Inês M. Micael Rosete

Licenciada em Química Aplicada - Perfil Química Aplicada

Gelation of Cellulose Derivatives: Searching for ionic liquid paper

Dissertação para obtenção do Grau de Mestre em
Química Bioorgânica

Adviser: Doutora Marta Cristina Parracho Cançado Corvo,
Investigadora PostDoc, Cenimat | i3N,
NOVA University of Lisbon

Co-adviser: Doutora Coro Echeverria,
Investigadora PostDoc, Cenimat | i3N,
NOVA University of Lisbon

Examination Committee

Chairperson: Prof. Doutora Paula Cristina de Sério Branco
Raporteur: Doutora Ana Sofia Diogo Ferreira
Member: Doutora Marta Cristina Parracho Cançado Corvo

FACULDADE DE
CIÊNCIAS E TECNOLOGIA
UNIVERSIDADE NOVA DE LISBOA

Setembro, 2016

Gelation of Cellulose Derivatives:
Searching for ionic liquid paper

Copyright © Inês M. Micael Rosete, Faculdade de Ciências e Tecnologia, Universidade NOVA de Lisboa.
A Faculty of Sciences and Technology e a NOVA University of Lisbon têm o direito, perpétuo e sem limites geográficos, de arquivar e publicar esta dissertação através de exemplares impressos reproduzidos em papel ou de forma digital, ou por qualquer outro meio conhecido ou que venha a ser inventado, e de a divulgar através de repositórios científicos e de admitir a sua cópia e distribuição com objetivos educacionais ou de investigação, não comerciais, desde que seja dado crédito ao autor e editor.

This document was created using the (pdf)LaTeX processor, based in the "unlthesis" template[1], developed at the Dep. Informática of FCT-NOVA [2].
[1] https://github.com/joaomlourenco/unlthesis [2] http://www.di.fct.unl.pt

Esta dissertação é dedicada aos meus avós
pelo seu exemplo de perseverança.

Acknowledgements

Em primeiro lugar, quero agradecer à minha orientadora, Dra. Marta Corvo, pela orientação, conhecimento e contribuições ao longo dos três anos de trabalho. Agradeço também à minha co-orientadora, Dra. Coro Echeverria, pela sua contribuição neste projeto. Quero ainda agradecer ao Professor Gabriel Feio e ao Dr. Pedro Almeida pelas sugestões e conhecimento que me permitiram conhecer a visão de um físico sobre o comportamento dos materiais (com maior foco sobre o seu "comportamento elástico").

Agradeço ainda à Dra. Joana Pinto e Professora Luísa Ferreira pelas análises dos polímeros por DRX e por ATR-FTIR, respectivamente. Gostava também de agradecer ao Leonardo Moreira dos Santos pelas análises de DSC e TGA.

Quero agradecer aos meus colegas de laboratório Ana, Gabriela e Jaime pelo espírito de companheirismo tido ao longo de toda a tese. Agradeço aos meus colegas de laboratório de RMN do departamento de química Ana Diniz e ao Micael pela motivação que sempre me deram, pelos jantares e voltas na 4L. Ao Diogo Poeira um especial agradecimento pelas longas conversas e conselhos nos momentos bons e menos bons da tese. Por fim, gostava de agradecer à Cláudia Afonso pelo seu exemplo de dedicação e pela constante motivação durante este ano.

Quero agradecer a todos os meus amigos pela sua amizade e suporte durante este ano. Em particular ao Tiago dos Santos e à Nivalda que me acompanharam ao longo destes cinco anos de estudo.

Quero agradecer ao meu namorado, Luís, pelo seu apoio, suporte e dedicação que se transformaram num pilar neste projecto. Agradeço ainda à minha família, em especial à minha mãe por todo o seu suporte e compreensão durante estes cinco anos.

Por fim, gostava de agradecer aos meus avós pelo seu humilde exemplo de vida que me ajudou no meu percurso académico. A eles dedico esta tese representativa do esforço e dedicação que me ensinaram a ter na vida.

Abstract

Cellulose is the world's most abundant, biocompatible, non-toxic, biodegradable polymer obtained from renewable sources. However its dissolution problems hampers a more generalized application. ILs are generally defined as organic/inorganic salts with a melting point lower than 100°C which present a good solubility for polar and non-polar compounds such as organic, inorganic or polymeric materials like cellulose. Cellulose solvents are scarce and, as such, the modification of its properties is a challenge.

In this dissertation the main goal was to combine some of the unique IL's properties with the intrinsic cellulose features. Thus, our strategy was to synthesize cellulose derivatives that enable the dissolution process in order to, later on, obtain a polymer gel. In the first stage we obtained ionic liquid grafted cellulose derivatives. Afterwards, we performed an extensive solubilization study to select the appropriate conditions to obtain the gel state. To further understand the solvents' dynamics and their relevance in the gelation process, these conditions were followed by NMR and Rheology.

The obtained results allowed the proposal of a gelation model for these cellulosic polymers. The proposed strategy could be a starting point to design and produce Ionic Liquid Paper (ILP), a material that could have potential for electrochemical applications.

Keywords: Cellulose; Cellulose derivatives; polymer ionic liquid; Gels; Nuclear Magnetic Resonance; Rheology.

Resumo

A celulose é um dos polímeros mais abundantes do mundo, é biocompatível, não tóxico, biodegradável e obtém-se a partir de fontes renováveis. No entanto, a sua difícil dissolução dificulta uma aplicação mais generalizada. Os líquidos iónicos são espécies iónicas geralmente definidas como sais orgânicos/inorgânicos com um ponto de fusão inferior a 100°C e apresentam boas capacidades de dissolução de compostos polares e não-polares tais como compostos orgânicos, inorgânicos ou polímeros como a celulose. Não existem muitos solventes capazes de dissolver a celulose por isso, a modificação das suas propriedades é um desafio.

Nesta dissertação o principal objectivo foi combinar algumas das propriedades dos LIs com as características da celulose. Assim, a nossa estratégia foi sintetizar derivados de celulose que facilitem o processo de dissolução para depois obter géis a partir dos mesmos. Numa primeira fase, sintetizou-se celulose derivatizada com líquidos iónicos e depois realizou-se um estudo intensivo de solubilização para selecionar as melhores condições para se obter o estado de gel. Para entender a dinâmica dos solventes e a sua relevância no processo de gelificação foram utilizadas RMN e Reologia como técnicas de referência.

Os resultados permitiram assim a obtenção de um possível modelo de gelificação para estes derivados de celulose. A estratégia proposta pode ser assim, um ponto de partida para aprofundar estudos e produzir Ionic Liquid Paper (ILP), um material que pode ter potencial para, por exemplo, aplicações eletroquímicas.

Palavras-chave: Celulose; Derivados de Cellulose; Líquidos Iónicos Poliméricos; Géis; Ressonância Magnética Nuclear; Reologia.

Contents

List of Figures

List of Tables

Symbols

δ Chemical Shift.

γ gyromagnetic ratio.

D Self-diffusion coefficient.

G' elastic modulus.

G" viscous modulus.

$\mathbf{T}_1$ Spin-lattice relaxation time.

$\mathbf{T}_2$ Spin-spin relaxation time.

$\mathbf{T}_{gel}$ gel point.

$\mathbf{t}_{cure}$ Cure time.

tan δ loss factor.

Acronyms

AGU Anhydroglucose unit(s).

AmimCl 1-allyl-3-methylimidazolium chloride.

ATR-FTIR Attenuated Total Reflectance -FTIR.

Bmim 1-butyl-3-methylimidazolium.

BmimCl 1-butyl-3-methylimidazolium chloride.

CDC 6-Chloro-6-deoxycellulose.

CellmimCl Cellulose anchored 1-methyl-imidazolium chloride.

CMC Carboxymethylcellulose.

CP-MAS Cross Polarization Magic Angle Spinning.

CPMG Carl-Purcel-Meiboom-Gill.

DMA Dimethylacetamide.

DMF Dimethylformamide.

DMSO Dimethyl Sulfoxide.

DOSY Diffusion Ordered Spectroscopy.

DP Degree of Polymerization.

DS Degree of Substitution.

DSC Differential Scanning Calorimetry.

DTG Derivative Thermogravimetric.

EmimAc 1-ethyl-3-methylimidazolium acetate.

FTIR Fourier Transform Infrared.

G* complex shear modulus.

HEC Hydroxyethylcellulose.

HPC Hydroxypropylcellulose.

HPMC Hydroxypropylmethylcellulose.

IL Ionic Liquid.

LVR linear viscoelastic range.

MC Methylcellulose.

mg milligrams.

MS Molar Substitution.

NMMO *N*- methylmorpholine -*N*-oxide.

NMR Nuclear Magnetic Resonance.

NOE Nuclear Overhauser Effect.

NOESY Nuclear Overhauser Effect Spectroscopy.

PF Paraformaldehyde.

PFG Pulse Field Gradient.

PILs Polymer Ionic Liquids.

POM Polarizing Optical Microscope.

ppm Parts per million.

RF Radio Frequency.

TGA Thermogravimetric Analysis.

VOC Volatile Organic Compound.

VT-NMR Variable Temperature NMR.

Chapter 1

Forward

This preliminary chapter intends to briefly introduce the motivation of this work and the main objectives in this dissertation. An outline of this manuscript is also presented.

1.1 Motivation

Cellulose is known to be the world's most abundant polymer. [1] It is biocompatible, non-toxic, biodegradable, renewable and environmentally friendly material. [2] All this interesting features are enough to arise curiosity and research into new applications for this material. Thus, cellulose and its derivatives have become an alternative to synthetic polymers, e. g., in gel state they are used in multiple fields like drug delivery system, [3] sensors [4] and tissue engineering [5].

In the last decades, scientists have designed a new family of polymer materials - Polymer ionic liquids (PILs).[6] These new materials are a class of polyelectrolytes which carry an Ionic Liquid (IL) species in each of the repeating units that are not soluble in water but instead in organic solvents. [7] PILs present some of the unique properties of ILs such as ionic condutivity, thermal and chemical stability. The use of cellulose as a backbone of PILs allows the production of new materials that bring together IL's properties with the intrinsic cellulose features.

This will be a new and promising material that could be explored in several fields (e. g., with optical properties, [8] as an healing agent [9] or with conductive properties [10]) after their development and structural and mechanical comprehension.

1.2 Goals and Expected Contributions

The goal of this work is the development of a new soft material that combines IL and cellulose properties toward the production of ionic liquid paper - a new polymer gels. For that purpose we take advantage of two advanced techniques, Nuclear Magnetic Resonance (NMR) and Rheology to study the micro- and macromolecular behavior.

Therefore, the four main contributions are:

- Development and characterization of a new cellulose derivative - Ionic liquid gel;
- Study the gelation process of cellulose derivatives in order to understand their physical and chemical properties for future applications;
- Understand the solvents' behavior and their relevance in the gelation process;
- Contribute with a detailed view on the dissolution and gelation process using NMR spectroscopy to study materials using Spin-lattice relaxation time (T_1), Spin-spin relaxation time (T_2), Nuclear Overhauser Effect Spectroscopy (NOESY) and Diffusion Ordered Spectroscopy (DOSY) experiments;

1.3 Outline

This document is organized as follows:

- Chapter 2 presents a detailed review of the literature on the dissertation research field. Firstly the cellulose's structural level understanding is carried out. Then an overview of the most used solvents in cellulose dissolution is presented. A short review of the most used cellulose derivatives is presented and polymer ionic liquids are introduced. Finally, we present the strategy of the outlined work in order to achieve the proposed goals.
- Chapter 3 presents a brief theoretical background of the techniques used. Herein is briefly explained each technique and their contributions in this work. It begins by NMR spectroscopy and then rheology technique is presented.
- Chapter 4 presents the experimental procedures used - a detailed description of the synthesis, systems characterization and gelation studies.
- Chapter 5 presents the polymer characterization through the interpretation of FTIR, CP-MAS and DRX diffraction experiments.
- Chapter 6 presents the results of this work. Here were made preliminary solubilization experiments of the polymers under study using BmimCl/DMSO binary mixture as solvent. Then for gelation process are presented both paths considered. For each one chemical shifts, ^{13}C - T_1 and ^{1}H - T_2 relaxations, ^{1}H-DOSY and ^{1}H,

^{1}H-NOESY were measured in order to understand the dynamics of the system at molecular level. Aiming to study the viscoelastic properties, rheology technique was used (temperature and frequency sweep tests).

- Conclusions and future work are presented in chapter 7.

Chapter 2

Introduction

As a consequence of the technological evolution and the new environmental challenges contemporary society faces, there is a need to create and develop sustainable and functional materials. In this context, Materials Science has been growing and currently plays an important role in society. For the scientific community the challenge is to create materials with specific physical, chemical or mechanical properties. Soft materials have a variety of physical states and are easily deformed by thermal stresses, thermal fluctuations or under stress.[11] These exist under different types, such as colloids, polymers or gels. In the last years the interest in soft functional materials having a fibrous network structure has been increasing. Electrochemical, drug delivery, catalysis or sensing are their most used technological applications. This master thesis focuses on the study of cellulose ionic liquid polymer gels.

2.1 Cellulose

Cellulose is a polysaccharide formed from repetitive D-glucose units, which are linked together by β (1→4)-glycosidic bonds, figure 2.1.[2] As the most abundant natural polymer on earth cellulose is a biocompatible, biodegradable, renewable and environmentally friendly material. Plants, cotton or ramie are the major natural sources of this polymer.[12] Cellulose is also produced by some green algae, bacteria and fungi. Due to its natural availability this polymer can be a good raw material to be explored in many fields, such as textile, food or pharmaceutical industry.[1, 13] These features make cellulose a polysaccharide capable of replacing synthetic polymers and reducing the dependence on fossil fuel resources.

With the increasing of environmental responsibility starting in the 19th century, the search for sustainable and environmentally friendly products and processes has become

imperative. In this context, the research on the renewable resource cellulose started. In 1838, the French chemist Anselme Payen found the cellulose's molecular formula, $C_6H_{10}0_5$ which increased the scientific interest in this material and later, in 1870,the synthesis of cellulose nitrate took place. [14]

In the last decades several scientific studies have been focusing on cellulose derivatives and their applications as coatings, optical films as well as property-determining additives in building materials or composites and nanocomposites as reflected by the review of Klemm *et al.*. [15] More recently, cellulose and its derivatives have become an important material due to its multiple applicability. This increasing interest results from the unique structure of cellulose.

2.1.1 Molecular Structure

As previously described, cellulose is made of repeating glucose units. Each two anhydroglucose rings are linked together through an oxygen covalently bonded to the C-1 of one glucose ring and the C-4 of the adjoining ring. This bond is called the β-1,4 glycosidic bond and is susceptible to the hydrolysis. As can be seen in figure 2.1 the Anhydroglucose unit(s) (AGU) contain hydroxyl groups at C-2, C-3 (secondary) and C-6 (primary) positions. In this conformation the free hydroxyl groups are positioned in the ring plane (equatorial) while the hydrogen atoms are in the axial position. The molecular size of cellulose depends on the number of repeating units and it can be defined as Degree of Polymerization (DP). The DP value depends on the pretreatment of cellulose.

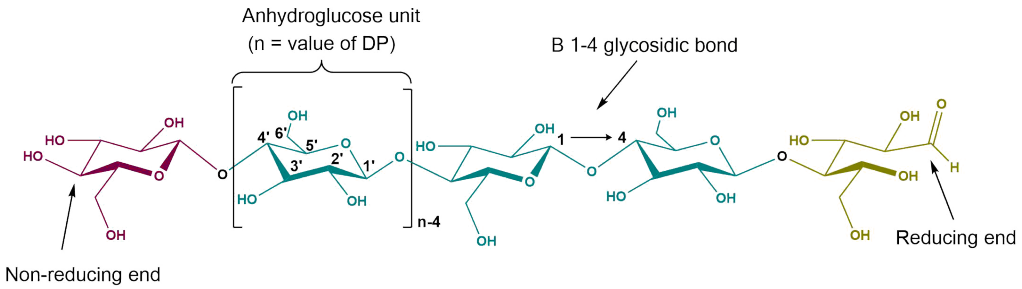

Figure 2.1: Molecular structure of cellulose. Adapted from reference [16].

The hydroxyl groups at both ends of the cellulose chain show different behavior. The glucose end group with a free C-1 hydroxyl group has reducing properties, while the C-4 end is non-reducing, figure 2.1.[1, 17] The presence of these hydroxyl groups and chirality offers a range of opportunities for synthesizing cellulose derivatives with desired properties for specific applications. The abundant hydroxyl groups lead to strong intra- and intermolecular hydrogen bonds, figure 2.2, making cellulose a relatively stable polymer. However, due to its hydrogen bonding cellulose can neither be melted nor dissolved in most organic solvents.[13] In section 2.2 this issue will be further addressed.

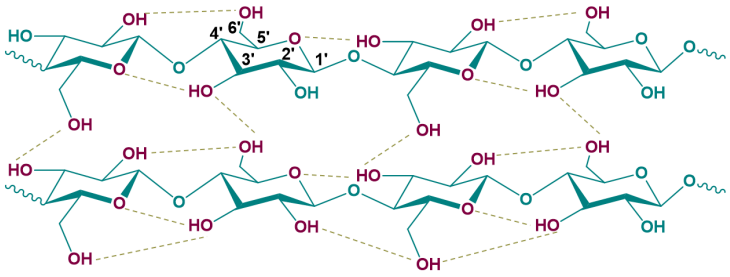

Figure 2.2: Molecular Structure of cellulose showing the intermolecular and intramolecular hydrogen bonds. Adapted from reference [18]

2.1.2 Supramolecular Structure

During cellulose formation, van der Waals and intermolecular hydrogen bonds between hydroxyl groups and oxygens of adjacent molecules promote aggregation of multiple cellulose chains, forming fibrils.[18] In turn, the chemical composition, conformation and hydrogen bonding system of cellulose is responsible for the tendency of cellulose to form crystalline aggregates. For this reason, within the cellulose fibrils there are regions where the cellulose chains are arranged in a highly ordered crystalline structure and regions that are low order, called amorphous regions.[1, 15] The different morphological structures of cellulose depend on its unit cell dimensions and their chain polarity.

There are four types of cellulose crystal structures - cellulose I, II, III and IV. [1, 15, 18] Cellulose I, or native cellulose, is the most abundant structure and can be converted to either cellulose II (most stable structure) and cellulose III by treatment with aqueous sodium hydroxide or by dissolution of the cellulose and subsequent precipitation. [15] Cellulose IV can be obtained through the treatment of the other structures (I, II and III) in a suitable liquid at high temperature under tension.[1]

There is not yet a defined hydrogen bonding pattern but according to the current state of the art, the intermolecular hydrogen bond between O-6-H and O-3 of another chain (figure 2.2) is generally considered the most important one for cellulose I.[1] As the most abundant structure, cellulose I has two polymorphs, a monoclinic structure Iβ and a triclinic structure Iα (Iβ is the most abundant polymorph). These two polymorphic structures only differ in the orientation of the hydrogen bonds on the plane [15, 17] and, therefore, they can be easily distinguished through X-ray crystallography. Cellulose crystallinity index can also be obtained through this technique.[18] Due to its supramolecular structure it becomes difficult to dissolve cellulose. Therefore, in the next section this theme will be explored.

2.2 Cellulose Dissolution

As already mentioned, cellulose cannot be dissolved in most organic solvents due to its intra- and intermolecular hydrogen bonds. For this reason, over the past few years

there has been an intensive research on the solvents which disrupt its hydrogen bonds. [1, 19] There are two different systems of solvents - derivatizing and non-derivatizing solvents. Herein will be presented the most important and used solvent systems on cellulose dissolution.

2.2.1 Derivatizing Solvents

With the derivatizing solvents the dissolution process occurs in combination with the formation of an unstable ester, ether or acetyl derivative.[16] The most important industrial method is the viscose process based on $CS_2/NaOH/H_2O$. The N_2O_4/Dimethylformamide (DMF) and Dimethyl Sulfoxide (DMSO)/ Paraformaldehyde (PF) systems herein summarize in table 2.1 will also be described bellow.

Table 2.1: Examples of derivatizing solvents and formed intermediaries. Adapted from reference [16]

Derivatizing solvents	Intermediate	R in (Cell-O-R)
$CS_2/NaOH/H_2O$	Cellulose Xanthate	CSSNa
N_2O_4/DMF	Cellulose nitrite	NO
DMSO/Paraformaldehyde	Methylol cellulose	CH_2OH

a) CS_2/NaOH/H_2O System

The most used method in the industry for cellulose dissolution is the CS_2/NaOH/H_2O system which forms cellulose xanthate from cellulose in seven steps. First, cellulose reacts with NaOH to form alkali cellulose. Then, it is oxidized and depolymerized. On the third step the white crumb produced is reacted with gaseous or liquid carbon disulfide (CS_2) to produce the intermediate cellulose xanthate. Afterwards, xanthate is dissolved again in NaOH and, finally undergoes washes and filtrations to obtain the final product. It is not a green process due to carbon disulfide production, an environmentally unfriendly waste product. [1, 16]

b) N_2O_4/DMF System

The N_2O_4/DMF system involves formation of the intermediate cellulose nitrite with the hydroxyl groups being converted to nitrite ester groups. [1] After the heterolytic cleavage of the N_2O_4, the process continues with the esterification of cellulose to the nitrite. The solvent system is able to dissolve cellulose within minutes without pretreatment. [20] The soluble cellulose nitrite has the ability to undergo ester exchange reactions. Toxicological hazards due to the formation of nitrous amines should be considered when using this system, which has also been studied for the preparation of cellulose derivatives.

c) DMSO/PF System

The derivative formed in the DMSO/PF system is methylol cellulose. [16] Methylol cellulose is able to participate in the synthesis of cellulose derivatives. Carboxymethylation, carbanilation, methylation and hydroxyalkylation of cellulose has been reported. [1] Finally, the major obstacles in this solvent system is the commercialization of DMSO/PF system. The solution requires a considerable excess of PF and the recovery is not optimized.

2.2.2 Non-derivatizing Solvents

Non-derivatizing solvents are defined as solvents that have the ability to dissolve cellulose only by intermolecular interactions.[16] Solvent systems such as *N*- methylmorpholine -*N*-oxide (NMMO), - Lyocell process - LiCl/Dimethylacetamide (DMA) and, more recently ionic liquids (ILs) are the most relevant non-derivatizing solvent systems on the cellulose dissolution process.[1]

a) *N*-methylmorpholine-*N*-oxide/water System

An alternative solvent used for cellulose dissolution is NMMO and its monohydrate, NMMO·H_2O. Due to its strong N-O dipole in combination with water NMMO can quickly dissolve cellulose at a temperature of about 85°C to a clear melted solution. [16] The interactions between NMMO and cellulose can be interpreted as a hydrogen bond-complex formation with cellulose hydroxyl groups, figure 2.3. [1] This NMMO/cellulose systems becomes unstable because at high temperatures cellulose undergoes severe degradations.[15]

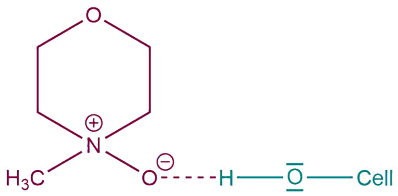

Figure 2.3: NMMO/Cellulose complex.[1]

b) Lithium Chloride/Dimethylacetamide System

A solution of LiCl (typically 10%) in DMA (DMA/LiCl) is one of the most relevant solvent systems in cellulose dissolution.[15] This system is based on the interactions of the $[Li(DMA)_x]Cl$ complex with the cellulose hydroxyl groups (figure 2.4) and was first reported by McCormick and Lichatowich in 1979. [21] Currently, this binary mixture is used for synthesis and analytical purposes. [15] It is very efficient and stable in homogeneous cellulose esterification and other reactions due to a full availability of cellulose hydroxyl groups in solution. With this feature, it is easier to control the Degree

of Substitution (DS) and cellulose can be dissolved without residue and detectable chain degradation. [1].

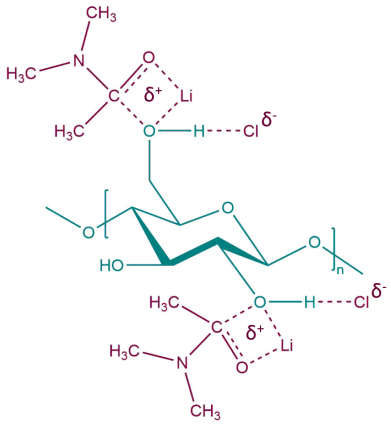

Figure 2.4: Li-DMA^{+}Cl^{-}/Cellulose complex.[16]

c) Ionic Liquids

ILs are generally defined as organic/inorganic salts with a melting point lower than 100 °C presenting a good chemical and electrochemical stability, low flammability, negligible vapor pressure, high ionic conductivity and a good solubility for polar and non-polar compounds such as organic, inorganic or polymeric materials. [6, 22] They can be used in electrochemistry,[23] nanotechnology[24] and biotechnology [25] and have the ability to dissolve polymeric compounds by ionic, hydrophobic and hydrogen bond interactions. Due to all of these properties they are able to replace traditional Volatile Organic Compound (VOC)s used in chemical reactions and extractions. [26, 27] Since there are a large number of cations and anions, there is a significantly large number of possible cation-anion conjugations. The ILs properties derive from its structure and the many variation possibilities have resulted in the capability to optimize them for specific applications, and as such ILs are called tailor made. Typically, the most reported ILs in literature are based on imidazolium, aliphatic ammonium, phosphonium and pyrrolidinium cations.[28] The anions can be selected according to the final properties, often modulating the viscosity, solubility, polarity, density, melting point and stability (chemical and thermal) of the final ionic liquid.

A study with *N*-ethylpyridinium chloride as a cellulose dissolving agent was made in 1969 by Husemann and Siefert.[29] In 2002, Swatloski et al. [30] reported a dissolution process of cellulose by 1-butyl-3-methylimidazolium chloride (BmimCl) and other ionic liquids. During the last years the scientific interest concerning the dissolution of cellulose in ILs has intensified [7, 31, 32] and currently several novel materials can be prepared from cellulose-ionic liquid solutions such as porous cellulose materials, [33] functionalized cellulose microparticles.[34] and bioactive cellulose films.[35] The anions of ILs disrupt the native hydrogen-bonded network in cellulose through interactions - which

are new hydrogen bonds - with hydroxyl groups of cellulose. On the other hand the cation can interact through hydrogen bonds, van der Walls, hydrophobic or non-specific interactions. [7] A interesting example of the cellulose dissolution power by imidazolium-based ionic liquids is 1-ethyl-3-methylimidazolium acetate (EmimAc) that can dissolve Avicel®PH101 up to 20% at room temperature within one hour. [36]

1-Butyl-3-Methylimidazolium Chloride (BmimCl)

BmimCl, figure 2.5, is reported to be a direct cellulose solvent. It is important to understand the mechanism of cellulose in ILs. Herein, the current state of the art about cellulose dissolution by BmimCl will be presented.

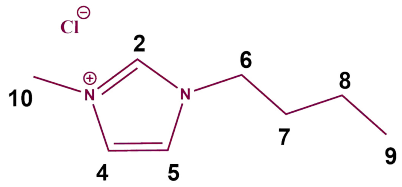

Figure 2.5: 1-Butyl-3-Methylimidazolium Chloride structure

In 2006, Remsing *et al.*[32] demonstrated through ^{13}C and $^{35/37}Cl$ NMR relaxations measurements that the solvation of cellulose by BmimCl involves hydrogen bonding between carbohydrate hydroxyl groups and the IL chloride anions in a 1:1 stoichiometry. Then, in 2011, Gross *et al.*[37] calculated the density distribution function of the chloride anions and 1-butyl-3-methylimidazolium (Bmim) cations around the dissolved cellulose and suggested that the imidazolium ring of Bmim cations had closer contacts with ether oxygen atoms and CH groups along the axial direction than with groups along the equatorial direction. In conclusion, they proposed that both the anion and the cation of BmimCl disrupt the cellulose inter-sheet contacts. More recently, Mostofian *et al.*[38] performed all-atom molecular dynamic simulations of a cellulose elementary fibril in BmimCl. The results suggested that Bmim cation interacted with cellulose in two different ways: stacking on cellulose strands on the hydrophobic surface and intercalating between chains in hydrophilic surfaces. It was believed that intercalation of the cations between cellulose strands on the two surfaces facilitated cellulose dissolution by loosening the layers of the cellulose structure. Finally, thermodynamic studies were also made by Gross *et al.*[39] and it was reported that the separation of the cellulose chains to the dissociated state in BmimCl led to an entropy reduction of the solvent. This result suggested that some solvent molecules were bound to cellulose chains and the intra-molecular degree of freedom of these chains was also reduced upon dissociation. The next section will introduce the most common cellulose derivatives with the aim of understanding their properties and applications. With this, we will have a broad overview of cellulose and its applications.

2.3 Cellulose Derivatives

In order to convert cellulose to a soluble compound, new water-soluble cellulose derivatives were produced. Herein is presented an overview of the three most synthesized cellulose derivatives. Typically, cellulose derivatives involve a chemical modification that disrupts the 2, 3 and 6-hydroxyl bonds. In 1905 Suida synthesized for the first time a cellulose derivative - Methylcellulose (MC)- [20] and in 1920 the synthesis of Carboxymethylcellulose (CMC) and Hydroxypropylcellulose (HPC) was reported. The most common reactions are esterification, etherification (figure 2.6) and grafting of cellulose.[40]

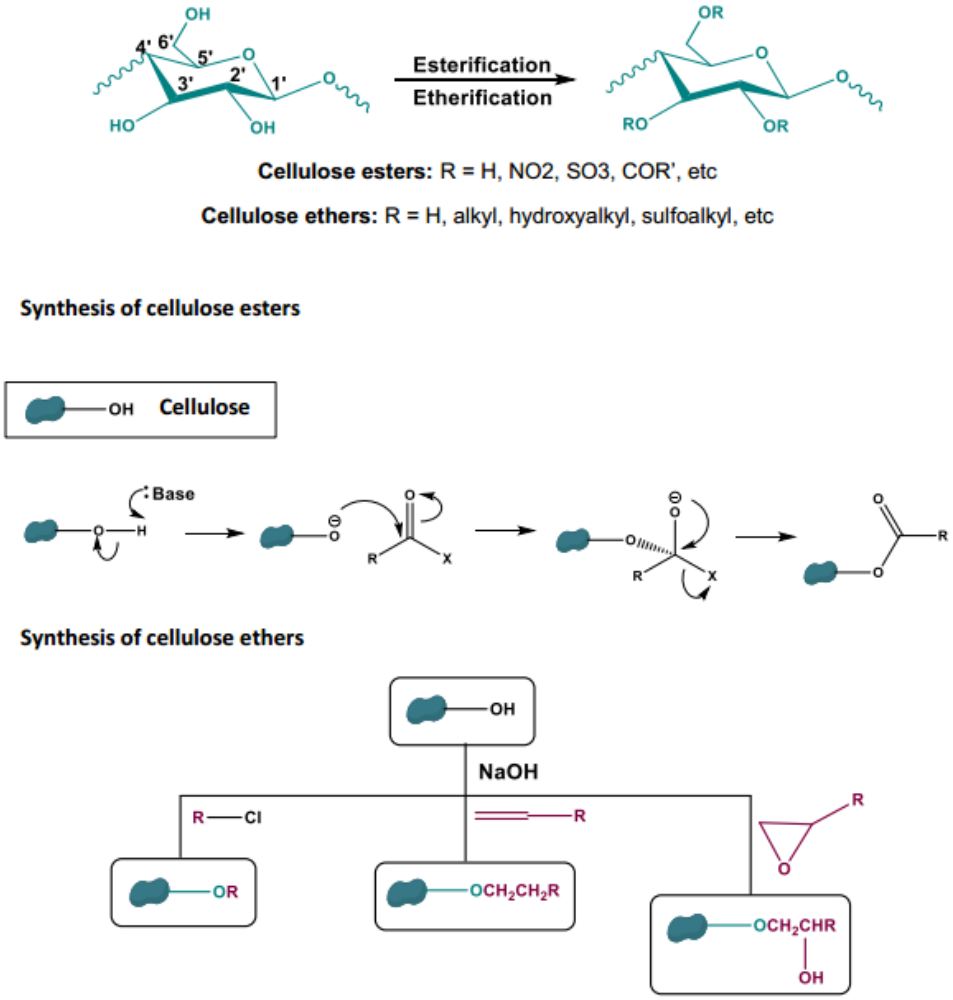

Figure 2.6: Synthetic approaches for cellulose derivatives. Adapted from reference [11]

Cellulose is esterified with acid anhydrides, acyl chlorides or with acids in the presence of dehydrating agents. It is etherified by Williamson ether synthesis with alkyl halides in the presence of a strong base, with alkylene oxides in a weakly basic medium and by a Michael addition of acrylic or related unsaturated compounds. [16, 40, 41] The three most relevant cellulose derivatives are MC, CMC and HPC, figure 2.7, that can be

obtained through etherification of cellulose. Solubility combined with chemical stability and non-toxicity are the most interesting features of these cellulose ethers.

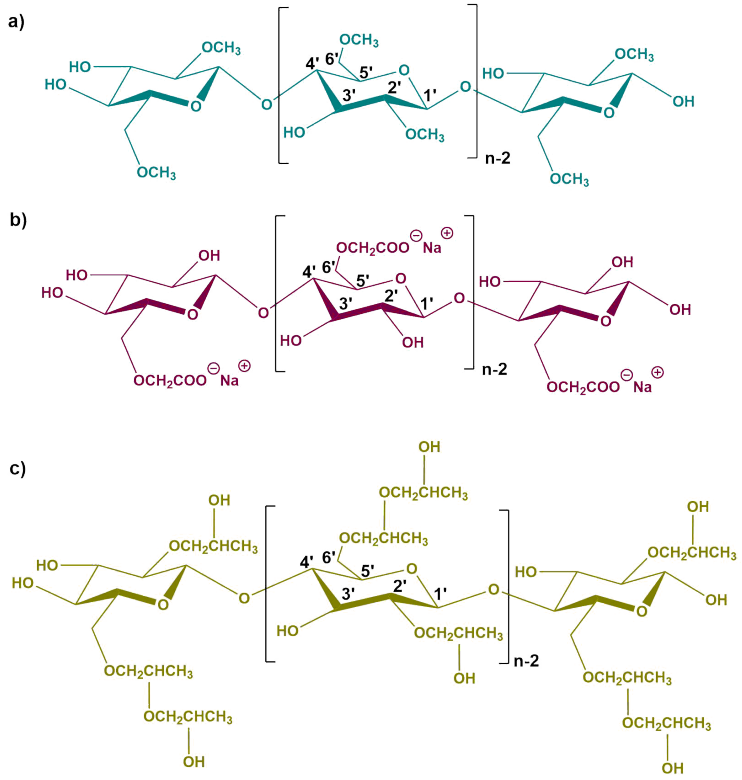

Figure 2.7: Cellulose Derivatives: a) MC, b) CMC and c) HPC

As a hydrophobically modified cellulose derivatives, methylcellulose results from a nucleophilic attack of an alkoxide group of cellulose on the acceptor carbon atom of the methyl chloride - an S_N2 reaction. [20] This methylation preferentially occurs at the C2 and C6 cellulose hydroxyl groups and commercially has a DS range of 1.5-2.0. [16] It has other interesting properties such as easy solubility in cold water and is amphiphilic due to the presence of hydrophilic and hydrophobic surfaces. One of the most relevant applications is the ability to form reversible gels in aqueous solutions. [1] Sodium Carboxymethylcellulose (CMC) is a polyelectrolyte water-soluble, anionic and linear polymer[41] with a DS range between 0.4 and 1.2. It is used in detergent, textile and food industries and cosmetics worldwide. [40] Finally, hydroxypropylcellulose is obtained through reaction of cellulose with propylene oxide. [41] Commercial HPC usually has a Molar Substitution (MS) (defined as the average number of hydroxyl groups per glucose unit) range of 3.5-4.5 and a DS between 2.2-2.8. [16, 20] It can act as a thickener, binder, film coating and suspension agent.

2.4 Polymeric Ionic Liquids

In the last decades, as a consequence of the research into new polymeric materials based on its future functionalities such as mechanical reinforcement or gas barrier properties, scientists have designed a new family of polymer materials - Polymer Ionic Liquids (PILs) - with particular properties and interesting applications.[42–44]. There is not a clear definition for PILs. Fundamentally, PILs refer to a special type of polyelectrolytes which carry an IL species in each of the repeating units that are not soluble in water but in organic solvents. [10] This is mainly due to the hydrophobic character of the counter-ion and the reduced coulombic interactions. [6] PILs present some of the unique properties of ILs (ionic conductivity, thermal stability, tunable solution properties and chemical stability) together with the intrinsic polymer properties.[6] The major advantages of forming a polymeric ionic liquid are enhanced stability, flexibility and durability, in addition to improved control over its meso-to nano-structure.[45] There are many interesting applications of these new polymeric materials. They can be used as novel polymer electrolytes [46], structuration agents of polymer matrices [47], plasticizers [48] or as surfactants [49] in the preparation of functional polymers. Currently, PILs are used as a medium for gas storage or transport, coatings for the detection of a number of environmental contaminants, matrix for enzyme immobilization, cellulose dissolution agent or as catalysts supports or precursors of *N*-heterocyclic carbene organic catalysts. These are the emerging applications of these new materials. [6]

2.5 Gels as Soft Materials

The scientific interest in gels as soft materials has been increasing due to the potential technological applications in multiple areas - such tissue engineering,[5] sensors[4] and drug delivery.[3] Significant progress has been achieved in the development of smart gels with the ability to respond to external stimuli, such as temperature,[50] electrical field,[51, 52] and light[4]. These unique properties have led to a diversity of applications such as sensors, actuators, cell/drug delivery systems, tissue engineering and regenerative medicine. There is not yet a consensus regarding a unique definition for the set of gel characteristics. Fundamentally, a gel is characterized by the presence of at least two components that trigger a three-dimensional (3D) solid scaffold, immobilizing a much larger liquid volume.[53] It has a continuous structure with macroscopic dimensions that is permanent on the time scale of an analytical experiment. Rheologically it exhibits mechanical solid properties and maintains its form under the stress of its own weight, behaving as a viscoelastic material.[54]

Gels can be classified according to the cross-linking type, source, medium and size. [55] Regarding the type of cross-linking of the gels, they can be divided in two classes - chemical and physical gels. Chemical gels are cross-linked by covalent bonds and are nonreversible. Physical gels' networks are held together by weak noncovalent interactions

like hydrogen bonding, π-π stacking, donor-acceptor interactions, metal coordination, host-guest interaction, van der Walls interactions and solvophobic forces. [56] This class of gels is reversible due to their easy-to-break interactions.

2.6 Cellulose and Cellulose Derivatives Gels

Cellulose and its derivatives are nontoxic, biocompatible, biodegradable and abundant in nature, thus it could be an alternative to synthetic polymer gels. Their strong inter- and intra-molecular hydrogen bonds together with the hydrophobic interactions between cellulose chains makes the dissolution process difficult which is crucial to obtain the polymer gel.

Currently, most relevant and used solvents to obtain cellulose gels are DMA/LiCl, DMSO and ILs (BmimCl and 1-allyl-3-methylimidazolium chloride (AmimCl)). H. Saito *et al.* [57] and M. Patchan *et al.* [58] studied the synthesis in DMA/LiCl and properties of cellulose-based hydrogels with high strength and transparency. They also evaluated the properties of the resulting hydrogels, water content, optical transparency and tensile and tear strengths. Finally, they correlated this features with cellulose concentration in order to optimize the gelation process. Their results suggested that overnight activation time (16 h) improves the optical transparency of the hydrogels from 77% to 97% at 550 nm and controlling cellulose concentration and gelation humidity improves their tear strength by as much as 200%. Even a small amount of water gave rise to a strong increase in viscosity resulting in gelation. Another relevant observation to consider for the development of the present master thesis is that Avicel®PH 101 hydrogels display good optical transparency.

Z. Wang *et al.* [59] have reported in 2012, a study using LiCl/DMSO for preparing cellulose gels. Although the previously described optical improvement wasn't achieved, the dissolved in LiCl/DMSO, could be coagulated by ethanol to give translucent cellulose gels, which could give rise to highly porous aerogels via solvent exchange drying.

Finally, the most recent and interesting solvents - ILs. They have revolutionized the cellulose dissolution process and their gelation studies. In the last few years the research focused on these solvents in cellulose dissolution has increased. [60] In addition studies regarding cellulose gels can be found in the literature although there is still a lack of experimental details. For instance in 2008, J. Kadokawa *et al.*[61] proposed the preparation of a flexible gel from a solution of cellulose (15% w/w) in an ionic liquid, BmimCl, by keeping it at room temperature for 7 days. The material was obtained by formation of cellulose aggregates in the solution of cellulose, attributed to a gradual absorption of water. Also, when the material was heated at 120^{o}C, it became soft and by keeping it at room temperature for 2 days, a more transparent gel was formed comparing with the primary gel. More recently, R. Ariño *et al.*[62] developed a new gelation process via coagulation. Cellulose was dissolved in an ionic liquid solvent and the resultant solution was maintained during 4 days under a coagulation agent (water or ethanol) vapor. The absorption of the coagulation agent was found to be related to the types of

ionic liquid and cellulose. The stiffness of the polymer gel increased with the polymer matrix content.

In 2016, C. Zhang *et al.*[63] reported new developments about the effect of DMSO on cellulose dissolution with ILs. The results suggested that DMSO has a dual effect depending on the concentration on solution. At lower concentrations it improves the cellulose solvating ability of AmimCl but weakens it at higher concentrations. The reason for this is the tight association between the cation and anion in the AmimCl network that is loosened at low DMSO concentrations.

Gelation of cellulose derivatives occurs as result of dehydration of the chains along with hydrophobic association of the chain segments, by which physical cross-links are formed, leading to three-dimensional polymer-network structures. This depends on the DS of the functional groups, polymer molar mass, temperature, etc. [11] A most relevant example is methylcellulose (MC). Thermally induced gelation is reversible in this polymer. Arvidson *et al.*[50] have reported, in 2013, new developments about MC thermo-reversible gelation. They conclude that MC gelation has a strong dependence on heating rate while the melting of the gel has little dependence on the cooling rate. Additionally, the T_{gel} decreases with increasing MC concentration. It is believed that water is the major factor for the gelation phenomena, since it disrupts the MC hydroxyl group interactions creating new hydroxyl bonds. Also, MC gels depend on the chain length, degree of substitution, substituents' position, salt and polymer concentration. [16]

2.7 Searching for Cellulose Derivatives - Ionic Liquid Gels

The aim of this dissertation is the development of a new cellulose derivative - ionic liquid gel. This brief literature review evidenced the difficulties found in cellulose dissolution. One possible path to solve this problem is the modification of the cellulose structure in order to increase the polymer solubility. Taking into account the interesting ionic liquids features we devised a strategy to improve cellulose solubility were we could both graft ionic liquids in the cellulose backbone and also use them as solvent systems, figure 2.8.

This increased solubility will be paramount for the pretended polymer gelation. In this sense it is crucial to characterize the polymer solvent interactions using NMR and Rheology techniques as a mean to gain a deeper insight into the micro- and macromolecular behavior of these systems.

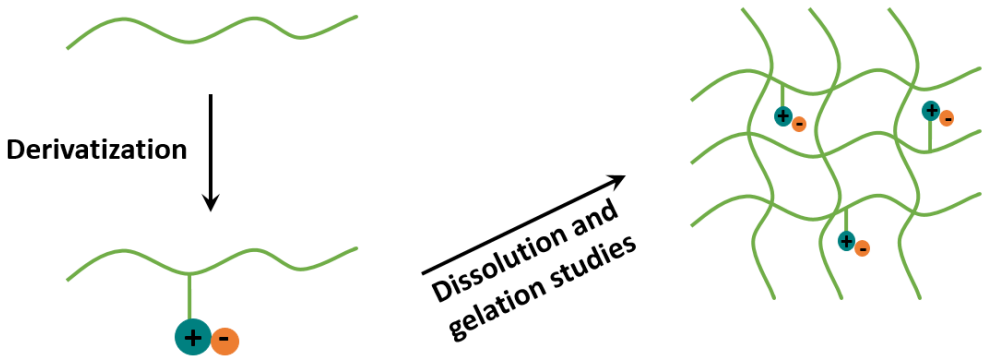

Figure 2.8: Pictorial representation of the strategy considered.

Chapter 3

Technical Background

This master thesis focuses on the molecular and mechanical studies of polymer gels. For these studies techniques such as NMR spectroscopy, Rheology were used. Herein the contributions of each technique for the studies will be presented.

3.1 NMR Spectroscopy

NMR spectroscopy can be defined as a technique that makes use of the interactions between nuclear spins ($I \neq 0$) and electromagnetic Radio Frequency (RF) pulses to allow the study of molecules at atomic scale (< angstrom). [64] Thus, it enables not only structural analysis but the study interaction between two molecules or even to determine the dynamic of molecules in different states of matter. One of the drawbacks of this technique is its relatively long timescale, which can be a disadvantage for observing fast phenomena [65].

In this work the NMR tools explored were chemical shifts for ^{1}H, T_1 and T_2, self-diffusion and Nuclear Overhauser Effect (NOE). The establishment of a 3D macromolecular arrangement and interactions were approached by chemical shift and NOE, respectively. Dynamics were followed by DOSY and relaxation T_1 and T_2.

A proton in a molecule is shielded to a very small extent by its electron cloud, the density of which varies with the chemical environment. This variations give rise to differences in chemical shift positions. [66] In a gelation process the electron density changes with the local structural changes and as such, the chemical shift variations can be used to follow this phenomena. Thus, knowing the chemical shift deviations, depending on the features described above, it is possible to study the gelation process.

The relaxation plays a relevant role in NMR spectroscopy. It is possible to correlate it

with the molecular dynamics, therefore allowing the understanding of the gelation process. The mobility of the molecules is influenced by viscosity, temperature and molecular weight. [65]

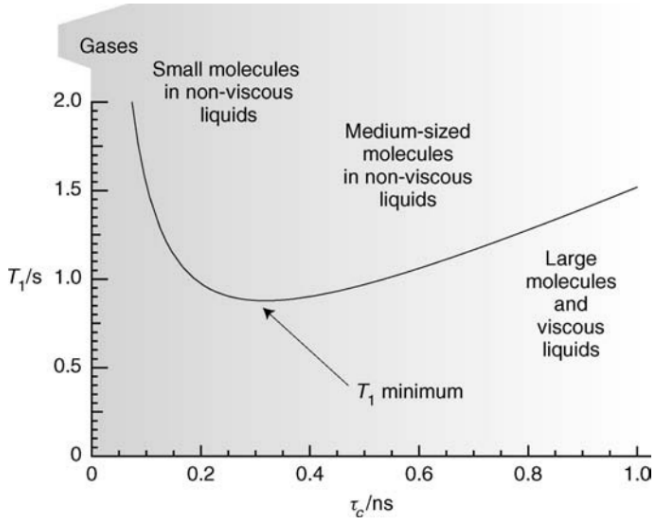

Figure 3.1: The spin-lattice relaxation time constant as a function of correlation time for random field fluctuations. Typical ranges of correlation time are shown. [65]

Small molecules in non-viscous solvents and at higher temperatures presents fast molecular reorientational tumbling. For solutions with higher viscosity or molecular weight and low temperatures the reorientational rates become progressively slower and consequently relaxation becomes more efficient, resulting in shorter T_1 values, figure 3.1. [64, 65]

T_2 relaxation is important because xy-plane magnetization is directly related with NMR signal appearance. In other words, this relaxation can be correlated with the spectral line width and consequently with molecular motion, figures 3.2.

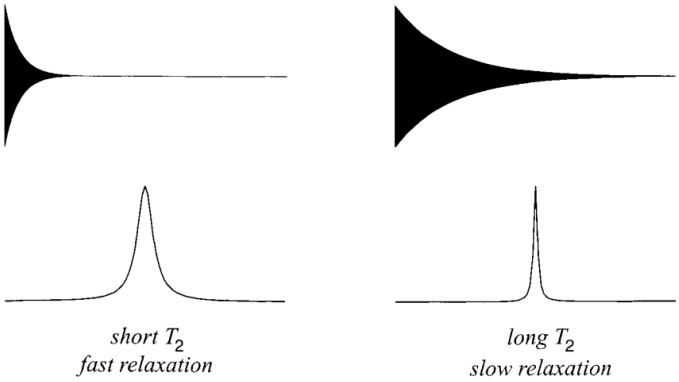

Figure 3.2: Effect of transverse relaxation process on NMR signal aspect. Adapted from reference [64]

There are two types of coupling: scalar and dipolar. Scalar coupling can be defined

as the indirect coupling that is transmitted through intermediate electron spins such as those in intervening chemical bonds. [64] Dipolar coupling consists in the spacial interactions between two spins, figure 3.3.

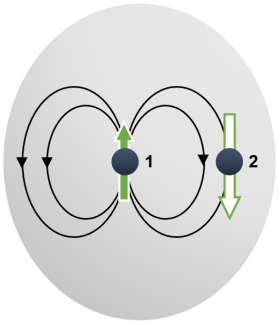

Figure 3.3: Dipolar interaction between two spins. Adapted from reference [65]

NOE is the change in intensity of one resonance when the spin transitions of a dipolarly coupled nucleus are somehow perturbed from their equilibrium populations. [65] It depends on the distance between interacting spins (<5Å), type and mobility of the nucleus, magnetic field strength and other relaxation processes. Therefore, acquiring NOESY spectra makes it possible to get spatial correlations of the closest nuclei. This technique allows the subsequent monitoring of the spatial intra- and intermolecular interactions of the cellulose derivative ionic liquid systems.

Diffusion Ordered Spectroscopy (DOSY) has been described as an effective technique to differentiate molecules according to their size.[64] It is based in the measurement of the signal attenuation in a gradient stimulated spin echo. In a usual pulse sequence it was added two Pulse Field Gradient (PFG). The PFG-NMR technique is the most used in these studies because it allows the measurement of the self-diffusion coefficients of one or several molecular constituents at a micrometric scale.[67] This technique can be useful in the study of molecular interactions between the polymer, the ionic liquid and the solvent.

3.2 Rheology

Defined as a field of physics which studies the deformation of bodies and flow behavior of matter,[68] rheology discloses information not only about flow behavior of liquids but also about deformation behavior of solids. Rheology measures the opposition of the material to flow due to an imposed deformation. Rheological behavior of matter can be consider to be between two extremes: i) flow of ideal viscous liquid and ii) deformation of ideal elastic solids. Materials in a non-ideal state show a combination of both, and are considered as viscoelastic.

Rheometers allow the precise measurement of a complex material's response to an applied force (stress) or deformation (strain). Linear oscillatory rheology put the material through a small oscillatory strain or stress of the form:

$$\gamma = Asin(\omega t) \tag{3.1}$$

where γ is the strain, A is the amplitude of the oscillation and ω is the frequency of oscillation. The response of the material to the applied strain is measured. In the case of a pure elastic solid the stress required to impose the deformation is proportional to the strain rate whereas for a viscous liquid, the stress is proportional to the strain rate [68]

$$\gamma = A\omega cos(\omega t) \tag{3.2}$$

As stated before, viscoelastic solids like gels will show a response to an applied deformation somewhere between ideal viscous liquid and ideal solid elastic. The rheological parameter that consider both characteristics is the complex shear modulus (G*) (equation 3.3). This parameter accounts for both the fraction that is in-phase with the deformation and the part that is out-of-phase. Those fractions are represented as elastic modulus, G', and viscous modulus, G" and $tan(\delta)$ is a correlation between them:

$$G^* = (G^{'2} + G^{''2})^{1/2} \tag{3.3}$$

$$G' = \alpha sin(\omega t) \tag{3.4}$$

$$G'' = \alpha cos(\omega t) \tag{3.5}$$

$$tan(\delta) = \frac{G''}{G'} \tag{3.6}$$

The analysis of the rheologic properties of the cellulose derivatives ionic liquid gel is an important topic in this dissertation. The determination of the viscoelastic properties would help the systems gel-like behavior at the macromolecular level.

Oscillatory rheology is a powerful tool in the field of a polymer science. Since by varying the amplitude or/and frequency of the applied deformation is possible to study a wide range of timescales and behavior. For instance, in the case of polymer gel oscillatory measurements allows the determination of gel-like behavior without destroying the gel structure. Rheologically, a polymer gel is characterized by i) an elastic modulus higher than viscous modulus (G'>G") and ii) an elastic modulus at zero frequency independent of the frequency. [69]

By means of oscillatory it is possible to study the influence of temperature in the gelation process of a physical gel. In fact, performing a temperature sweep test at a non-destructive frequency under a LVR, it is possible to analyze the evolution of G' and G" with temperature, and to detect the temperature at which the liquid-like to gel-like behavior occurs (where G' and G" crossover (G'=G")). Finally, with all of these measurements it is possible to characterize macroscopically the materials under study.

Chapter 4

Experimental

4.1 Preamble

The methods and characterization studies of the cellulose derivatives synthesized are based on general framework procedures described below:

- The solvents *N, N'* – dimethylformamide (DMF) and toluene were obtained from Merck and Sigma Aldrich respectively, and distilled with CaH_2. *N*-methylimidazole was purchased from Alfa Aesar and distilled with CaH_2. Ammonium hydroxide, methanol and acetone were used without prior purification. Microcrystalline cellulose (MCC) Avicel®PH-101 (DP 200-300) was obtained from Fluka, Sigma Aldrich and dried at 60 °C at least 24h in a vacuum oven before used. The water used was always Millipore water. Finally, BmimCl purchased from io-li-tec and was dried in vacuum at 45 °C for at least 24h.
- Elemental analysis was obtained from elemental analyzer Thermo Finnigan-CE Instruments Flash EA 1112 CHNS series. The data are presented through percentage (%).
- Attenuated Total Reflectance -FTIR (ATR-FTIR) spectra were acquired from spectrometer Perkin Elmer UATR Two in a range of 400-4000 cm^{-1}. Spectra were acquired with 16 scans and the most intense bands characterizing each synthesized compound were interpreted. Data are shown as follows: maximum frequency absorption, υ_{max}, in cm^{-1} (functional group), intensity and shape (s – strong; m – medium; w – weak; br – broad; sh – sharp)
- Thermogravimetric Analysis (TGA) analysis were obtained from TA Instruments model Q20 equipment and SDT equipment (TA Instruments model Q600), respectively. During the TGA scan, the samples were first heated from room temperature

to 80 °C within 5 minutes, then cooled to -50 °C at a rate of 20 °C/min. After 2 minutes at -50 °C, samples were heated until 230 °C at a rate of 10 °C/min. After 2 minutes at 230 °C the temperature process was reversed, i.e., from 230 °C to -50 °C (10 °C/min). Finally, after 2 minutes at -50 °C the temperature was ramped up to 300 °C (10 °C/min).

- The X-ray diffractions were performed using a PANalytical's X'Pert PRO MRD X-ray diffractometer with 2θ in the 5-75° interval, using the CuKα radiation source with a wavelength of 1.54 Å at room temperature.

- The NMR experiments were acquired in a Bruker Avance III 300 MHz (7.2 T) spectrometer and a Bruker Avance III 400 MHz (9.4 T) spectrometer.

  300 MHz:

  - The solid state Cross Polarization Magic Angle Spinning (CP-MAS) ^{13}C NMR spectra operating at 75.47 MHz equipped with a BBO probehead. The samples were spun at the magic angle at a frequency of 5 KHz in 4 mm diameter rotors at room temperature with pulse repetitions of 2 s and contact times of 1200 ms.
  - ^{1}H-NMR experiments were acquired with ^{13}C/^{1}H/^{2}H 5mm dual probe (VT) operating at 300.02 MHz with 64 k time domain points over a spectral window of 8012.820Hz (20.0244 ppm) centered at 2471.09 Hz (6.175 ppm) and with 64 scans per FID. Relaxation delay was 5 s. Typical 90 degree pulse lengths were 12.125 μs. VT-NMR were carried out using DMSO-d_6 as reference with a temperature range from 296 to 346 K (296, 301, 306, 311, 316, 321, 326, 331, 336, 341 and 346 K). A standard BVT 3000 variable temperature control unit with an accuracy of +/-0.5 °C was used.
  - ^{13}C Spin-lattice (T_1) relaxation times were obtained with ^{13}C/^{1}H/^{2}H 5mm dual probe (VT) operating at 75.47 MHz by means of the usual inversion recovery (180-τ-90-acquisition) sequence. Typically, for a T_1 determination 12 spectra of 64 K data points with τ values in the range of 1 ms to 25 s were acquired. Relaxation delay was 5 s. A quick T_1 estimation was performed for all samples in order to set the appropriate relaxation delay.
  - Transverse (T_2) relaxation times were obtained by means of the usual CPMG sequence. Typically, for a T_2 determination a number of 8 spectra of 14 K data points were collected, with 14 τ values in the range of 3 ms to 35 s.
  - ^{1}H Diffusion measurements were acquired with a micro-imaging probe PH Micro 2.5 with a ^{1}H insert using a magnetic field pulsed gradient in the z-direction of 1.47 T.m^{-1} and were performed using the stimulated echo sequence using bipolar sine gradient pulses and eddy current delay before the detection (diffSTE). Self-diffusion coefficients were obtained by varying the

gradient strength (g) while keeping the gradient pulse length (δ) and the gradient pulse intervals constant within each experimental run. Typically, in each experiment a number of 32 spectra of 16 K data points were collected, with values for the duration of the magnetic field pulse gradients (δ) of 12 to 16 ms and diffusion times (Δ) of 180 to 200 ms. The sine shaped pulsed gradient (g) was incremented from 5 to 95% of the maximum gradient strength in a linear ramp. The spectral width was 8333.33 Hz (27.77 ppm) centered on 2214.96 Hz (7.38 ppm) in direct dimension (t2) and of 3001.20 Hz (9.99 ppm) centered on 2214.96 Hz (7.38 ppm) in indirect dimension (t1). The phase was corrected with 1D spectrum obtained by 1H-NMR. All experiments were acquired at 298 Kelvin (K).

400 MHz:

- NOESY experiments were acquired with a 5 mm high-resolution BBO probe operating at 400.15 MHz for ^{1}H with pulsed gradient units, capable of producing magnetic field pulsed gradients in the z-direction of 0.54 T.m^{-1}. Two dimensional nuclear Overhauser effect spectra, 2D ^{1}H-NOESY, were acquired with 4096 points in the direct dimension (t2) and 256 increments in the indirect dimension (t1) with 8 scans per increment. A spectral window of 5197.505 Hz (12.99 ppm) centered at 2240.84 Hz (5.60 ppm) was identical in both dimensions. The relaxation delay was 5 s long and the mixing times was 50 to 300 ms. The phase were corrected using the 1D spectra obtained through NOESY.

- Rheological properties were characterized using a Bohlin Gemini HR nano rheometer in a stress-controlled mode with a diameter steel parallel plates of 20 mm.

  Three different experiments were performed:

  - Strain sweep test was carried out to determine the linear viscoelastic range (LVR) that was fixed at 0.002.
  - Temperature sweep test were performed under the LVR at constant frequency ω = 1 Hz at 2 °C/min. In a temperature range between 70°C and 20°C.
  - Frequency sweep test were performed under the LVR in the range of 0.1-10 Hz at 70°C.

4.2 Synthesis

4.2.1 Synthesis of CDC

General Procedure

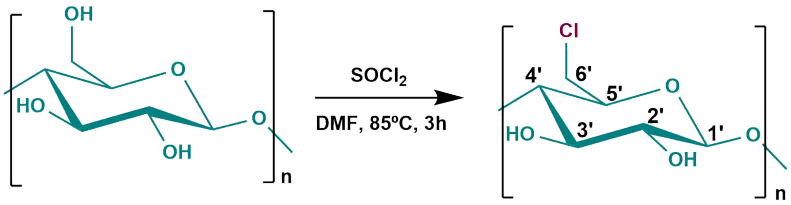

Figure 4.1: 6-chloro-6-deoxycellulose (CDC) synthesis

The CDC was prepared according to procedures described in the literature, figure 4.1. [42] Microcrystalline cellulose Avicel®PH-101 (1g, 6x10^{-3} mol, 1 equiv.) was suspended in DMF (20 mL) and heated to 80 °C under magnetic stirring during 20 minutes. Thionyl chloride (3.5 mL, 4.8x10^{-2} mol, 8 equiv.) was gradually added to the suspension. After the addition was complete, the reaction was continued for 3 h at 85 °C. The viscous solution was cooled to room temperature and poured into ice water (500 mL) with agitation. The precipitated CDC was filtered, washed with dilute ammonium hydroxide and then washed with water to bring the pH to neutral. Finally, CDC was dialyzed for 48 h and lyophilized during 24h. The yield is 94.7%. CP-MAS ^{13}C NMR (75 MHz) δ (ppm): 104.68 (C1'); 85.40 (C4'); 74.46 (C3',2',5'); 45.15 (C6'). IV υmáx (cm^{-1}: 3404 (s, (O-H)); 2884 (sh, (C-H)); 1626 and 1176 (CH-OH); 1314 (C-H, C-O); 1028 (s, (C-O, O-H)); 866 (C-O β glycosidic linkage); 753 and 719 (C-Cl). Appendix figures: A.4 and A.6. EA (%): 4.92 (N); 37.80 (C); 5.89 (H); 1.82 (S).

In the appendix, table A.1 a summary of all the synthesis and corresponding spectra can be found.

4.2.2 Synthesis of cellulose anchored 1-methyl-imidazolium chloride (CellmimCl)

General Procedure

The CellmimCl was prepared according to the literature procedure, figure 4.2. [42] 6-chloro- 6-deoxycellulose (0.5 g) was reacted with *N*-methylimidazole (5 mL) at 95 °C under magnetic stirring for 24 h. The solution was poured into methanol (150 mL) and the precipitate was washed with methanol, then dried in vacuum at 45 °C. Finally, CellmimCl was dialyzed for 48 h and dried again in vacuum at 45 °C. The degree of methylimidazolium substitution is 0.37 determined by elementar analysis [42] and the yield is 92.3%. CP-MAS ^{13}C NMR (75 MHz) δ (ppm): 139.60 (C7'); 128.77 (C8'); 123.37 (C9'); 105.36 (C1'); 86.5 (C4'); 74.65 (C3',2',5'); 49.46 (C6"); 45.49 (C6'); 37.04 (C10'). IV υmáx (cm^{-1}: 3446 (s, (O-H)); 2904 (sh, (C-H)); 1734 (C=O); 1634 and 1112 (CH-OH);

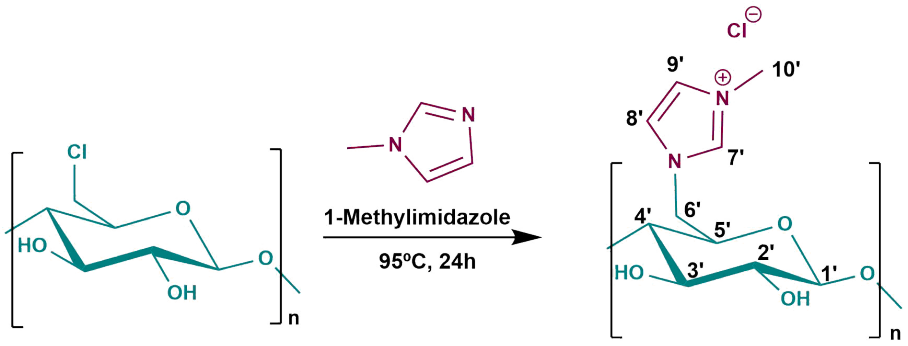

Figure 4.2: Cellulose anchored 1-methyl-imidazolium chloride (CellmimCl) synthesis

1526 (C= N); 1314 (C-H, C-O); 1064 (s, (C-O, O-H)); 866 (C-O β glycosidic linkage); 753 and 719 (C-Cl). Appendix figures: A.5 and A.7.

In the appendix, table A.2 a summary of all the synthesis and corresponding spectra can be found.

4.3 Gelation Studies

The pursue of the gelation of CDC and CellmimCl was attempted through several approaches. Herein, their experimental procedures are presented.

4.3.1 Approach I

In a closed vial Avicel®, CDC or CellmimCl was dissolved in BmimCl and DMSO at different ratios for each sample, tables 4.1, 4.2 and 4.3. After 8 hours at 70°C the mixture each sample was put through heating/cooling cycles (heating the sample to 343 K and cooling down to 298 K), see figure 4.3. Initially the cycles were of 30 minutes (32 cycles) , 1 hour (7 cycles) and 12 hours (3 cycles).

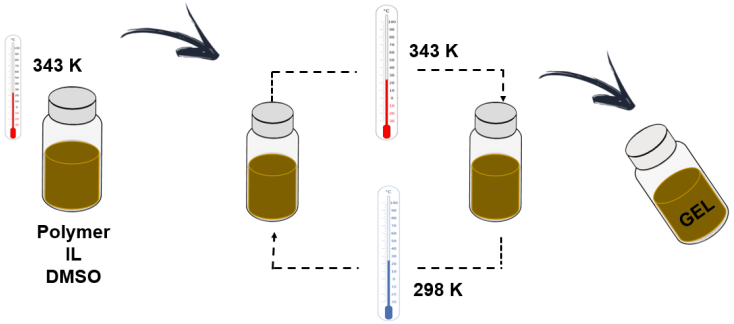

Figure 4.3: Gelation process - heating/cooling cycles.

Table 4.1: Experimental conditions for Cellulose samples used in Approach I. (Solubility: - No soluble; +/- swelling; + Soluble)

ID	Total (g)	Cellulose (mg) - (%)	BmimCl (mg) - (%)	BmimCl/Cellulose ratio	DMSO (mL) - (%)	DMSO/Cellulose ratio	Solubility
D1	1.09	4 (0.37)	60 (5.2)	14	0.95 (94.4)	258	-
D2	1.06	4 (0.38)	140 (12.7)	34	0.85 (86.9)	231	-
D3	1.06	4 (0.38)	240 (23.0)	61	0.75 (76.6)	204	-

Table 4.2: Main experimental conditions for CDC samples used in Approach I. (Solubility: - No soluble; +/- swelling; + Soluble)

ID	Total (g)	CDC (mg) - (%)	BmimCl (mg) - (%)	BmimCl/CDC ratio	DMSO (mL) - (%)	DMSO/CDC ratio	Solubility
E2	1.07	4 (0.37)	250 (23.4)	63	0.75 (76.2)	204	+
E1	1.17	4 (0.34)	250 (20.9)	61	0.85 (78.7)	231	+
H1	1.08	4 (0.37)	100 (9.2)	25	0.90 (90.4)	244	+
H3	1.12	4 (3.57)	50 (4.5)	1	0.95 (92.0)	26	+

Table 4.3: Main experimental conditions for CellmimCl samples used in Approach I. (Solubility: - No soluble; +/- swelling; + Soluble)

ID	Total (g)	CellmimCl (mg) - (%)	BmimCl (mg) - (%)	BmimCl/CellmimCl ratio	DMSO (mL) - (%)	DMSO/CellmimCl ratio	Solubility
F2	1.07	4.7 (0.44)	470 (43.9)	100	0.550 (55.7)	127	-
F3	0.54	4.0 (0.75)	125 (23.4)	31	0.375 (75.9)	102	+
F1	1.09	2.6 (2.40)	250 (23.0)	10	0.750 (74.6)	31	+/-
F4	0.27	4.0 (1.48)	63 (23.2)	16	0.188 (75.3)	51	+/-
PC	1.11	40.0 (3.60)	256 (23.1)	6	0.750 (73.3)	20	+
H4	1.08	40.0 (3.70)	50 (4.6)	1	0.950 (95.4)	26	+

4.3.2 Approach II

CDC (50, 100 and 150 mg) was dissolved in the BmimCl (475, 450 and 425 mg) and DMSO (475, 450 and 425 mg) at 70 °C overnight in a closed vial to obtain solutions with (matrix:IL:DMSO) (p/p) ratios of (5:47.5:47.5), (10:45:45) and (15:42.5:42.5), respectively. CellmimCl was dissolved in the BmimCl/DMSO with (matrix:IL:DMSO) (p/p) ratio of (10:25:65). The solution was kept in an oven at 100°C for 10 min to minimize any heterogeneity in the solution and to remove residual air bubbles. The vial containing the solution was placed under an overturned glass bowl together with a vial with water, coagulation agent, in order to obtain a slow absorption of the latter into the solution. The gelling period was set to 4 days and, in order to prevent any side-effect from light exposure, the system was placed in the dark. Excess ionic liquid was rinsed off with coagulation agent and the gels were bench-dried for 4 days, figure 4.4.

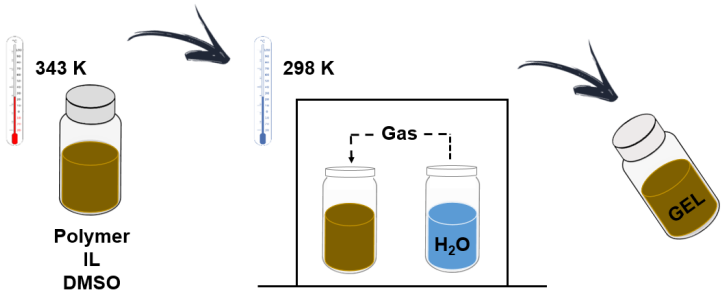

Figure 4.4: Gelation process with coagulation agent.

Table 4.4: Main experimental conditions for all samples used in Approach II. (Solubility: - No soluble; +/- swelling; + Soluble)

ID	Total (g)	Polymer (mg) - (%)	BmimCl (mg) - (%)	BmimCl/Polymer ratio	DMSO (mg) - (%)	DMSO/Polymer ratio	Solubility
A	1.0	0.05 (5)	0.48 (47.5)	10	0.475 (47.5)	10	+
B	1.0	0.10 (10)	0.45 (45.0)	5	0.450 (45.0)	5	+
C	1.0	0.15 (15)	0.43 (42.5)	3	0.425 (42.5)	3	+
CellmimCl	1.0	0.10 (10)	0.25 (25)	3	0.650 (65.0)	7	+

Chapter 5

Cellulose Derivatives Characterization

CDC was obtained from Avicel®chlorination with a similar yield as previously reported in literature.[42] The addition of *N*-methylimidazolium to CDC allowed the production of CellmimCl in 92.3% yield. The results were analyzed by ATR-FTIR, X-ray diffraction, CP-MAS NMR.

5.1 ATR-FTIR

ATR-FTIR measurements were carried out in order to verify whether the desired product was synthesized. Avicel®, CDC and CellmimCl are shown in figure 5.1. From these spectra it is possible to observe the bands characterizing each of the products. The FTIR spectra of all synthesized samples can be found in appendix A.3.

In the Avicel®spectrum the absorption band at 3338 cm^{-1} is attributed to the stretching vibrations of the hydroxyl groups (OH ring and the side chains -CH-OH and CH_2-OH). The stretching and deformation vibrations of C-H group in the glucose unit are shown at 2900 cm^{-1} and 1317 cm^{-1} bands. The absorption bands at 1162 cm^{-1} and 1056 cm^{-1} are assigned to the stretching bands of the CO groups. The absorption band at 894 cm^{-1} is characteristic of β-glycosidic linkage between glucose units. Finally, the band at 1642 cm^{-1} is assigned to the deformation vibration of the hydroxyl groups. All the bands are in agreement with the literature values. [70–72]

Comparing CDC with the Avicel®spectrum, two new absorption bands at 752 cm^{-1} and 722 cm^{-1} were observed in the former. These bands are associated with the stretching vibration of the C-Cl bond. The bands between 1500 cm^{-1} and 1200 cm^{-1} have decreased intensity due to the substitution of the hydroxyl group on C6. [70, 72] In the CellmimCl spectrum it is possible to observe new bands (1564 cm^{-1}, 1110 cm^{-1} and 1062 cm^{-1}) corresponding to the ionic liquid. [42, 73] The absorption band at 3342 cm^{-1} exhibits

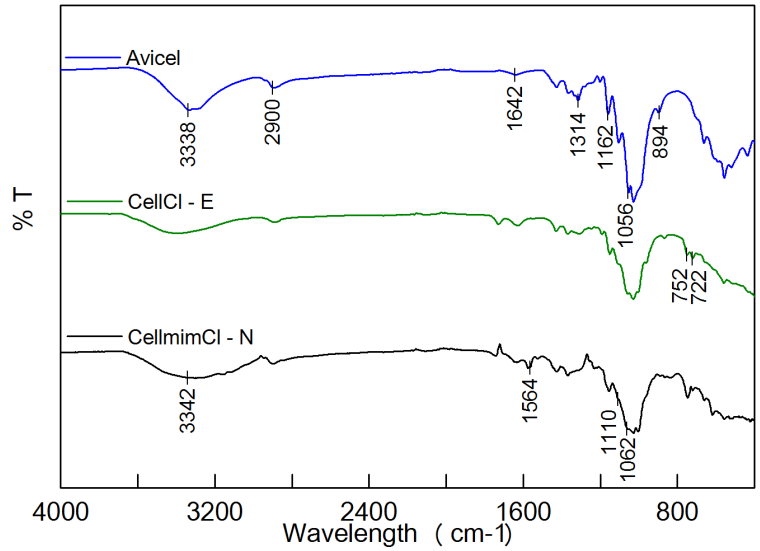

Figure 5.1: FTIR patterns of avicel®, CDC - E and CellmimCl - N.

increased intensity due to the hydrophilic property of the BmimCl.

5.2 X-ray Diffraction

Avicel®, CDC and CellmimCl X-ray diffraction patterns were carried out in order to follow the changes in polymer structure aggregation at the molecular-level, figure 5.2. In Avicel XRD pattern three distinct peaks (101, 002 and 040 planes) can be observed, which are characteristic of microcrystalline cellulose. [72, 74]

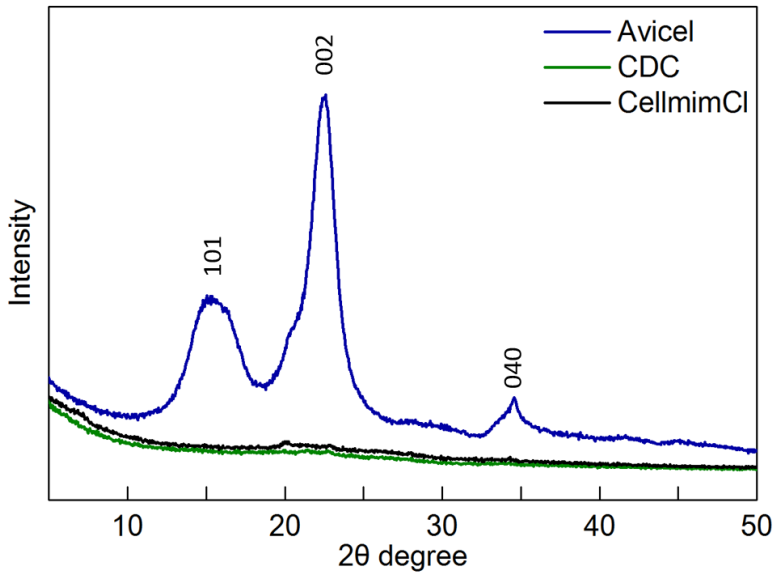

Figure 5.2: X-ray diffraction patterns of Avicel®, CDC and CellmimCl.

Crystallinity is a parameter that determine the availability of hydroxyl groups to interact with other molecules. In crystalline regions the arrangement is more ordered and, consequently the intermolecular interactions with solvents are more difficult. In contrast, in non-crystalline regions these interactions are less intense and the arrangement is not ordered. [72] In CDC and CellmimCl no clear diffraction pattern is identified except for the vestigial peak at $2\theta = 20°$. For that reason no conclusions are extracted from these analysis. However, as reported in the literature it is expected that the incorporation of chloride or the imidazolium within the cellulose backbone could derive to a less crystalline structure.

5.3 CP-MAS

^{13}C CP-MAS spectra of Avicel®, CDC and CellmimCl shown in figure 5.3 were performed to confirm if the synthesis was successful. The Avicel®spectrum exhibits the chemical shifts expected for this polymer. The signal at 106.70 ppm is attributed to C1', bonded to two oxygen atoms. C4' appears at 90.00 ppm, which is connected to only one oxygen atom and is responsible for binding 1,4-β-glucoside bonds. The chemical shifts between 70 and 80 ppm correspond to C2',3',5'. Finally, the signal at 65.60 ppm is assigned to C6' which is a primary carbon connected to -OH and -CH_2 groups.

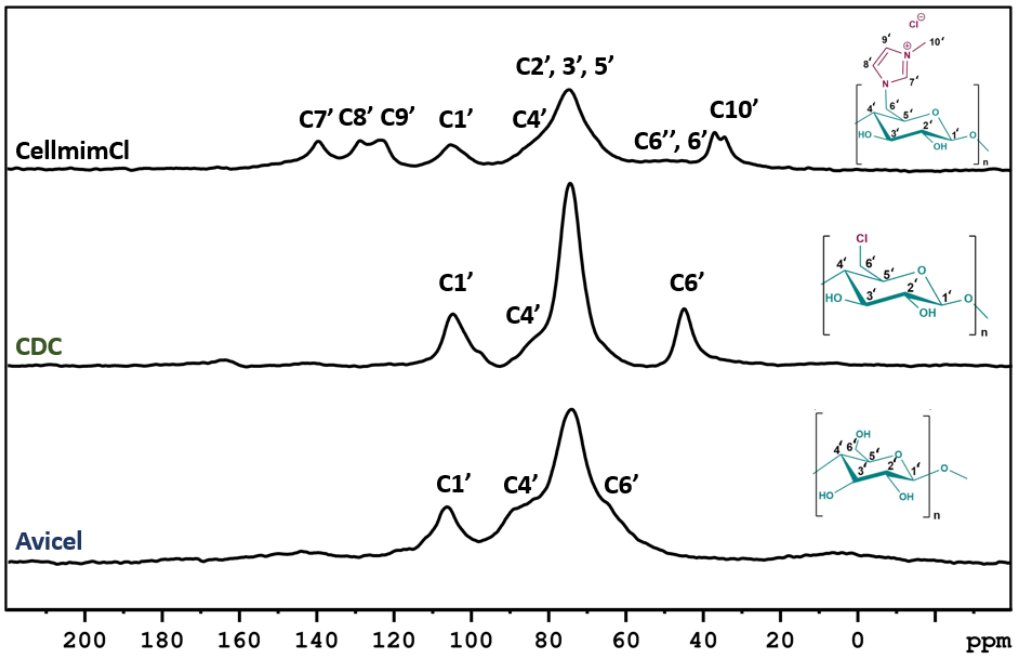

Figure 5.3: CP-MAS ^{13}C-NMR spectra of Avicel®, CDC and CellmimCl.

Comparing CDC with the Avicel®spectrum, the most significant change is the chemical shift of C6' from 65.60 ppm to 45.15 ppm (this synthesis results in a partial substitution of the -OH by chloride at C6' position). Other slight changes occurred, namely the C1' chemical shift changes from 106.70 ppm to 104.68 ppm. Finally, on CellmimCl

synthesis 1-methylimidazolium was covalently bonded to the C6' position, as confirmed by the presence of the signals at 139.60 ppm (C7'), 128.77 ppm (C8'), 123.37 ppm (C9') and 37.04 ppm (C10').These results are in agreement with the values described in the literature. [42, 74].

5.4 TGA

TGA curves of Avicel®, CDC and CellmimCl are shown in figure 5.4. CDC exhibits lower thermal stability than Avicel and CellmimCl has lower thermal stability than both cellulose and CDC. The onset degradation temperature of Avicel is 280°C and shows only one decomposing process from 280 to 400°C with a mass loss of 88% (Appendix, figure A.17) due to pyrolytic degradation of the carbon skeleton. [42] CDC can remain stable until 200°C and has a mass loss of 77% up to 600°C. (Appendix, figure A.18) Two decomposition stage can be seen in CDC. The first stage between 200 and 260°C is caused by the cleavage of C-Cl bond and the condensation of hydroxyl groups on C2 and C3. The second stage from 260 to 360°C corresponds to the depolymerization of cellulose polymeric chain. [42] CellmimCl also presents two stage of decomposition behaviour with a mass loss of 69%. (Appendix, figure A.19) The first mass loss from 100 to 200°C can be interpreted as losing of the immobilized imidazolium group on cellulose backbone together with the condensation of hydroxyl groups of C2 and C3. The second stage from 200°C is correlated with the loss of cellulose fiber. Finally, with the compound derivatization there was a lower degradation temperature. It may be explain by the destroyed crystalline structure and the different chemical structures.

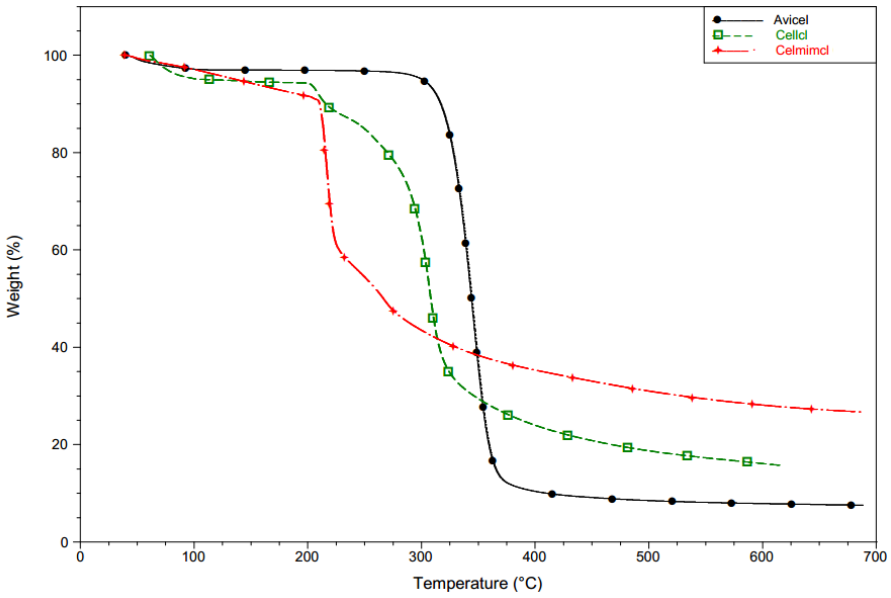

Figure 5.4: TGA curves of Avicel®, CDC and CellmimCl.

Chapter 6

Gelation Studies

One of the main targets of this work is the investigation of a gelation process for new cellulose derivatives. The solvent system that emerged from the literature review (sections 2.2 and 2.6) - BmimCl and DMSO was chosen for the dissolution/gelation studies of cellulose and cellulose derivatives obtained in this work. A dissolution study will now be discussed in this chapter.

6.1 Early studies on gelation of cellulose and cellulose derivatives

One of the main issues with cellulose is its solubility problems that affect the processing and further applications. Aiming to solve this problem the strategy that we followed consisted of the cellulose derivatization with ionic liquids and the study of solvents' behavior and their respective relevance in order to achieve the gelation of cellulose derivates.

In a first stage we studied a variation of conditions (composition of the solvents system and polymer matrix ratio) in order to obtain the suitable composition towards the gel obtainment. This study was performed for Avicel®, CDC and CellmimCl and the corresponding results are presented in table 6.1.

Avicel®

Avicel®samples were prepared using a fixed polymer weight of 4 milligrams (mg) and different solvent ratios. This mixtures were submitted to heating/cooling cycles, see section 4.3.1, to induce the gelation. The results of this procedure is presented in table 6.1.

Table 6.1: Experimental conditions for Cellulose, CDC and CellmimCl samples used in Approach I. Cellulose: D1-D3; CDC: E2-H3; CellmimCl: F2-H4. (Solubility: - No soluble; +/- swelling; + Soluble)

ID	Total (g)	Polymer (mg) - (%)	BmimCl (mg) - (%)	BmimCl/Polymer ratio	DMSO (mL) - (%)	DMSO/Polymer ratio	Solubility
D1	1.09	4 (0.37)	60 (5.2)	14	0.95 (94.4)	258	-
D2	1.06	4 (0.38)	140 (12.7)	34	0.85 (86.9)	231	-
D3	1.06	4 (0.38)	240 (23.0)	61	0.75 (76.6)	204	-
E2	1.07	4 (0.37)	250 (23.4)	63	0.75 (76.2)	204	+
E1	1.17	4 (0.34)	250 (20.9)	61	0.85 (78.7)	231	+
H1	1.08	4 (0.37)	100 (9.2)	25	0.90 (90.4)	244	+
H3	1.12	4 (3.57)	50 (4.5)	1	0.95 (92.0)	26	+
F2	1.07	4.7 (0.44)	470 (43.9)	100	0.550 (55.7)	127	-
F3	0.54	4.0 (0.75)	125 (23.4)	31	0.375 (75.9)	102	+
F1	1.09	2.6 (2.40)	250 (23.0)	10	0.750 (74.6)	31	+/-
F4	0.27	4.0 (1.48)	63 (23.2)	16	0.188 (75.3)	51	+/-
PC	1.11	40.0 (3.60)	256 (23.1)	6	0.750 (73.3)	20	+
H4	1.08	40.0 (3.52)	50 (4.4)	1	0.950 (92.1)	26	+

Several studies have been carried out about BmimCl/DMSO system and the effect on cellulose dissolution. [75–77] From those studies was suggest that the increased cellulose solubility resulted from the preferential solvation of the cation by the aprotic polar solvent which leaves the anion more free to engage in cellulose interactions. Our results did not show polymer solubilization in this range of concentrations (5-23%) which is a clear indication of the need for a higher amount of BmimCl to accomplish the dissolution.

CDC

With the substitution of a hydroxyl group in the C6 position of cellulose for a chloride, some inter- and intra-molecular hydrogen bonds are affected, figure 6.1, which is expected to decrease the crystallinity of the polymer. As such it should be easier to dissolve the resulting polymer.

From table 6.1 is possible to confirm that all BmimCl/DMSO binary mixtures (E and H samples) were able to dissolve CDC. With increasing concentration of DMSO there is a decreased ability to dissolve the CDC. In every case, the polymer is dissolved but the samples with the highest DMSO concentration the dissolution process takes longer. Sample H3 is fairly viscous and therefore was studied through NMR technique in order to study the solvents-polymer interactions and verify whether or not a gel was present.

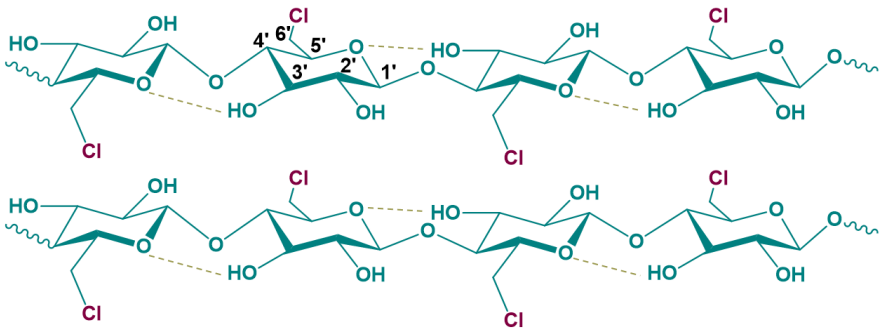

Figure 6.1: Molecular structure of CDC illustrating the intermolecular and intra-molecular hydrogen bonds.

CellmimCl

This system is slightly more complex than the previous one, figure 6.2. The imidazolium cation grafted in the cellulose backbone is expected to further decrease the crystallinity of the polymer and to enable additional interactions namely ionic interactions.

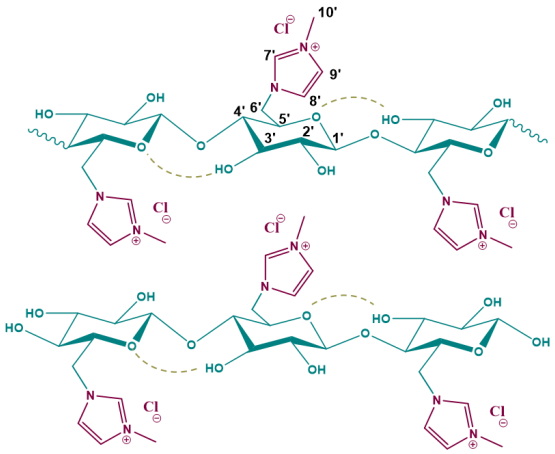

Figure 6.2: Molecular structure of CellmimCl illustrating the intra-molecular hydrogen bonds.

From table 6.1 is possible to observe that in sample F3 there is polymer dissolution, in F1 and F4 there is the formation of swollen aggregates and sample F2 does not appear to have any dissolution. The behavior of sample F3 can be explained by the lower polymer amount in relation to the remaining samples. F1 and F4 suggest that the IL concentration of 23% is close to the minimum concentration necessary to achieve polymer dissolution. Regarding sample F2 where no polymer dissolution is observed, the result is probably related to the amount of DMSO in the system, in sample F2 the solvation of IL might not be as effective as in sample F3. In sample H4 only a slight dissolution occurs, indicating that the IL concentration below 23% does not dissolve the polymer. Also, it is observed that with a DMSO concentration above 95% there is no polymer dissolution. A DMSO

concentration of 75% promotes an effective dissolution process.

Summary

In summary, the exchange of the polymer's hydroxyl group in position C6 by chloride and imidazolium cation could allows a reduction in the amount of IL that could be necessary to dissolve the polymer when compared with cellulose.[75, 76, 78] These results can be related to the decrease of crystallinity in these cellulose derivatives that allows a easier solvent interaction and a new favorable ionic interactions. Besides it was determined the most suitable solvent ratios that could give rise to polymer gelation. In the case of CDC 50:50 (BmimCl/DMSO) was found to be the adequate ratio whereas for CellmimCl this ratio was of 27:73 (BmimCl/DMSO).

In order to gain a deeper insight into the dissolution phenomena sample H3 was selected to perform NMR experiments since it was consider the most suitable in terms of composition and closest to the intended gel state.

6.1.1 Dissolution study - Sample H3

NMR measurements

The dissolution phenomena of the CDC/BmimCl/DMSO-d_6 system was studied using the NMR technique ^{1}H-NMR spectra (figure 6.3) ^{1}H,^{1}H-NOESY, ^{1}H-DOSY and ^{13}C- T_1 and ^{1}H-T_2 relaxation.

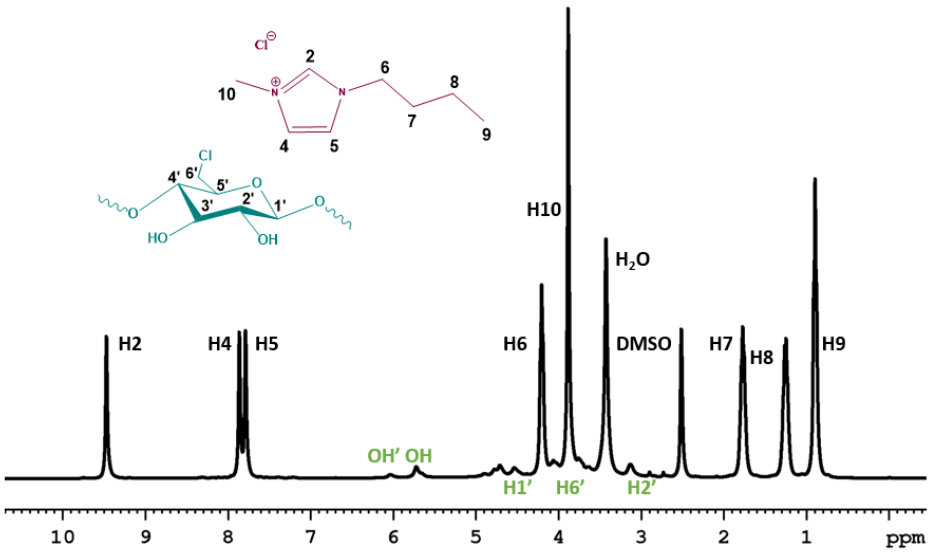

Figure 6.3: Sample H3 - ^{1}H-NMR spectra of CDC/BmimCl/DMSO-d_6 system at 298 K.

^{1}H - VT-NMR

In the ^{1}H-NMR spectrum is possible to identify the imidazolium cation, DMSO and water protons. Also is possible to observe cellulose broaden proton signals.

In order to understand the solvents interactions a variable temperature analysis was studied with the aim of observing the chemical shift deviations with Variable Temperature NMR (VT-NMR). Depending on the interactions during this process, some chemical shifts are shielded and others are deshielded, figure 6.4.

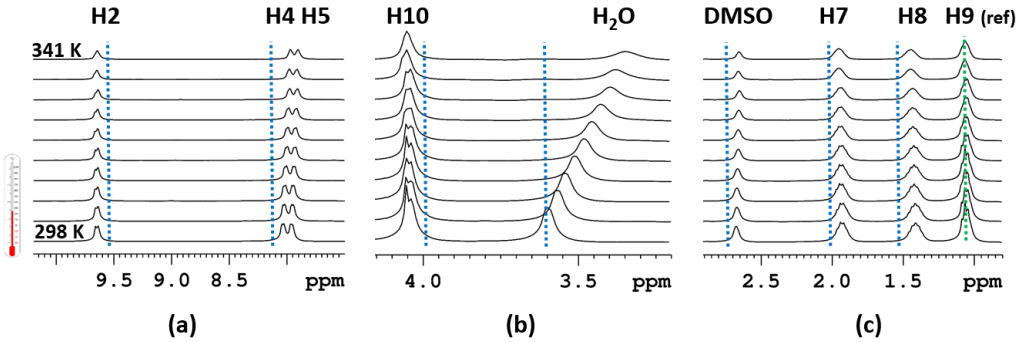

Figure 6.4: ^{1}H-NMR spectra of CDC gel with temperature gradient - local changes in the IL polar domain region H2,4,5 (a); in IL H10 and H_2O (b); DMSO and IL H7,8,9 (c).

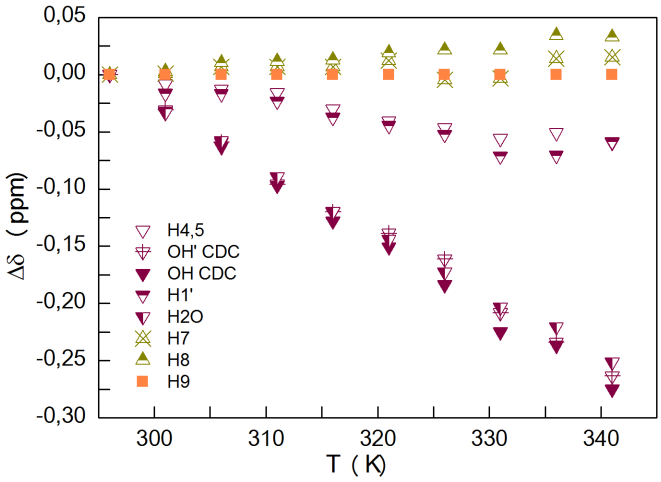

Figure 6.5: Relevant chemical shift deviations with gradient temperature.

In figure 6.5 a pictorial view of the chemical shift deviations is depicted (Table and graphic of all protons are in appendix A.5 and A.21, respectively.). When sample H3 is heated it is possible to see that water changes its local environment in a more drastic way compared to the rest of the nuclei. H4 and H5 also have a slight deviation which probably means that IL cation is more efficiently solvated with DMSO. H7 and H8 are the protons that are less affected. These results point to a relevance of the cation in the dissolution process. Water has the same $\Delta\delta$ range as CDC OH', OH. For this reason, they are probably influenced by the same rearrangement of the hydrogen bond system.

^{1}H - DOSY

The diffusion coefficients for sample H3 allow the observation of different diffusional regimes within the analyzed mixture, table 6.2.

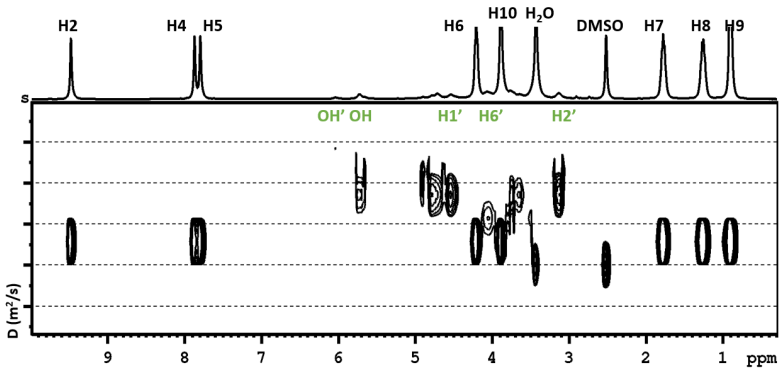

Figure 6.6: Sample H3 - ^{1}H – DOSY CDC/BmimCl/DMSO-d_6 system at 293 K.

Table 6.2: Sample H3 - ^{1}H Diffusion Coefficients at 293 K.

	δ (ppm)	Diffusion Coeff. x 10^{-10} (m^2/s)
H2	9,64	2.308±0.001
H4,5	7,99	2.304±0.003
OH CDC	6,20	**0.110±0.025**
H1 CDC	4,88	**0.219±0.153**
H6	4,37	2.183±0.032
H10	4,05	2.352±0.005
		0.164±0.066
H_2O	3,60	6.000±0.033
		0.178±0.074
DMSO	2,68	4.596±0.038
H7	1,94	2.307±0.001
H8	1,41	2.296±0.002
H9	1,07	2.303±0.002

The results show two distinct diffusional regimes (figure 6.6) - a faster regime which corresponds to IL, water and DMSO protons and a slower regime that corresponds to CDC protons. This difference is justified by their respective dimensions.

An important finding is that H10 IL and water exhibit a bi-exponential behavior, i.e., each nuclei's populations are distributed in two different regimes. A faster regime, which is the free molecule, with higher mobility and a slower regime in the same order of magnitude as CDC protons. Thus, this is evidence of the interaction between the polymer

with IL and water in the dissolution process at 293 K, figure 6.6.

^{13}C - T_1 Relaxation

The longitudinal relaxation times T_1 can be used to establish a correlation between the system rigidity and the molecular tumbling rate with the temperature gradient. The results, figure 6.3 suggest that C10 denotes a change between 310 K and 320 K probably associated to a conformational change, figure 6.7.

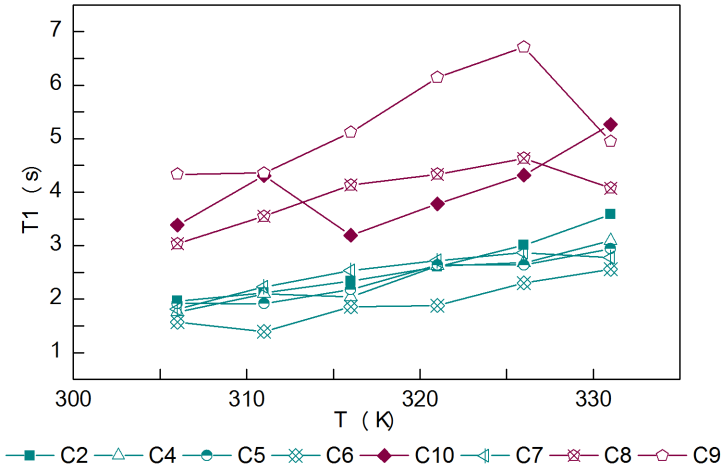

Figure 6.7: Sample H3 - ^{13}C T_1 relaxation with increasing temperature.

Table 6.3: Sample H3 - T_1 values with gradient temperature.

	T_1 (s)							
T(K)	**C2**	**C4**	**C5**	**C6**	**C10**	**C7**	**C8**	**C9**
306	1.96±0.06	1.76±0.07	1.92±0.05	1.57±0.08	3.39±0.40	1.81±0.06	3.04±0.10	4.34±0.44
311	2.12±0.10	2.10±0.11	1.92±0.05	1.40±0.07	4.31±0.26	2.23±0.08	3.55±0.23	4.36±0.31
316	2.34±0.24	2.04±0.12	2.18±0.15	1.86±0.12	3.19±0.28	2.53±0.16	4.13±0.18	5.12±0.53
321	2.61±0.22	2.62±0.19	2.64±0.19	1.88±0.14	3.78±0.39	2.72±0.31	4.34±0.34	6.14±1.00
326	3.01±0.31	2.68±0.24	2.64±0.18	2.30±0.18	4.32±0.58	2.87±0.22	4.63±0.48	6.71±0.90
331	3.59±0.44	3.10±0.19	2.94±0.22	2.56±0.13	5.27±0.69	2.78±0.20	4.08±0.57	4.95±0.67

C8 and C9 also present a pronounced change however being a part of the end of the aliphatic chain a higher mobility with the temperature increase is expected.

^{1}H - T_2 Relaxation

The transverse relaxation time T_2 can be correlated with molecular motion. When measurements are made with a temperature gradient the variation of the mobility of each nuclei enable understanding changes on T_2 relaxation. Increasing temperature results in a decreasing viscosity and increasing of the solvents and polymer degrees of freedom. The results of our measurements, figure 6.8 and table 6.4, suggest that at 321 K the system

decreased its T_2 value, which means above 313 K and below 328 K probably occurs some conformational changes.

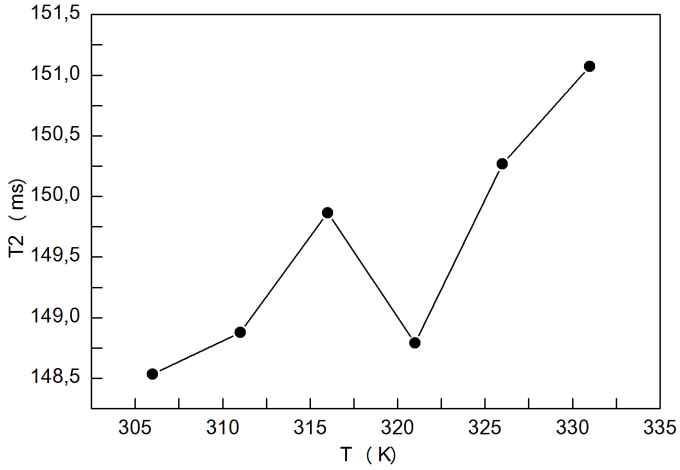

Figure 6.8: Samples H3 - ^{1}H T_2 Relaxation values with increasing temperature.

Table 6.4: Sample H3 - ^{1}H T_2 Relaxation values with gradient temperature.

T (K)	**T_2 (ms)**
306	148.53±0.35
311	148.88±0.37
316	149.87±0.34
321	148.79±0.32
326	150.27±0.34
331	151.07±0.26

Looking at each nuclei, graphic 6.9 and table 6.5, there are changes in relaxation trend with increasing temperature. Between 308 K and 313 K H10 and OH CDC are affected by conformational changes in this range of temperature.

Table 6.5: Sample H3 - T_2^* values with gradient temperature.

	T_2^* (ms)									
T (K)	**H2**	**H4,5**	**OH CDC**	**H6**	**H10**	**H_2O**	**DMSO**	**H7**	**H8**	**H9**
306	14,94	7.51	6.02	11.75	15.45	13.17	14.47	9.74	9.22	11.88
311	15.67	7.72	4.81	12.21	17.76	13.29	15.00	9.91	9.62	12.08
316	15.25	7.61	6.84	12.48	16.42	12.72	15.13	9.97	9.81	11.75
321	15.95	7.76	7.76	12.85	15.78	12.38	14.66	10.29	9.32	12.13
326	15.57	7.66	6.24	12.47	15.56	12.15	14.83	10.16	9.34	12.05
331	15.87	7.70	5.27	12.24	16.38	12.50	15.67	10.11	9.93	12.00

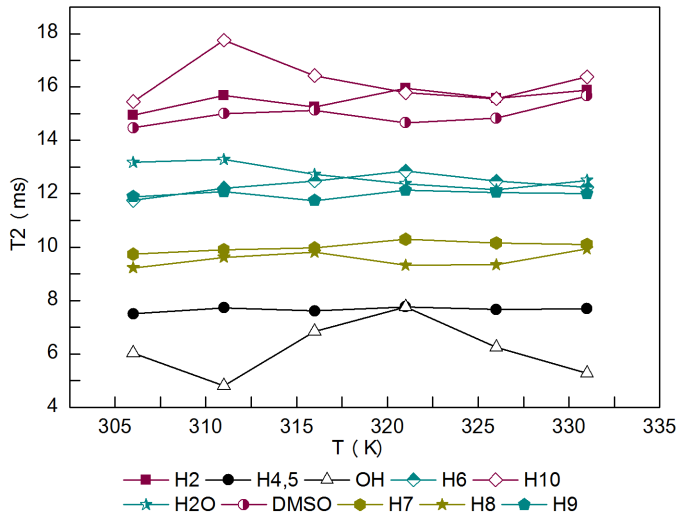

Figure 6.9: Sample H3 - ^{1}H T_2* relaxation values with increasing temperature.

^{1}H, ^{1}H - NOESY

The ^{1}H, ^{1}H– NOESY spectrum (300 ms mixing time) presented in figure 6.10 allows the observation of the correlations between the CDC protons, IL, DMSO and water species.

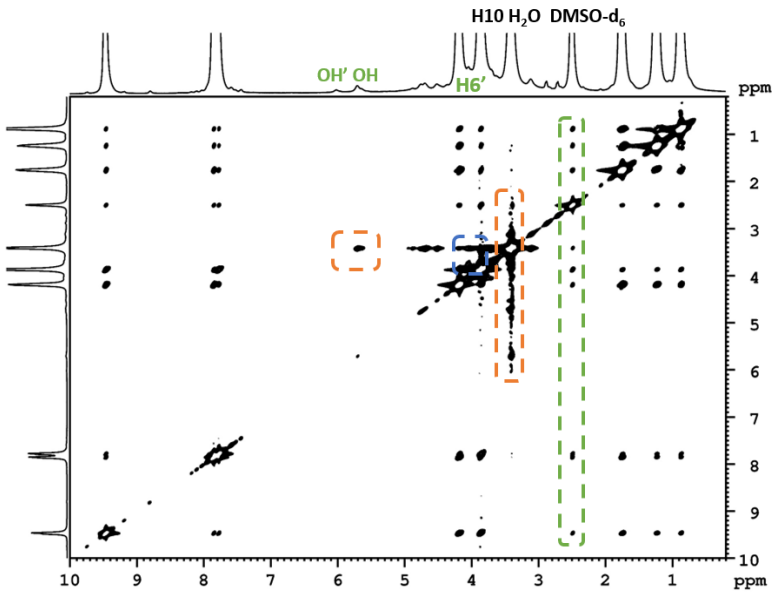

Figure 6.10: ^{1}H, ^{1}H– NOESY CDC/BmimCl/DMSO-d_6 system at 293 K.

At 293 K besides the usual cation-cation interactions it is possible to observe three main correlations - the H6' from CDC has a correlation with H10 from the IL and water; OH, H1' and H2' from CDC show correlation with water; and DMSO shows spatial proximity with all IL nuclei and water, figure 6.11. These correlations are indicative of the spatial proximity between BmimCl, DMSO and the polymer.

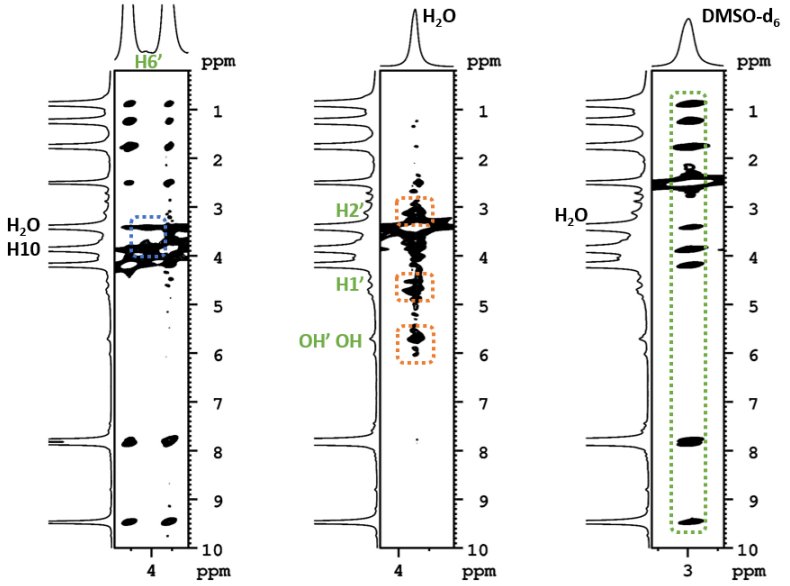

Figure 6.11: Expansions of ^{1}H, ^{1}H– NOESY CDC/BmimCl/DMSO-d_6 system at 293 K.

Summarizing all NMR experiments is possible to conclude that i) IL cation establishes interactions with CDC through the polar IL domain; ii) between 308 K and 320 K the system undergoes conformational changes that could be the starting point of the solution/gelation phenomena. iii) From the diffusion experiments it is possible to observe some degree of association between the polymer and the IL's cation. iv) From NOE experiments the IL's cation exhibits interactions with part of the polymer.

The results described suggest a hypothetical network system for sample H3, figure 6.12 in which the material is ordered into aggregates in the solvent mixtures and at structural level water interacts with the hydroxyl groups and H6' of the polymer and the IL polar domain region interacts with polymer H1' and H6'.

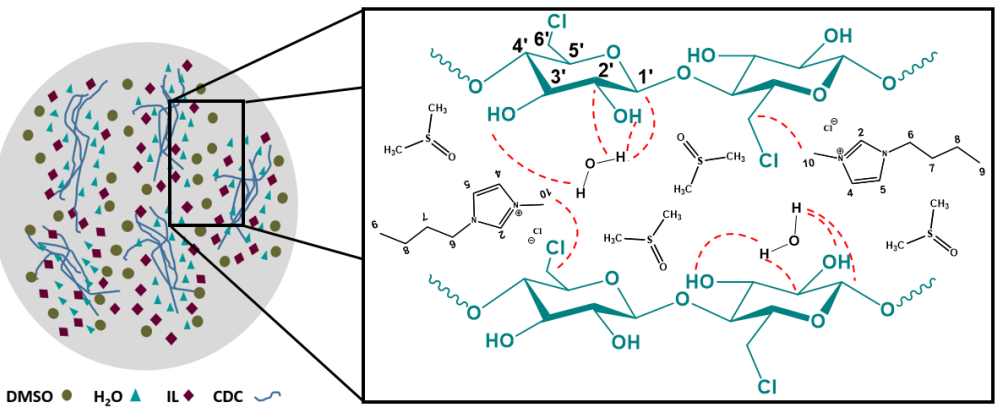

Figure 6.12: Pictorial representation of the hypothetical network system of sample H3.

From these set of NMR experiments it is not possible to arrived a conclusion regarding to a plausible gel-like behavior however, it is possible to extract relevant information from

these distinct pattern of interactions. The IL and water are establishing interactions with the polymer. A complete polymer dissolution is necessary step prior the gelation and as such a two step approach was followed from here on (approach II of the section 4.3.2).

6.2 Gelation studies on cellulose derivatives

The second approach studied in this dissertation will now be discussed. The gelation process was followed for three CDC samples and a CellmimCl sample, table 6.6, and in all presented studies were analyzed the cooled process from 343 K to 298 K.

Table 6.6: Amounts of Polymer, BmimCl and DMSO in each sample studied.

	CDC			CellmimCl
	A	**B**	**C**	**D**
Polymer (%)	5.0	10.0	15.0	10.0
BmimCl (%)	47.5	45.0	42.5	25.0
DMSO (%)	47.5	45.0	42.5	65.0

Here in, in CDC samples three different polymer loadings were used, 5%, 10% and 15%. The objective of this study is to discuss the influence of the polymer amount in the gel stiffness and the solvents dynamic in gelation process with increasing polymer.

CDC/BmimCl/DMSO-d_6 and CellmimCl/BmimCl/ DMSO-d_6 systems after their characterization (figures 6.3 and 6.13) were studied through NMR techniques, such as ^{1}H -VT-NMR, ^{13}C - T_1 and ^{1}H - T_2 relaxation times, ^{1}H-DOSY and ^{1}H,^{1}H-NOESY. Rheology measurements were also made in order to confirm the matter physical state.

NMR measurements

^{1}H -VT-NMR

As explained above, the chemical shifts of protons are essentially influenced by the chemical groups locations and interactions between them. With this in mind, our focus is in chemical shift deviations between liquid-like (343K) and gel-like behavior (298K), table 6.7. The change of physical state can may cause the chemical shifts change to up or downfield.

Interpreting the figure 6.14(a) (table is in appendix A.7) it is possible to observe that samples A and B exhibit a similar trend. Particularly, H2 changes its local environment to upfield and DMSO to downfield. Sample B doubled the polymer amount however when compared with sample A the chemical shift deviations have the same behavior. These results probably means that the nuclei in both samples were influenced by the same local environment and in these conditions range there are no dynamic changes in the system. Sample C shows a significant pattern change, figure 6.14(b), H2's changes is downfield

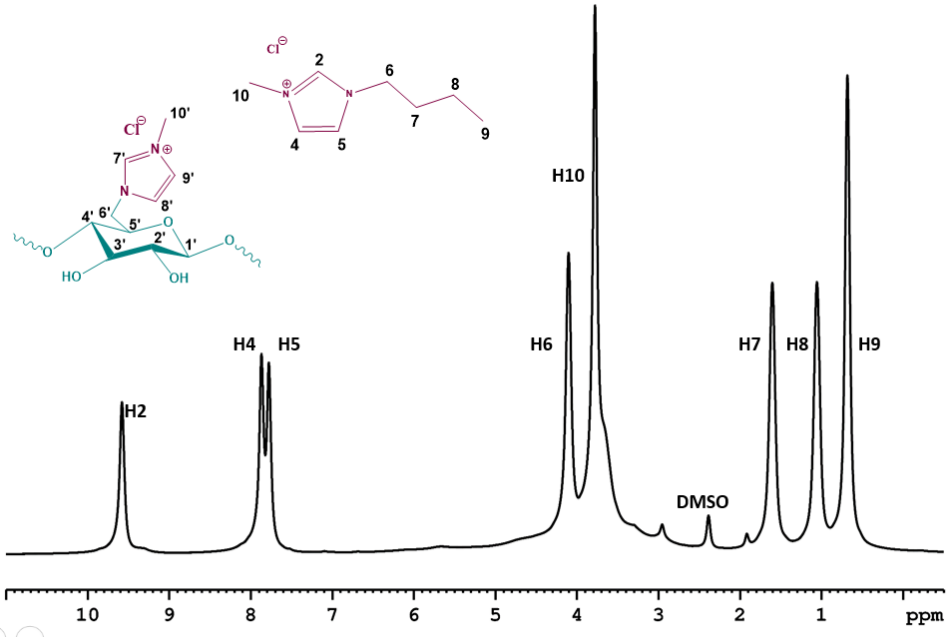

Figure 6.13: ^{1}H-NMR spectra of CellmimCl/BmimCl/DMSO-d_6 system at 298 K.

Table 6.7: ^{1}H-NMR chemical shifts of CDC samples at 298K.

	298 K			343 K		
	A	B	C	A	B	C
H2	9.763	9.635	9.680	9.882	9.800	9.671
H4	8.074	7.965	7.969	8.057	7.960	7.913
H5	7.966	7.867	7.871	7.958	7.870	7.831
H_2O	4.622	-	-	-	-	4.853
H6	4.235	4.184	4.175	4.219	4.170	4.178
H10	3.914	3.859	3.851	3.899	3.850	3.864
DMSO	2.511	2.465	2.451	2.458	2.412	2.443
H7	1.665	1.649	1.637	1.672	1.649	1.660
H8	1.084	1.080	1.080	1.110	1.091	1.104
H9	0.682	0.682	0.682	0.682	0.682	0.682

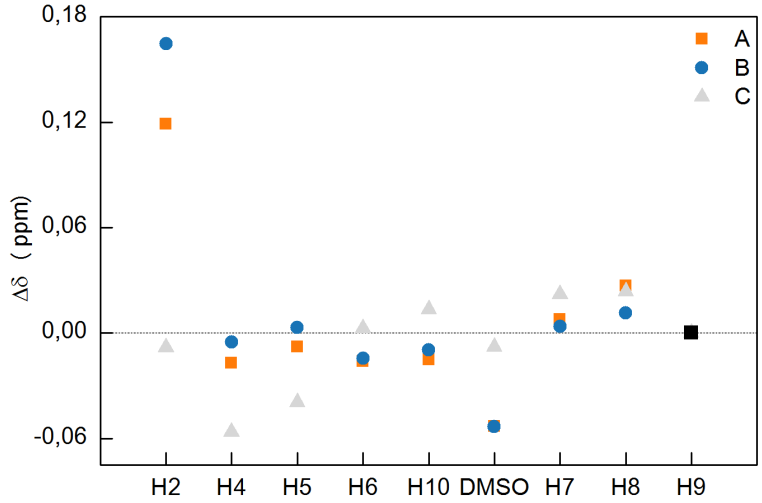

(a) Sample A and B have the same pattern.

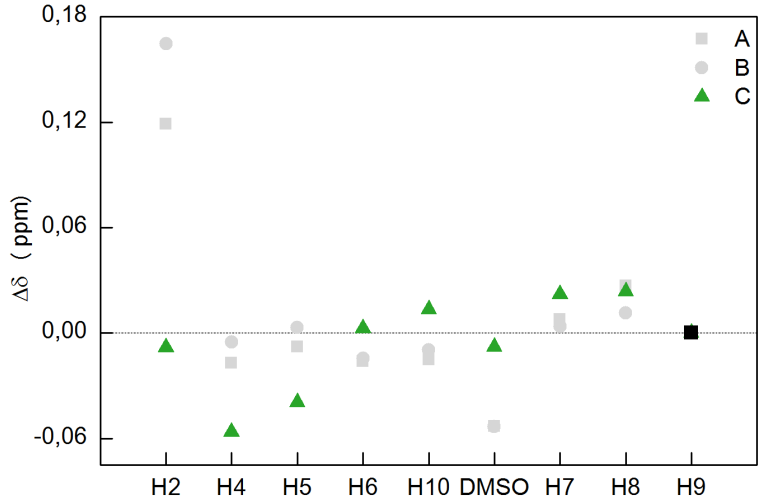

(b) Sample C have a different pattern.

Figure 6.14: CDC samples - Chemical shift deviations ($\delta_{343\,\mathrm{K}} - \delta_{298\,\mathrm{K}}$) — ■ is the reference point.

shifted which can be related with the ionic liquid pair (cation-anion) interactions changes at this polymer concentration.

In BmimCl, chloride anion mainly governs the cellulose dissolution through the polymer hydrogen bonds disruption [79, 80] and therefore, the cation-anion interactions can change. This being said in samples A and B the anion interactions with the polymer network decreases the ionic interactions between cation and anion. This means that the cation establish interactions with the anion but probably suffers from constraints due to macromolecular organization of the polymer. On the other hand, in sample C where there is increased polymer amount, the cation exhibits an opposite trend.Here the polymer must be in a different type of organization, more constrained, where the structure does not need the ILs ions to be stabilized, and therefore we only observe minor changes in the cation's chemical shifts. Based on these observations, from 5-10% polymer, figure 6.14(a), the local organization and ions interactions reflect a similar arrangement while the 15%, figure 6.14(b), loading the polymer as a different behavior.

^{13}C - T_1 Relaxation

^{13}C - T_1 relaxation time can be correlated with nuclei's mobility. At 298 K samples A/B/C have a very similar pattern of relaxation times, figure 6.15, except for the methyl groups C9 and C10, where slight changes can be detected. This could be an indication that all of these samples are in a similar physical state at this temperature.

Analyzing the changes in ^{13}C - T_1 relaxation of each nuclei with the temperature change, it is possible to observe that in samples A and B, methyl group C10 present the most pronounced change. However this is not observed for sample C, this nuclei exhibit only a slight change, table 6.8, probably this is indicative that at 343 K the system is very constraint and the local mobility of the cation is not as influenced by temperature as in the previous samples. The imidazolium cation in CellmimCl sample presents a very similar relaxation profile to the CDC however the absence of data in a different temperature prevents further conclusions to be drawn.

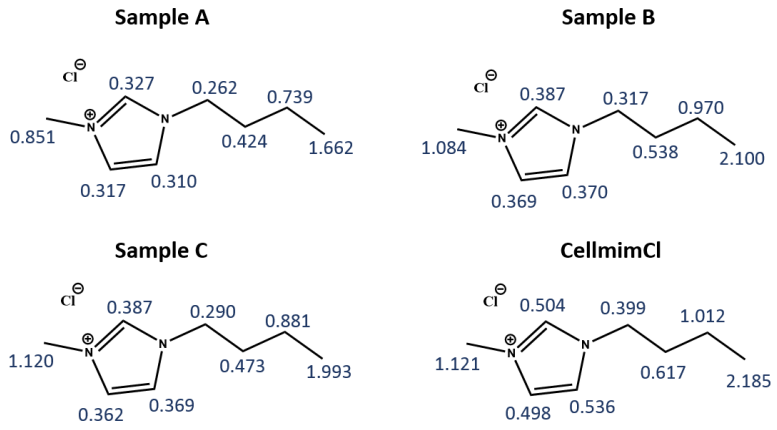

Figure 6.15: Deviations of T_1 relaxation times of CDC and CellmimCl samples at 298 K.

Table 6.8: CDC and CellmimCl samples - ^{13}C - T_1 relaxation time (seconds) at 298 K and 343 K.

	CDC						CellmimCl
	A		B		C		D
	298 K	343 K	298 K	343 K	298 K	343 K	298 K
C2	0.327±0.003	1.139±0.007	0.387±0.003	1.302±0.009	0.387±0.003	0.751±0.007	0.504±0.009
C4	0.317±0.002	1.103±0.008	0.369±0.003	1.262±0.011	0.362±0.004	0.749±0.003	0.498±0.008
C5	0.310±0.001	1.109±0.006	0.370±0.003	1.266±0.006	0.369±0.005	0.766±0.009	0.536±0.012
C6	0.262±0.006	0.966±0.007	0.317±0.005	1.119±0.007	0.290±0.012	0.646±0.012	0.399±0.026
C10	0.851±0.027	2.646±0.081	1.084±0.040	3.011±0.082	1.120±0.042	1.679±0.034	1.121±0.043
C7	0.424±0.008	1.675±0.006	0.538±0.007	1.823±0.012	0.473±0.012	1.131±0.013	0.617±0.030
C8	0.739±0.007	2.882±0.013	0.970±0.006	3.129±0.022	0.881±0.006	1.901±0.016	1.012±0.047
C9	1.662±0.021	5.259±0.033	2.100±0.011	5.587±0.038	1.993±0.018	3.451±0.036	2.185±0.035

^{1}H - T_2 Relaxation

The transverse relaxation time can be correlated with molecular motion and therefore, with the system rigidity. Looking at table 6.9 we can observe that all samples decreased its ^{1}H - T_2 values from 343 K to 298 K, i.e., the molecules' mobility decreases. Thus, at 298 K all system show gel-like behavior.

Sample C presents the smallest ^{1}H - T_2 difference between 343 K and 298 K among all samples, figure 6.16, which means that probably at 343 K this system presents a gel-like behavior (this is in agreement with ^{13}C - T_1 relaxation time results).

Sample B has the highest ^{1}H - T_2 value at 298 K therefore, possible exchange effect or system viscosity may be affecting the measurements.

Table 6.9: CDC and CellmimCl samples - ^{1}H - T_2 Relaxation times at 298 K and 343 K.

	T_2 (ms)	
	298 K	**343 K**
A	160.152±0.112	500.336±0.185
B	267.484±0.092	399.718±0.314
C	129.469±0.112	220.954±0.146
CellmimCl	124.825±0.164	-

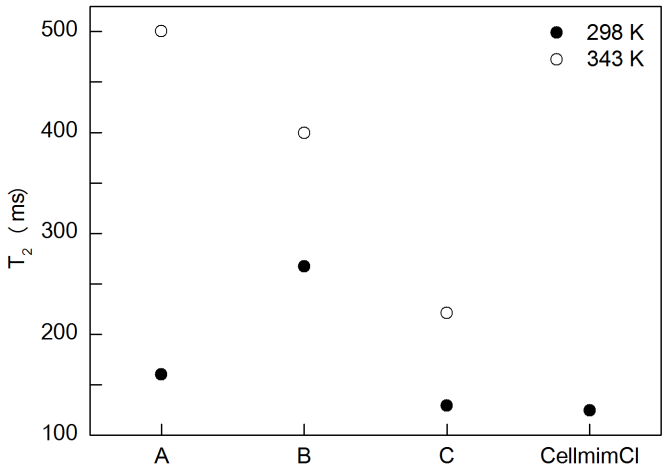

Figure 6.16: ^{1}H - T_2 Relaxation times of all samples at 298 K and 343 K.

^{1}H - DOSY

The determination of the diffusion coefficients in a sample with polymer and ions and solvents allows us to observe possible associations between them (the effective decay of H2 for sample B of CDC is in Appendix A.10 and A.22). Looking at table table 6.10 to 6.13, it is possible to observe that sample B exhibits diffusion coefficients one order of magnitude below than samples A and C, which can be a reflection of the viscosity, and the local interactions. This can be explained, with a more effective association of the ILs cation with the polymer for sample B. In samples A and C some of the ILs cation nuclei exhibit a bi-exponential behavior, meaning that part of the cations population is associated with the polymer and the rest is flowing more freely in the solution. In sample A there is a lesser amount of polymer and because of that less cations are in fact associated with the matrix. From A to B an increased amount of polymer means that probably more cations are establishing interactions within the polymer, in sample C which has even more polymer the dual behavior detected can be a reflection of a decreased association of the cation with the matrix when compared to sample B. The IL population in excess (that does not participate in hydrogen bonds disruption) diffuses quickly. Regarding CellmimCl sample, all nuclei present mono-exponential diffusion except DMSO nucleus. This nucleus is responsible for solvating BmimCl, thus these results show the populations that is solvating and the one that is not.

Table 6.10: CDC - Sample A (x 10^{-11}).

	δ (ppm)	Diffusion Coeff. x 10^{-11} (m^2/s)
H2	9.76	0.204±0.002
H4,5	8.02	0.197±0.001
H6	4.24	0.771±0.111
		-
H10	3.91	0.183±0.005
DMSO	2.51	1.912±0.186
		0.194±0.005
H7	1.67	3.207±0.272
		0.199±0.002
H8	1.08	3.212±0.273
		0.208±0.002
H9	0.68	0.184±0.003

Table 6.11: CDC - Sample B (x 10^{-13}).

	δ (ppm)	Diffusion Coeff. x 10^{-13} (m^2/s)
H2	9.64	1.662±0.014
H4,5	7.92	1.683±0.013
H6	4.18	7.655±1.099
		1.581±0.022
H10	3.86	1.598±0.011
DMSO	2.47	4.988±0.739
		1.479±0.058
H7	1.65	6.882±0.895
		1.539±0.020
H8	1.08	6.882±0.950
		1.539±0.020
H9	0.68	1.577±0.010

Table 6.12: CDC - Sample C (x 10^{-11}).

	δ (ppm)	Diffusion Coeff. x 10^{-11} (m^2/s)
H2	9.68	0.228±0.005
H4,5	7.92	0.224±0.004
H6	4.18	4.110±0.392
		0.241±0.003
H10	3.85	0.212±0.001
DMSO	2.45	1.964±0.358
		0.269±0.024
H7	1.64	3.605±0.640
		0.225±0.002
H8	1.08	3.491±0.498
		0.235±0.003
H9	0.68	0.201±0.004

Table 6.13: CellmimCl - (x 10^{-12}).

	δ (ppm)	Diffusion Coeff. x 10^{-12} (m^2/s)
H2	9.579	4.341±0.029
H4,5	7.823	4.218±0.032
H6	4.103	4.496±0.031
		-
H10	3.778	4.103±0.038
DMSO	2.386	9.584±0.297
		3.038±0.224
H7	1.603	4.292±0.031
		-
H8	1.055	4.240±0.035
		-
H9	0.682	4.019±0.037

^{1}H, ^{1}H - NOESY

Herein will be presented the spatial correlations by ^{1}H, ^{1}H– NOESY experiment in all samples considered. In all spectra all the ILs cation protons show correlation with every other cation nucleus.

The ^{1}H, ^{1}H– NOESY spectrum (150 ms mixing time) presented in figure 6.17 allows the observation of the correlations between CDC protons, IL, DMSO and water species. At 298 K this spectrum shows three main correlations - IL protons and H2' from CDC have correlations with water; H6' from CDC has correlations with H10 IL proton; and DMSO shows spatial proximity with H7 IL proton and water, figure 6.18.

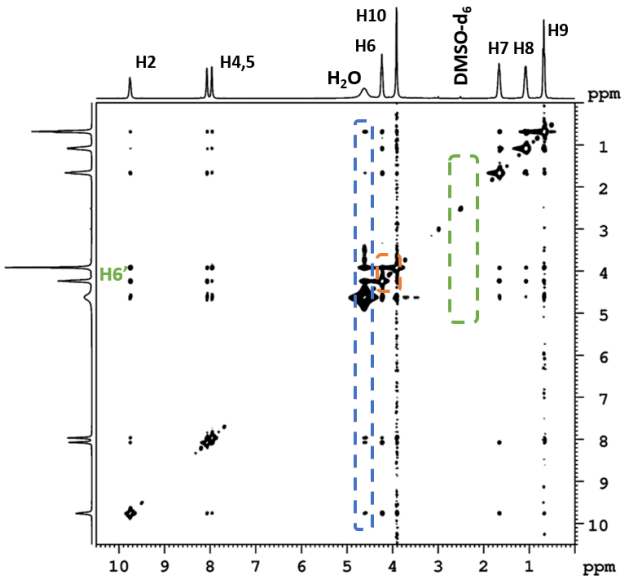

Figure 6.17: Sample A - ^{1}H, ^{1}H-NOESY CDC/BmimCl/DMSO-d_6 system at 298 K.

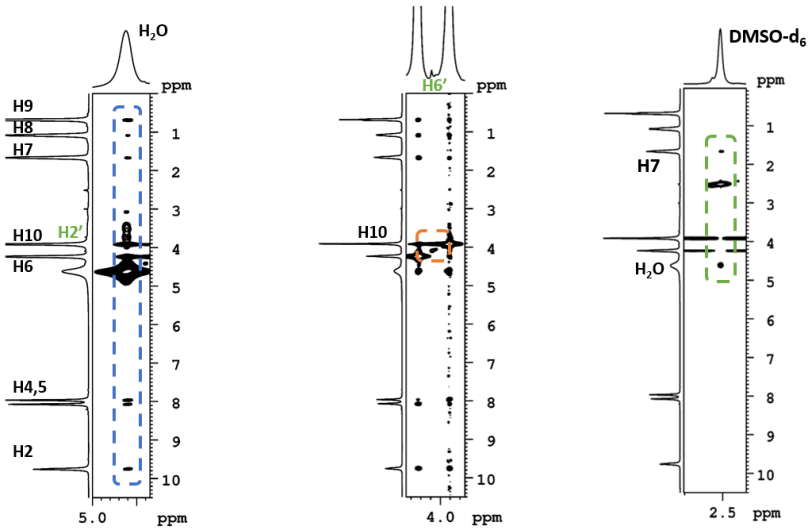

Figure 6.18: Sample A - Expansions of ^{1}H, ^{1}H-NOESY CDC/BmimCl/DMSO-d_6 system at 298 K.

In sample B, at 298 K the ^{1}H, ^{1}H - NOESY (150 ms mixing time) spectrum, figure 6.19, present two main correlations - IL protons has correlations with water; and DMSO shows spatial proximity mainly with H6 and H10 IL protons and water, figure 6.20.

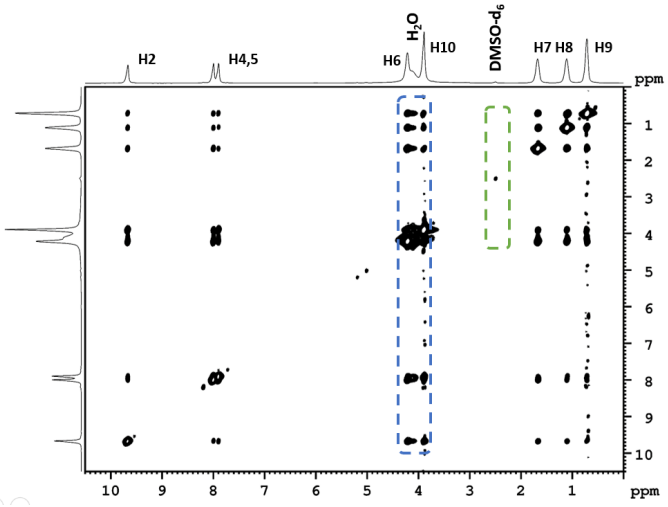

Figure 6.19: Sample B - ^{1}H, ^{1}H-NOESY CDC/BmimCl/DMSO-d_6 system at 298 K.

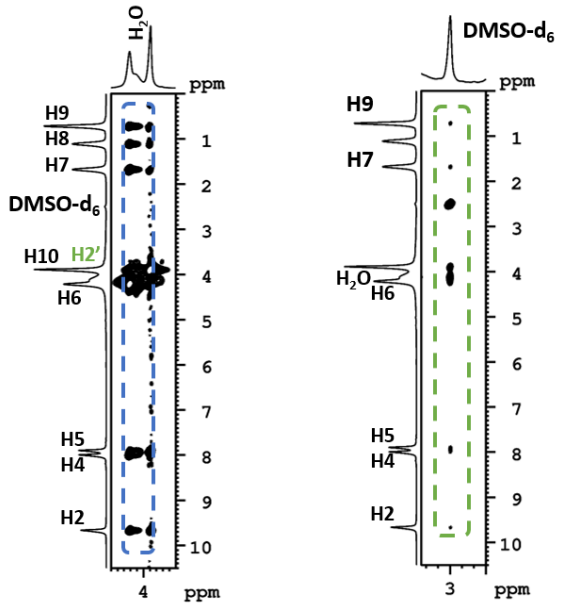

Figure 6.20: Sample B - Expansions of ^{1}H, ^{1}H-NOESY CDC/BmimCl/DMSO-d_6 system at 298 K.

Regarding to sample C, at 298 K the ^{1}H, ^{1}H - NOESY (150 ms mixing time) spectrum, figure 6.21, shows two main correlations - water has correlations with H2'; and DMSO shows spatial proximity with all IL protons and water, figure 6.22.

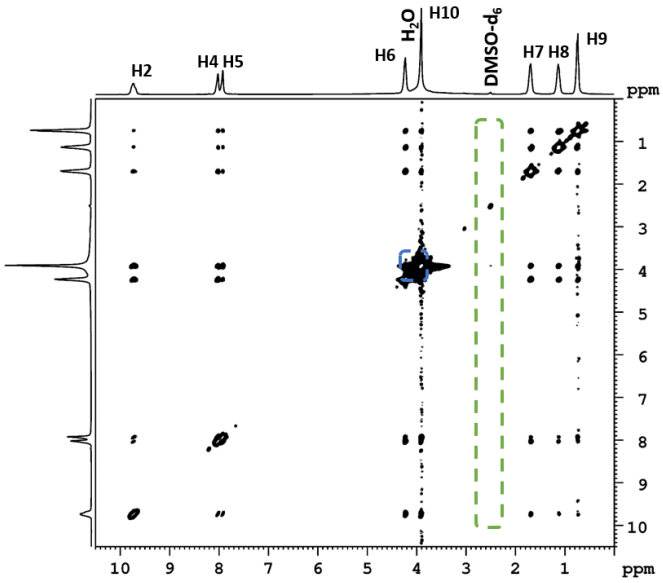

Figure 6.21: Sample C - ^{1}H, ^{1}H-NOESY CDC/BmimCl/DMSO-d_6 system at 298 K.

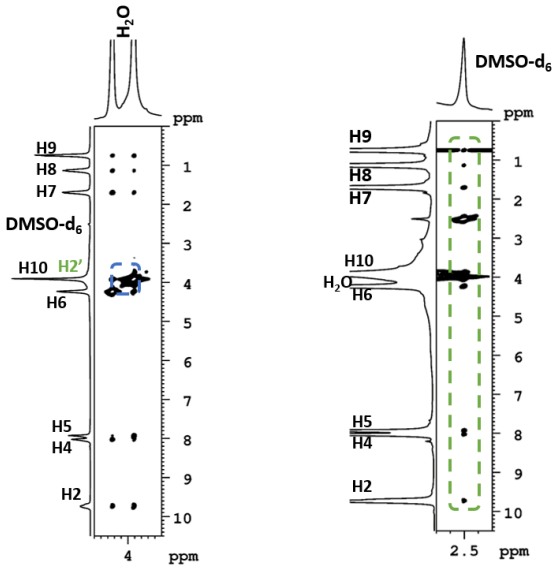

Figure 6.22: Sample C - Expansions of ^{1}H, ^{1}H-NOESY CDC/BmimCl/DMSO-d_6 system at 298 K.

Summary

Based on NMR experiments the pattern of interactions observed in each sample is depicted in figure 6.23. In every sample the correlation between the polymer and water is present which means that it must be in the vicinity of the polymer matrix, the interaction between IL and DMSO is also detected, which points to some degree of dissociation of the cation/anion pair, which was no doubt important for the dissolution step. The correlation between the ILs cation and the polymer is only detected in samples A and B, in agreement with what the VT-NMR, the relaxation measurements and even diffusion were suggesting. Namely that in sample C the polymer is stabilized without the need for the ILs cation to engage in further interactions. In samples A and B this interaction seems to be a part of the system.

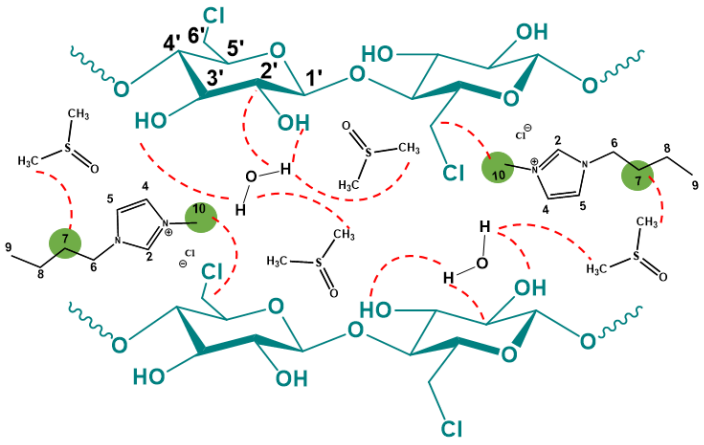

(a) Sample A

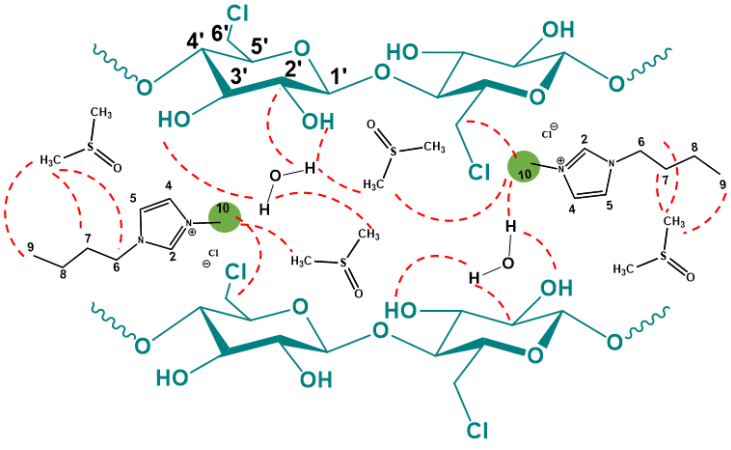

(b) Sample B

Figure 6.23: Representation of the three CDC hypothetical system models.

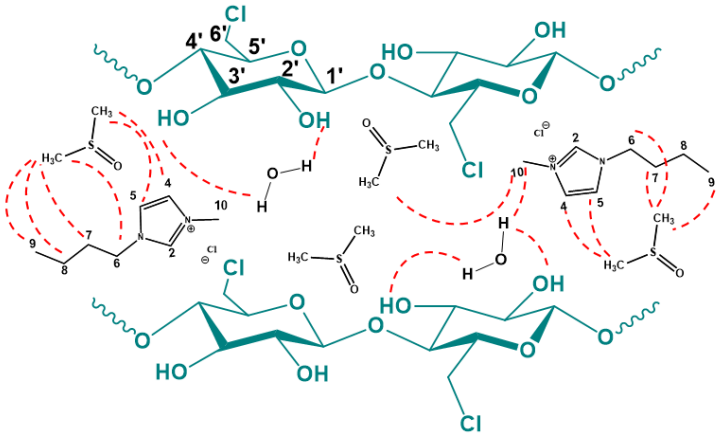

(c) Sample C

Figure 6.23: (Continued) Representation of the three CDC hypothetical system models.

Regarding to CellmimCl sample at 298 K in ^{1}H, ^{1}H - NOESY (150 ms mixing time) spectrum, figure 6.24, it is possible to observe three main correlations: H7' CellmimCl shows spatial proximity with H10' and H6' CellmimCl; water has correlations with H2', H10', H1' and OH, OH' CellmimCl; and DMSO shows spatial proximity with all IL protons, figure 6.25.

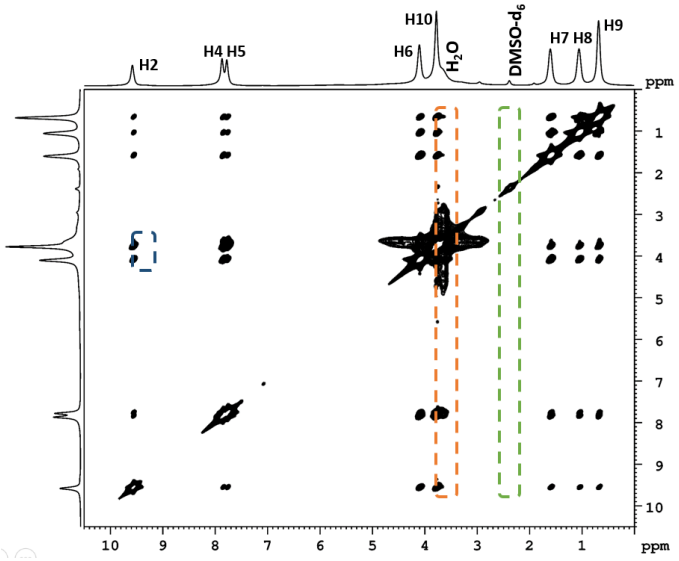

Figure 6.24: CellmimCl - ^{1}H, ^{1}H-NOESY CellmimCl/BmimCl/DMSO-d_6 system at 298 K.

The imidazolium cation grafted in the cellulose backbone enabled new system ionic interactions. The imidazolium cation grafted in the cellulose backbone enabled an additional set of interactions to be established – from the ionic moiety 6.26. An important conclusion is that H7' CellmimCl correlations with H10'and H6'allows us to conclude that the introduction of the ionic liquid moiety in the cellulose backbone brought a new

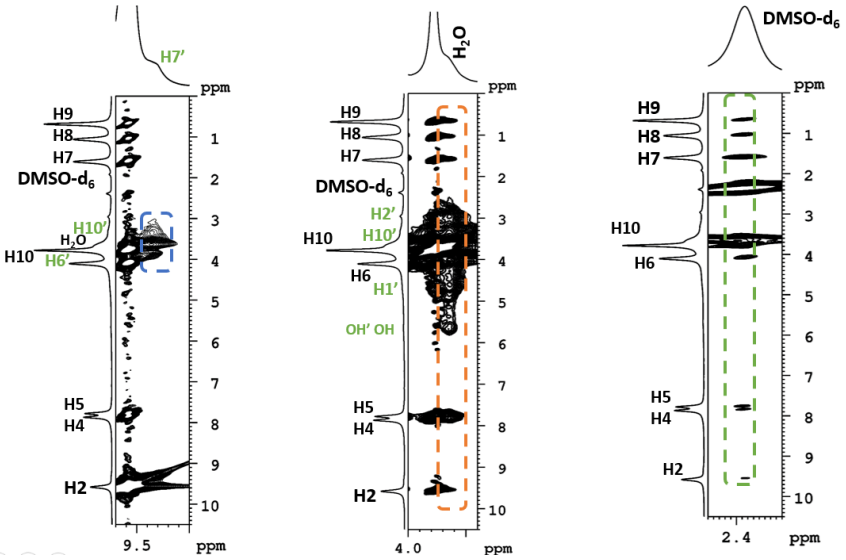

Figure 6.25: CellmimCl - Expansions of ^{1}H, ^{1}H-NOESY CellmimCl/BmimCl/DMSO-d_6 system at 298 K.

set of interactions, since it is possible to correlate the ILs cation in the solvent with the imidazolium grafted in the cellulose. The modification of the polymer's structure enabled additional interactions with the solvent.

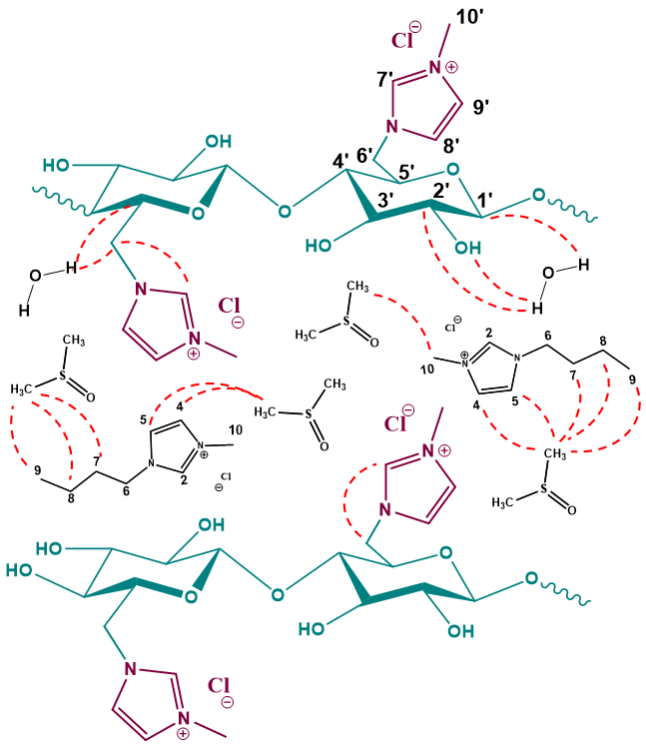

Figure 6.26: Representation of CellmimCl hypothetical system model.

Rheology measurements

In order to study the viscoelastic properties of CDC and CellmimCl samples, dynamic measurements were performed by means of rotational rheometer.

From the results obtained by different NMR measurements it was advanced that the gelation of the system may occur upon cooling. Thus, in order to confirm the gelation of the polymer, temperature sweep test as well as frequency sweep test were performed for all samples.

Figure 6.27(a) shows the temperature sweep test where the evolution of both elastic and viscous modulus are analyzed upon cooling from 70 to 20 °C for the sample A. The experiment was carried out at constant non-destructive frequency, 1 Hz, and a cooling rate of 2°C/min, under the LVR (region where the elastic and viscous moduli are independent of the applied deformation). As observed from the figure 6.27(a), above 32.6°C there is a high dispersion of points from which no conclusions can be drawn. At this range of temperatures the rheometer is not sensitive enough to acquired real G', G" values, instead we are measuring the inertia of the sample. In contrast, below 32.6°C the elastic modulus, G', become higher than viscous modulus, G" which is indicative of a more solid-like behavior. However, from this experiment it is not possible to confirm a gel-like behavior. In order to determine if the sample showed a gel-like behavior, we performed a frequency sweep test at 20°C , immediately after the temperature sweep test and represented in figure 6.27(b). From the evolution of G' and G" with frequency, two main results can be extracted: (i) G' is higher than G" in the whole range of studied frequencies, which confirms that the sample present a solid-like behavior and (ii) that the sample shows an elastic modulus at zero frequency and independent of the frequency, which is the rheological definition of a gel-like behavior. Therefore, the performed study confirmed the gel formation.

The described behavior is also observed for the samples B, C and CellmimCl as shown from figure 6.27(c) to 6.28(h), thus confirming the gel formation.

By comparing the results of CDC samples, table 6.14, which corresponds to gels with different polymer matrix content, it is observed that as the polymer amount increases the obtained gel present higher modulus. Besides, the temperature where the cross-over of G' and G" (G'=G") occurs increases with polymer content, being of 32, 33 and 43°C, for A, B and C samples, respectively.

If we compare the results of CDC (sample B, 10% of polymer matrix) and CellmimCl (also containing 10% of polymer matrix), the latter presents G' almost two orders of magnitude lower than the moduli of CDC. In addition, the temperature where the crossover of G' and G" occurs is lower, being of 33.8°C for sample B and of 28.0°C for CellmimCl. This result indicates that the grafting of IL into the cellulose backbone give rise to a less stiff gel.

The analysis of rheology data demonstrates that the system presents a gel-like behavior and allows us to verify that the NMR results were reflecting the gelation of the system.

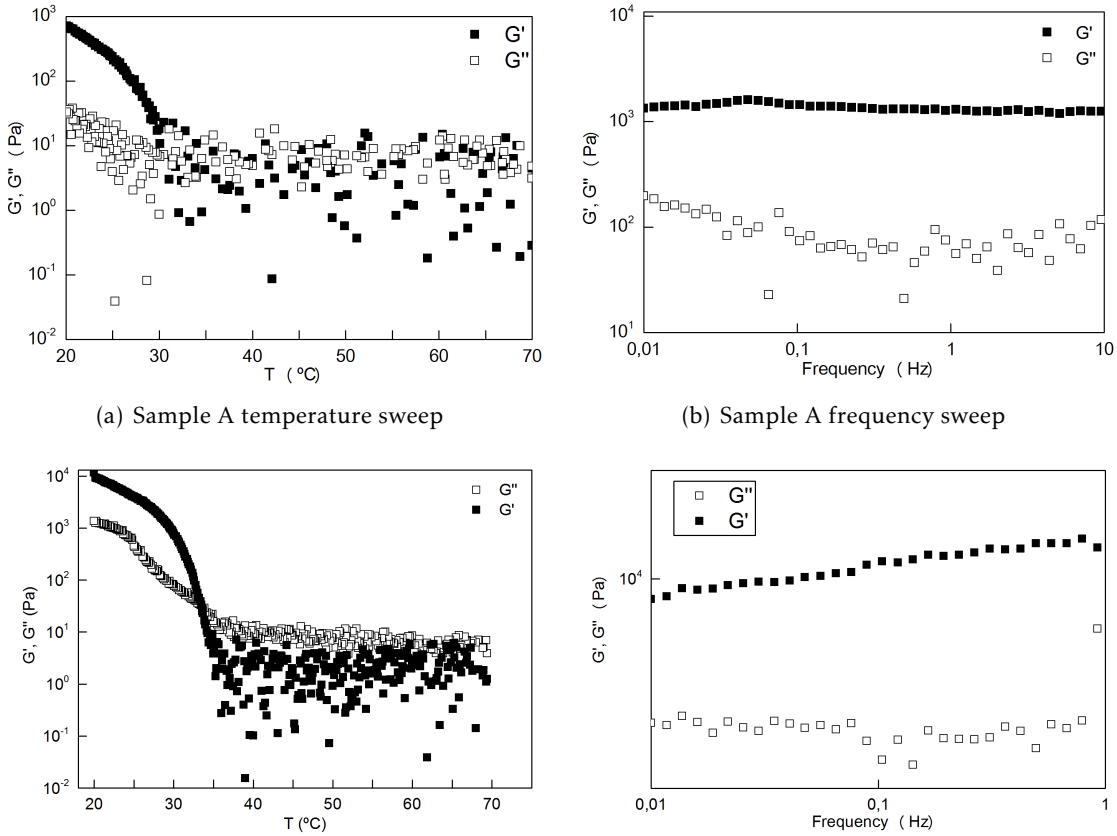

(a) Sample A temperature sweep

(b) Sample A frequency sweep

(c) Sample B temperature sweep

(d) Sample B frequency sweep

Figure 6.27: Temperature sweep test performed at a cooling rate of 2°C/min (a, c, e, g) and frequency sweep test performed at 20°C (b, d, f, h) corresponding to samples CDC (A, B, C) with different polymer content, and to CellmimCl are shown.

In fact, the difference observed in the rheological behavior of CDC samples was previously observed in the relaxation profiles. For instance sample C that presents a $T_{G'=G''}$ temperature at 43.3° is the one that exhibits no significant difference in IL cation ^{13}C - T_1 relaxation profile.

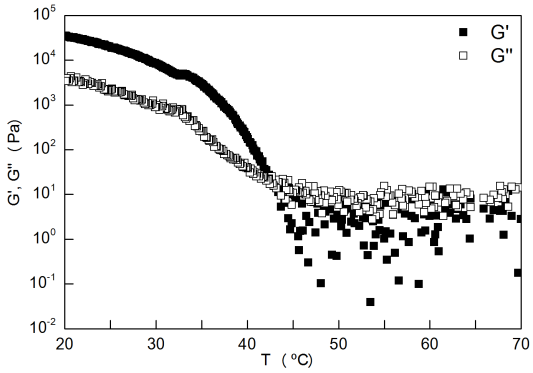

(e) Sample C temperature sweep

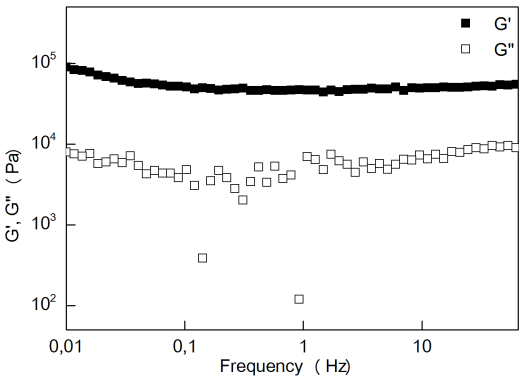

(f) Sample C frequency sweep

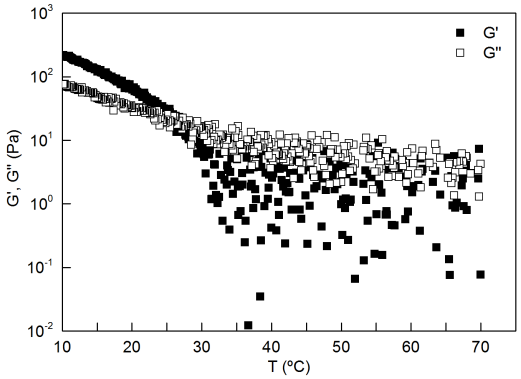

(g) CellmimCl sample temperature sweep

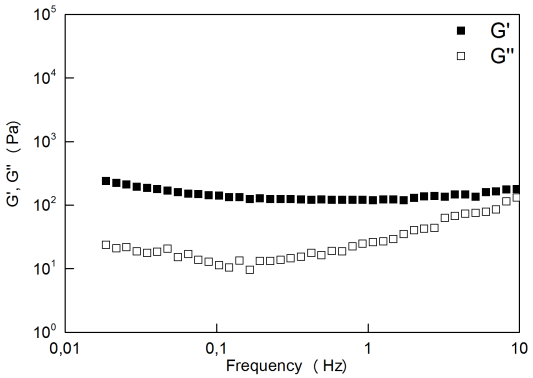

(h) CellmimCl sample frequency sweep

Figure 6.27: (Continued) Temperature sweep test performed at a cooling rate of 2°C/min (a, c, e, g) and frequency sweep test performed at 20°C (b, d, f, h) corresponding to samples CDC (A, B, C) with different polymer content, and to CellmimCl are shown.

Table 6.14: Cross-over temperature (G'=G") was extracted from temperature sweep test and G' and G" was obtained from frequency sweep test.

	$T_{G'=G''}$ (°C)	G' (Pa)	G" (Pa)
A	32.6	709.3	32.7
B	33.8	9,333.0	1,254.8
C	43.3	57,209.0	5,401.6
CellmimCl	28.0	237.6	23.6

CHAPTER 7

Conclusions and Future work

Cellulose is a polymer with a set of relevant features for several fields, however its dissolution process is a relevant issue for further applications. The main goal of this dissertation was to develop a new cellulose derivative - ionic liquid gel. In order to improve the polymer solubility ILs were grafted to cellulose backbone and also used as solvent system in the dissolution/gelation process. To study the gelation process and understand the physical and chemical properties of the new cellulose derivative NMR techniques and Rheology measurements were performed.

The polymer dissolution with BmimCl/DMSO system (figure 7.1) benefits from the IL ions solvation. The dissolution process is crucial for the sucess of the subsequent gelation.

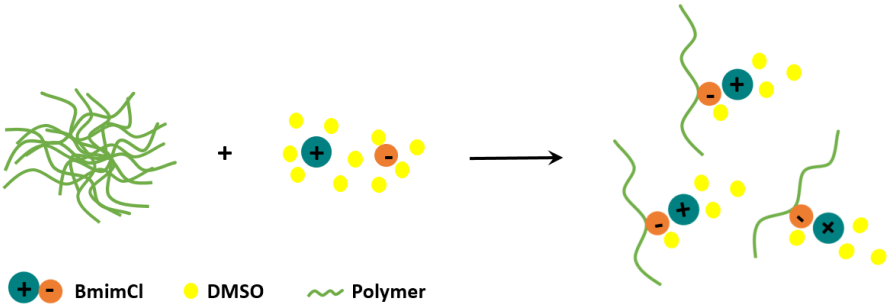

Figure 7.1: Pictorial representation of dissolution step.

For the gelation to occur a minor amount of water is needed as observed by NMR. Depending of polymer matrix amount the gels present distinct behavior. In CDC, for A and B samples the structure has less constraints, figure 7.2.1), and in the gelation process the anion-cation interactions decreases due to anion interaction with polymer network.

Moreover, sample C structure has more constraints, figure 7.2.2) - in these conditions, the cation still interacts with polymer network although to a lesser extent. In this system

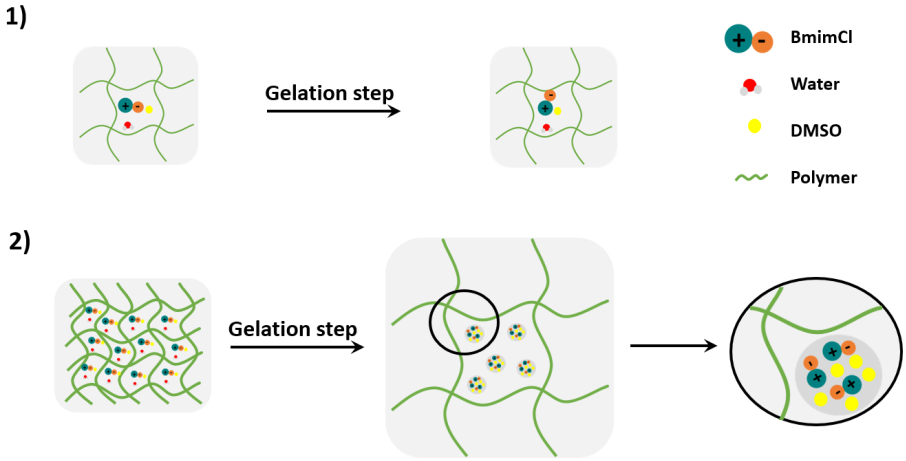

Figure 7.2: Pictorial representation of gelation step.

probably there are the formation of clusters of IL solvated by DMSO. CellmimCl sample has similar behavior.

It is the anion that is expected to governs the hydrogen bond disruption process but it is possible to follow the dissolution/gelation process through the cation. In the gelation process probably it is necessary less IL amount than the needed to dissolve the polymer.

The rheological experiments allow to confirm the gel-like behavior of the obtained system, moreover, the increasing of polymer matrix content in CDC samples increases the viscoelastic properties.

The derivatization of cellulose with ionic liquids allowed the improvement of the polymer solubility as intended however the obtained gel is weaker.

As above described it is possible to follow the dissolution and gelation processes through the IL cation. Thus, it is important to do studies with the polymer amount gradient in order to comprehend the IL critical concentration for each considered system. The relaxation behavior of the polymer can be using in the future to followed the gelation process by NMR. In the future, will be interesting to explore the versatility of the polymer ionic liquids by grafting different moiety in cellulose backbone.

Bibliography

[1] D. Klemm, B. Philipp, T. Heinze, U. Heinze, and W. Wagenknecht. *Comprehensive Cellulose Chemistry; Volume 1: Fundamentals and Analytical Methods*. Wiley-VCH, 1998.

[2] D. F. Caulfield, J. D. Passaretti, and S. F. Sobczynski. In: *Materials Research Society* 197 (1990), pp. 89–98.

[3] Y. Shen, X. Li, and Y. e. a. Huang. In: *Macromol. Res.* 24 (2016), pp. 602–608.

[4] M. L. S. C. R. Palomero and M. Valcárcel. In: *Sensors and Actuators B: Chemical* 229 (2016), pp. 31–37.

[5] S. Tanpichai and K. Oksman. In: *Composites Part A: Applied Science and Manufacturing* 88 (2016), pp. 226–233.

[6] D. Mecerreyes. In: *Progress in Polymeric Science* 36 (2011), pp. 1629–1648.

[7] X. Yuan and G. Cheng. In: *Phys. Chem. Chem. Phys.* 17 (2015), pp. 31592–31607.

[8] J. E. Stumpel, D. J. Broer, and A. P.H. J. Schenning. In: *Chem. Commun.* 50 (2014), pp. 15839–15848.

[9] A. Feula, X. Tang, I. Giannakopoulos, A. M. Chippindale, I. W. Hamley, F. Greco, C. P. Buckley, C. R. Siviour, and W. Hayes. In: *Chem. Sci.* 7 (2016), pp. 4291–4300.

[10] J. Yuan and M. Antonietti. In: *Polymer* 52 (2011), pp. 1469–1482.

[11] S. Seiffert. *Supramolecular Polymer Networks and Gels*. Springer International Publishing AG Switzerland, 2015.

[12] M. Imai, K. Ikari, and I. Suzuki. In: *Biochemical Engineering Journal* 17 (2004), pp. 79 –83.

[13] H. Kang, R. Liu, and Y. Huang. In: *Polym Int* 62 (2013), pp. 338 –344.

[14] M. Isik, H. Sardon, and D. Mecerreyes. In: *Int. J. Mol. Sci.* 15 (2014), pp. 11922–11940.

[15] D. Klemm, B. Heublein, H. Fink, and A. Bohn. In: *Angew. Chem. Int.* 44 (2005), pp. 3358–3393.

[16] J. Wertz, O. Bédué, and J. P. Mercier. *Cellulose Science and Technology*. EPFL Press, 2010.

[17] R. Moon, A. Martini, J. Nairn, J. Simonsen, and J. Youngblood. In: *Chem. Soc. Rev.* 40 (2011), pp. 3941–3994.

[18] M. Poletto, V. Pistor, and A. J. Zattera. *Structural Characteristics and Thermal Properties of Native Cellulose*, *Cellulose - Fundamental Aspects*. InTech, 2013.

[19] T. Wustenberg. *Cellulose and Cellulose Derviatives in the Food Industry . Fundamentals and Applications*. Wiley-VCH, 2015.

[20] D. Klemm, B. Philipp, T. Heinze, U. Heinze, and W. Wagenknecht. *Comprehensive Cellulose Chemistry; Volume 2: Functionalization of Cellulose*. Wiley-VCH, 1998.

[21] C. McCormick and D. Lichatowich. In: *J. Polym. Sci. Polym. Lett. Ed.* 17 (1979), p. 479.

[22] A. Modaressi, H. Sifaoui, M. Mielcarz, U. Domanska, and M. Rogalski. In: *Colloids and Surfaces A: Physicochemical and Engineering Aspects* 302 (2007), pp. 181–185.

[23] P. Hapiot and C. Lagrost. In: *Chemical Reviews* 108 (2008), pp. 2238–2264.

[24] T. Ichikawa, M. Yoshio, A. Hamasaki, T. Mukai, H. Ohno, and T. Kato. In: *Journal of the American Chemical Society* 129 (2007), pp. 10662–10663.

[25] F. van Rantwijk and R. A. Sheldon. In: *Chemical Reviews* 107 (2007), pp. 2757–2785.

[26] M. J. Earle and K. R. Seddon. In: *Pure Appl. Chem.* 72 (2000), pp. 1391–1398.

[27] X. Han and D. W. Armstrong. In: *Accounts of Chemical Research* 40 (2007), pp. 1079–1086.

[28] P. Wasserscheid and T. Welton. *Ionic Liquids in Synthesis - Volume 1*. Wiley-VCH, 2008.

[29] E. Husemann and E. Siefert. In: *Makromol. Chem.* 128 (1969), p. 288.

[30] R. P. Swatloski, S. K. Spear, J. D. Holbrey, and R. D. Rogers. In: *J. Am. Chem. Soc.* 124 (2002), pp. 4974–4975.

[31] R. Sescousse, K. A. Le, M. E. Ries, and T. Budtova. In: *J. Phys. Chem* 114 (2010), pp. 7222–7228.

[32] R. C. Remsing, R. P. Swatloski, R. D. Rogers, and G. Moyna. In: *Chem. Commun.* 12 (2006), pp. 1271–1273.

[33] C. Tsioptsias, A. Stefopoulos, I. Kokkinomalis, L. Papadopoulou, and C. Panayiotou. In: *Green Chem.* 10 (2008), pp. 965–971.

[34] C. X. Lin, H. Y. Zhan, M. H. Liu, S. Y. Fu, and L. A. Lucia. In: *Langmuir* 25 (2009), pp. 10116–10120.

[35] M. B. Turner, S. K. Spear, J. D. Holbrey, and D. R. Rogers. In: *Biomacromolecules* 5 (2004), pp. 1379–1384.

[36] G. Cheng, P. Varanasi, R. Arora, V. Stavila, B. A. Simmons, M. S. Kent, and S. Singh. In: *J. Phys. Chem. B* 116 (2012), pp. 10049–10054.

[37] A. S. Gross, A. T. Bell, and J. W. Chu. In: *J. Phys. Chem.* 115 (2011), pp. 13433–13440.

[38] B. Mostofian, J. C. Smith, and X. Cheng. In: *Cellulose* 21 (2014), pp. 983–997.

[39] A. S. Gross, A. T. Bell, and J. W. Chu. In: *Phys. Chem. Chem. Phys.* 14 (2012), pp. 8425–8430.

[40] P. Zugenmaier. *Crystalline Cellulose and Derivatives: Characterization and Structures*. Springer-Verlag, 2008.

[41] A. Nussinovitch. *Hydrocolloid Applications*. Chapman & Hall, 1997.

[42] Q. Chen, C. Peng, H. Xie, Z. k. Zhao, and M. Bao. In: *RSC Adv.* 5 (2015), pp. 44598–44603.

[43] J. Lu, F. Yan, and J. Texter. In: *Progr. Polym. Sci.* 34 (2009), pp. 431–448.

[44] H. Ohn. *Design of Ion Conductive Polymers Based on Ionic Liquids*. Wiley-VCH, 2007.

[45] O. Green, S. Grubjesic, S. Lee, and A. Millicent. In: *Polymer Reviews* 49 (2009), pp. 339–360.

[46] J. Fuller, A. C. Breda, and R. T. J. Carlin. In: *Electrochem. Soc.* 144 (1998), p. 67.

[47] S. Livi, V. Bugatti, B. G. Soares, and J. Duchet-Rumeau. In: *Green. Chem.* 16 (2014), p. 3758.

[48] M. Rahman and C. S. Brazel. In: *Polym. Degrad. Stabil.* 91 (2006), p. 3371.

[49] A. Usuki, M. Kawasumi, A. Okada, Y. Fukushima, T. Kurauchi, and O. Kamigaito. In: *J. Mater. Res.* 8 (1993), p. 1179.

[50] S. A. Arvidson, J. R. Lott, J. W. McAllister, J. Zhang, F. S. Bates, and T. P. Lodge. In: *Macromolecules* 46 (2013), pp. 300–309.

[51] R. Mantravadi, P. R. Chinnam, D. A. Dikin, and S. L. Wunder. In: *ACS Appl. Matter. Interfaces* 21 (2016), pp. 13426–13436.

[52] M. S. A. Rani, N. H. Hassan, A. Ahmad, H. Kaddami, and N. S. Mohamed. In: *Ionics* (2016).

[53] W. Zhao, Y. J. Hai, Z. Jinxiong, X. Feng, Z. Miklos, D. H. Patrick, O. Yoshihito, and C. Y. Mei. In: *Chem Soc. Rev.* 43 (2014), pp. 8114–8131.

[54] M. George and R. G. Weiss. In: *Accounts of Chemical Research* 39 (2006), pp. 489–497.

[55] A. Nussinovitch. *Polymer Macro- and Micro-Gel beads: Fundamentals and Applications*. Soringer, 2010.

[56] M. Djabourov, K. Nishinari, and S. B. Ross-Murphy. *Physical Gels from Biological and Synthetic Polymers*. Cambridge University Press, 2013.

[57] H. Saito, A. Sakurai, M. Sakakibara, and H. Saga. In: *Journal of Applied Polymer Science* 90 (2003), pp. 3020–3025.

[58] M. Patchan, J. L. Graham, Z. Xia, J. P. Maranchi, R. McCally, O. Schein, J. H. Elisseeff, and M. M. Trexler. In: *Materials Science and Engineering C* 33 (2013), pp. 3069–3076.

[59] Z. Wang, S. Liu, and Y. Matsumoto. In: *Celulose* 19 (2012), pp. 393–399.

[60] M. Gericke, P. Fardim, and T. Heinze. In: *Molecules* 17 (2012), pp. 7458–7502.

[61] J. Kadokawa, M. Murakami, and Y. Kaneko. In: *Carbohydrate Research* 343 (2008), pp. 769–772.

[62] R. Ariño, M. Brodin, A. Boldizar, and G. Westman. In: *Bioresources* 8 (2013), pp. 2209–2221.

[63] C. Zhang, H. Kang, P. Li, Z. Liu, Y. Zhang, R. Liu, J. Xiang, and Y. Huang. In: *Cellulose* 23 (2016), pp. 1165–1175.

[64] T. D. W. Claridge. *High-Resolution NMR Techniques in Organic Chemistry*. Tetrahedron Organic CHemistry Series, 2005.

[65] M. H. Levitt. *Spin Dynamics: Basics of Nuclear Magnetic Resonance*. Wiley, 2008.

[66] R. M. Silverstein, F. X. Webster, and D. J. Kiemle. *Spectrometric identification of organic compounds - Seven edition*. Wiley, 2005.

[67] S. L. Feunteun, M. Ouethrani, and F. Mariette. In: *Food Hydrocolloids* 27 (2012), pp. 456–463.

[68] S. A. Khan, J. R. Royer, and S. R. Raghavan. In: *The National Academy of Sciences* (1997), pp. 31–46.

[69] T. Osswald and N. Rudolph. *Polymer Rheology*. Hanser, 2015.

[70] S. Coseri, G. Biliuta, L. F. Zemljic, J. S. Srndovic, P. T.L. S. Strnad, T. Kreze, A. Naderi, and T. Lindstrom. In: *RSC Adv.* 5 (2015), pp. 85889–85897.

[71] B. Abderrahim, E. Abderrahman, A. Mohamed, T. Fatima, T. Abdesselam, and O. Krim. In: *W. J. Environmental Engineering* 3 (2015), pp. 95–110.

[72] E. C. S. Filho, L. C. B. Lima, F. C. Silva, K. S. Sousa, M. G. Fonseca, and S. A. A. Santana. In: *Carbohydr. Polym.* 92 (2013), pp. 1203–1210.

[73] J. Sun, W. Cheng, W. Fan, Y. Wang, Z. Meng, and S. Zhang. In: *Catalysis Today* 148 (2009), pp. 361–367.

[74] E. C. S. Filho, S. A. A. Santana, J. C. P. Melo, F. J.V. E. Oliveira, and C. Airoldi. In: *J. Therm. Anal. Calorim.* 100 (2010), pp. 315–321.

[75] F. Huo, Z. Liu, and W. Wang. In: *J. Phys. Chem.* 117 (2013), pp. 11780–11792.

[76] J. M. Andanson, E. Bordes, J. Devemy, F. Leroux, A. A. H. Padua, and M. F. C. Gomes. In: *Green Chem.* 16 (2014), pp. 2528–2538.

[77] Y. L. Zhao, J. J. Wang, H. Y. Wang, Z. Y. Li, X. M. Liu, and S. J. Zhang. In: *J. Phys. Chem. B* 119 (2015), pp. 6686–6695.

[78] B. D. Rabideau, A. Agarwal, and A. E. Ismail. In: *J. Phys. Chem. B* 118 (2014), pp. 1621–1629.

[79] A. Brandt, J. P. Hallett, D. J. leak, R. J. Murphy, and T. Welton. In: *Green Chem.* 12 (2010), pp. 672–679.

[80] A. Xu, Y. Z. Y. Zhang, and J. Wang. In: *Carbohydrate Polymers* 92 (2013), pp. 540–544.

[81] H. Olivier-Bourbigou, L. Magna, and D. Morvan. In: *Applied Catalysis A: General* 373 (2010), pp. 1–56.

APPENDIX

A.1 Technical Background

A.1.1 NMR processes

Inversion recovery process

In this process the first step is inverting the population by applying 180° pulse. The magnetization vector will recover only along the z-axis as there is no xy magnetization. The recovery is measured by placing the vector in the xy-plane with a 90° pulse after a suitable period, τ, as reproduced in figure A.1.

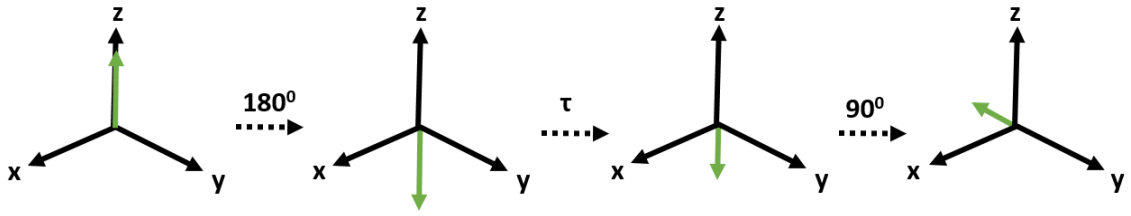

Figure A.1: The inversion recovery process

Spin-echo process

This experiment is reproduced in figure A.2. The first step is a 90° pulse that places the magnetization in the xy-plane. The magnetization will then lose coherence due to field inhomogeneity during a time period, τ. The second step is to apply a 180° pulse that will rotate the vectors towards to $-y$ axis and, after a second period time, τ, the magnetization will be refocused. Carl-Purcel-Meiboom-Gill (CPMG) sequence is the same but in the 180° pulse the vectors will rotate around $+y$ axis, figure A.3.

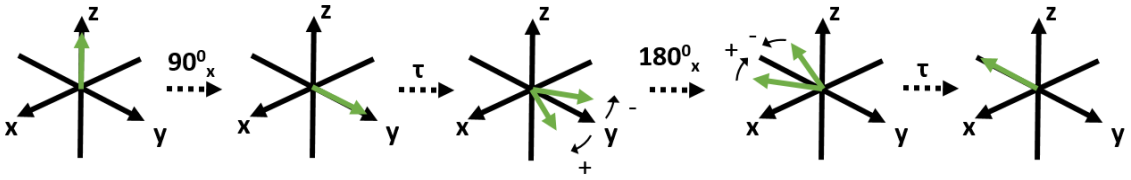

Figure A.2: Spin-echo sequence.

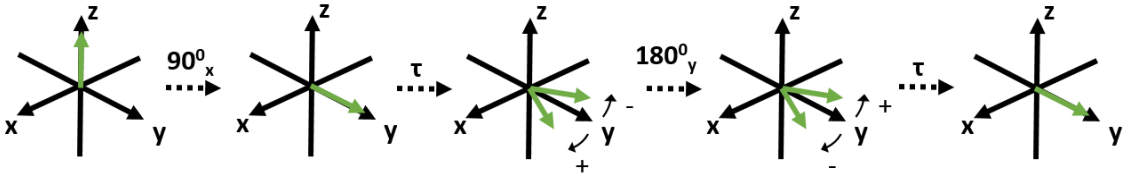

Figure A.3: CPMG process

A.2 Experimental

A.2.1 Syntheses Results

Table A.1: Summary of CDC syntheses

CDC	Avicel m(g)	Initial Conditions	T(°C)	t(h)	Yield (%)
A	1	20 min. at 80 °C	85	3.0	65.1
B	2	20 min. at 80 °C	85	3.0	86.7
C	2	20 min. at 75 °C	85	4.5	94.7
D	2	20 min. at 80 °C	85	4.0	92.3
E	1	60 min. at 80 °C	85	3.0	73.4
F	1	60 min. at 80 °C	85	3.0	69.9
G	1	60 min. at 80 °C	85	3.0	80.0

Table A.2: Summary of CellmimCl syntheses

CellmimCl	CDC m(g)	Initial Conditions	T(°C)	t(h)	Yield (%)
H	0.5	3 h at 36.4 °C	95	24	72.6
I	1.0	-	95	24	63.4
J	0.5	-	95	24	68.6
K	0.5	0.6 mL *N*-methylimidazole 30 min. before start	90	24	63.9
L	0.5	-	95	24	34.5
M	0.5	1 mL *N*-methylimidazole 6h before start	95	28	92.3
N	1.0	-	90	24	43.4
O	0.2	-	90	24	48.7
P	0.2	-	90	24	52.9

A.2.2 Spectra Characterization

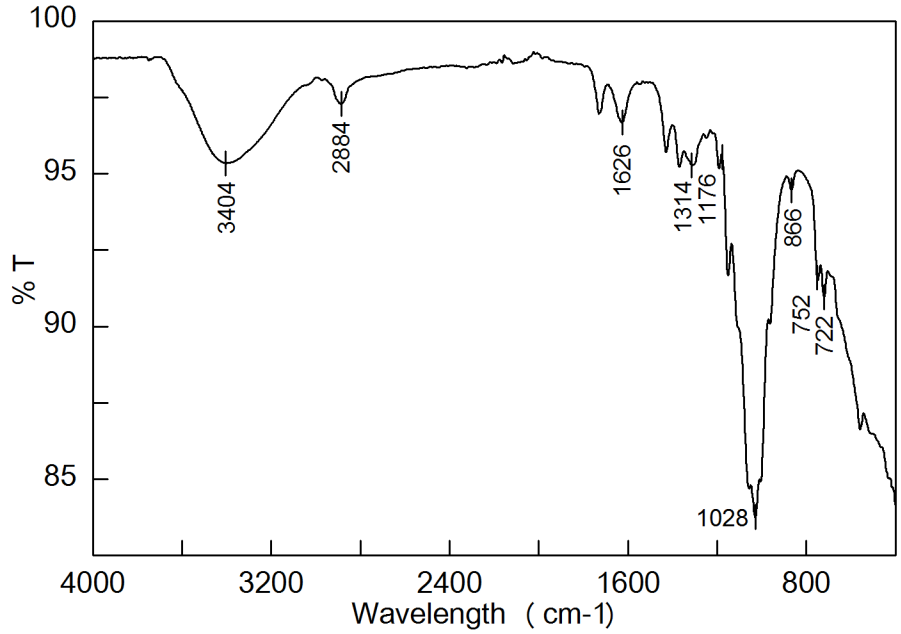

Figure A.4: IV spectrum of sample E.

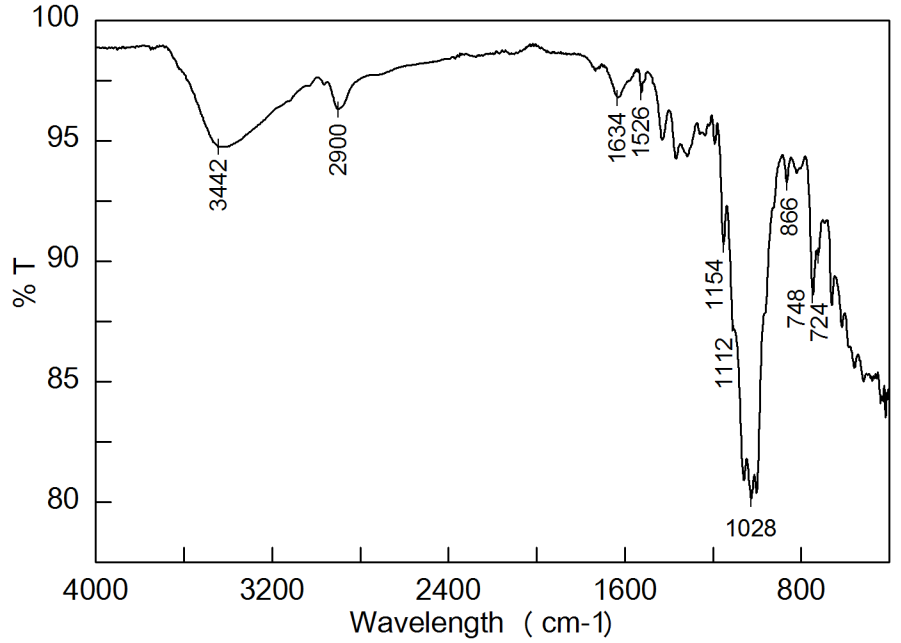

Figure A.5: IV spectrum of sample N.

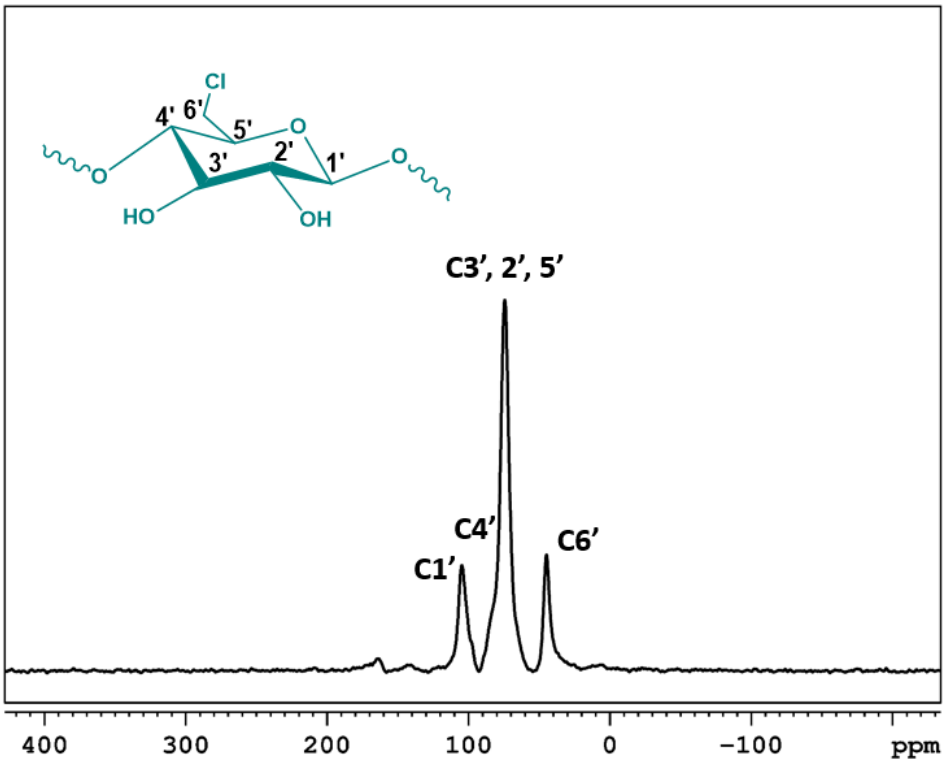

Figure A.6: CP-MAS ^{13}C-NMR spectrum of CDC.

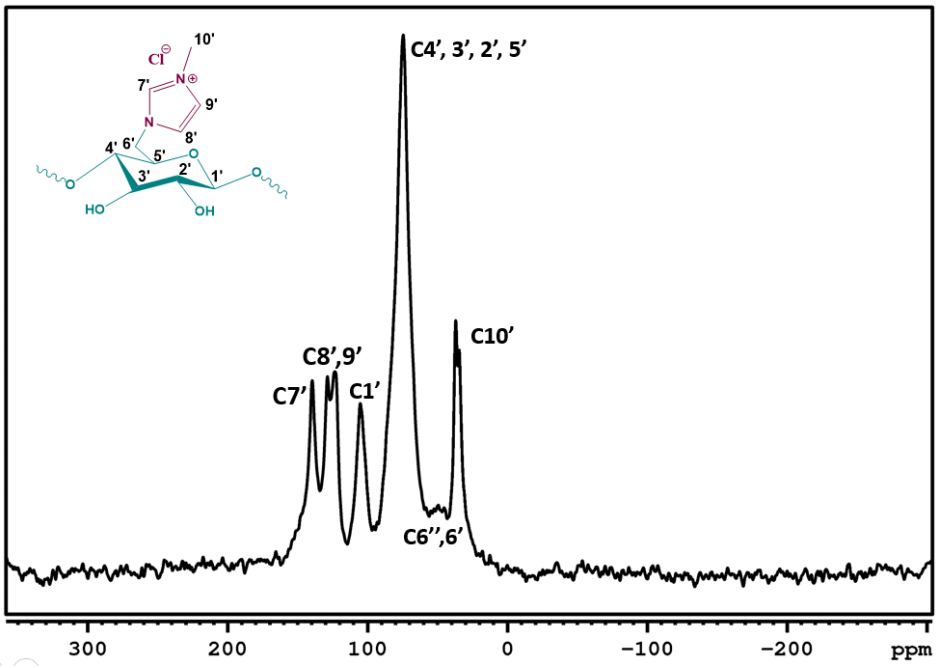

Figure A.7: CP-MAS ^{13}C-NMR spectrum of CellmimCl.

A.3 Polymer Characterization

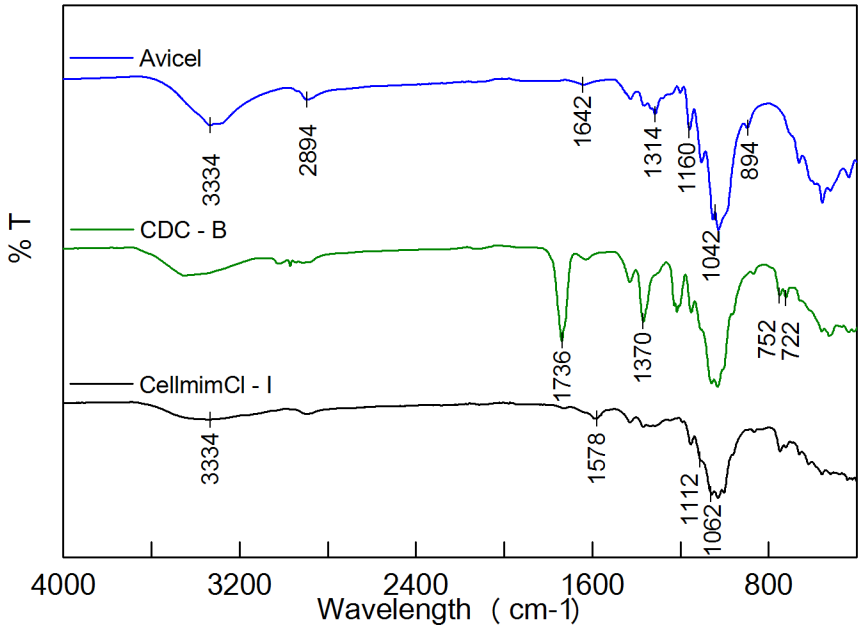

Figure A.8: FTIR patterns of avicel®, CDC - B and CellmimCl - I.

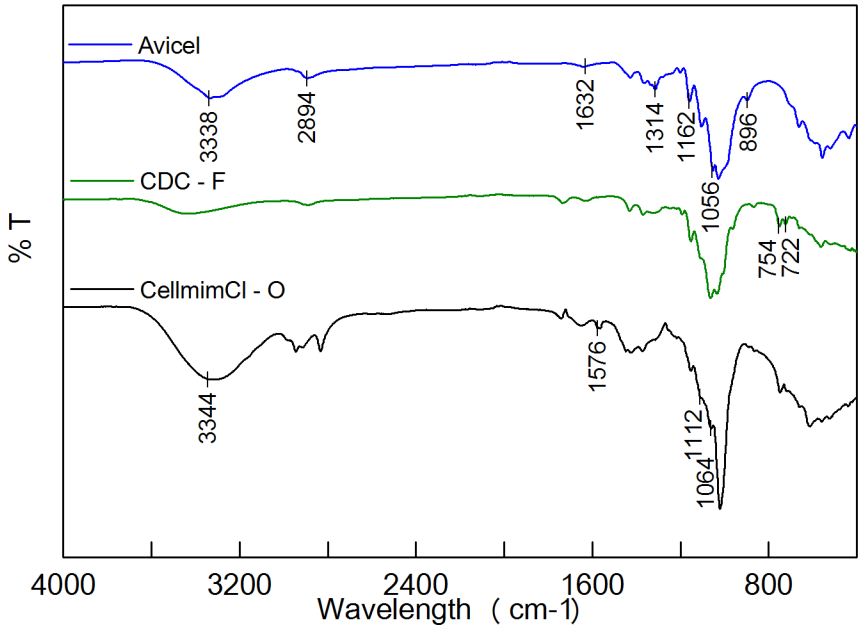

Figure A.9: FTIR patterns of avicel®, CDC - F and CellmimCl - O.

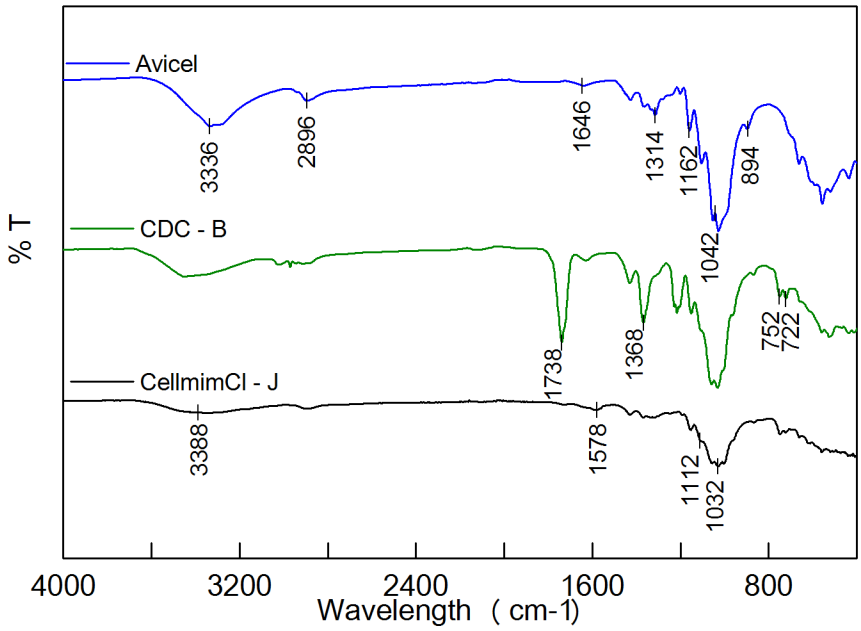

Figure A.10: FTIR patterns of avicel®, CDC - B and CellmimCl - J.

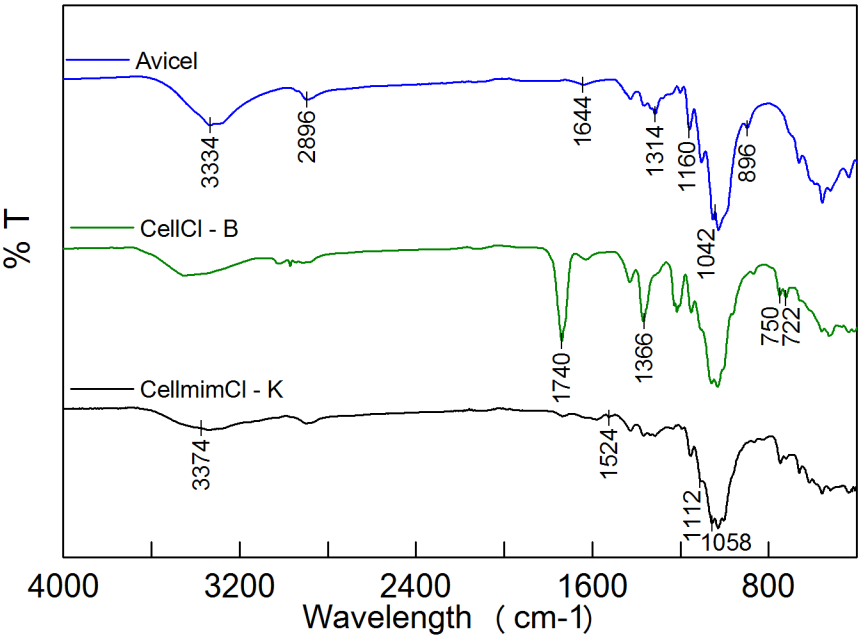

Figure A.11: FTIR patterns of avicel®, CDC - B and CellmimCl - K.

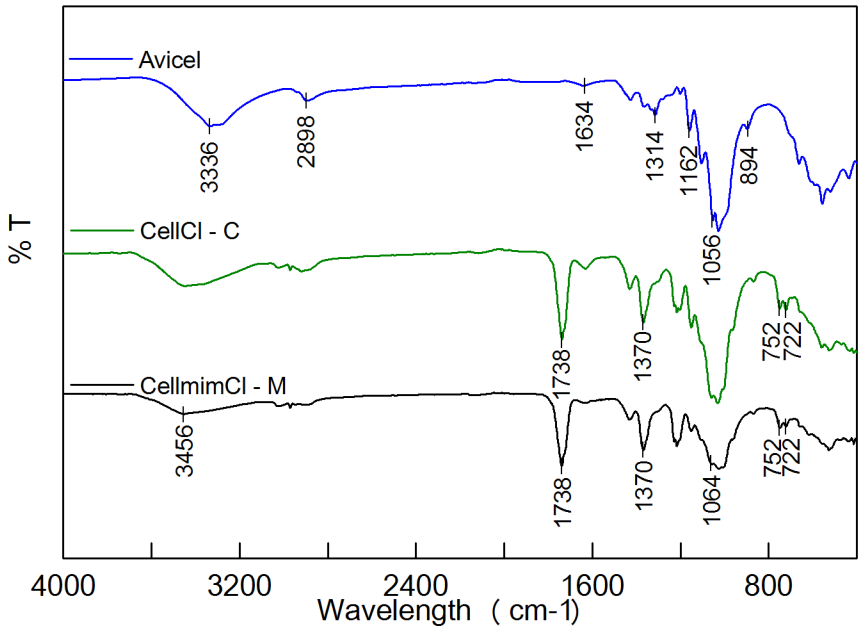

Figure A.12: FTIR patterns of avicel®, CDC - C and CellmimCl - M.

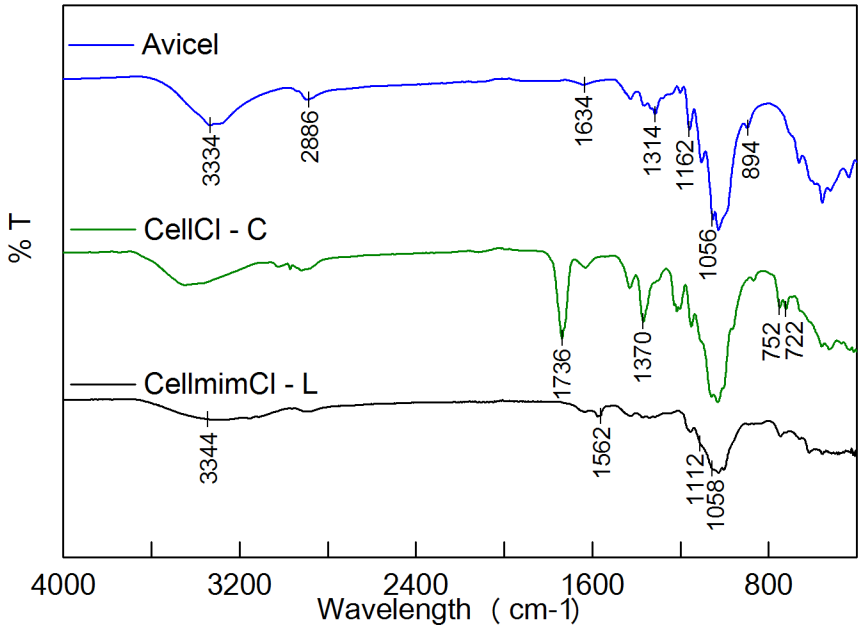

Figure A.13: FTIR patterns of avicel®, CDC - C and CellmimCl - L.

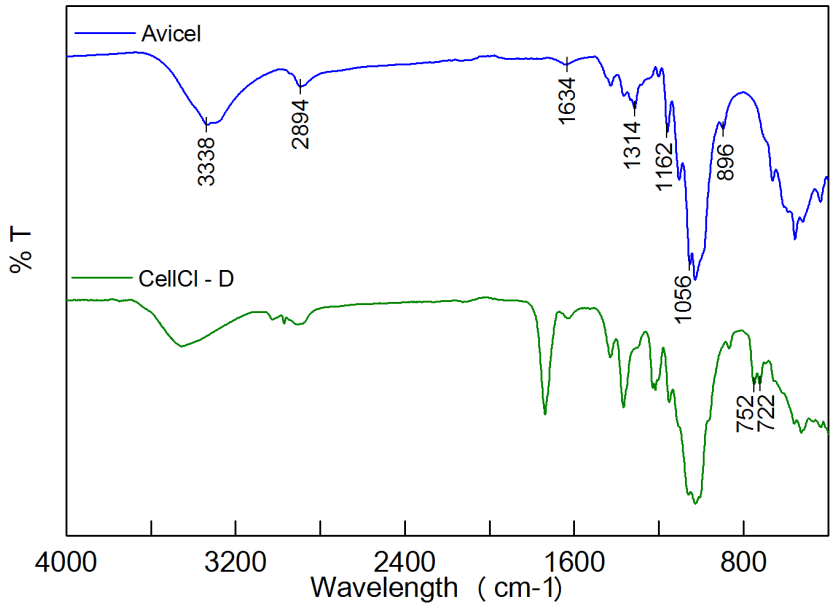

Figure A.14: FTIR patterns of avicel®and CDC - D.

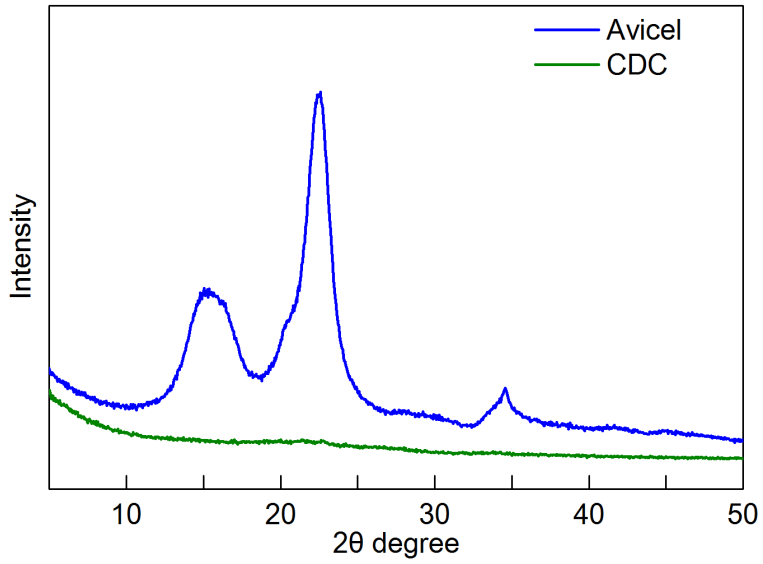

Figure A.15: X-ray diffraction patterns of Avicel®and CDC.

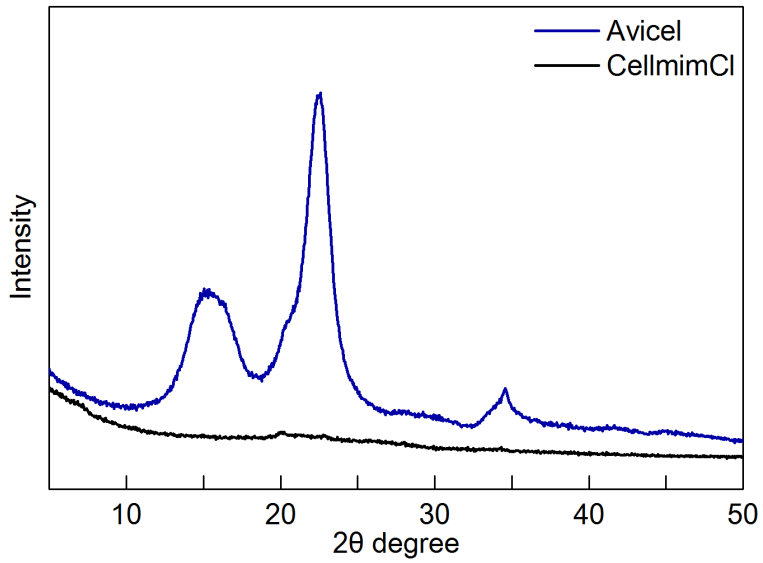

Figure A.16: X-ray diffraction patterns of Avicel®and CellmimCl.

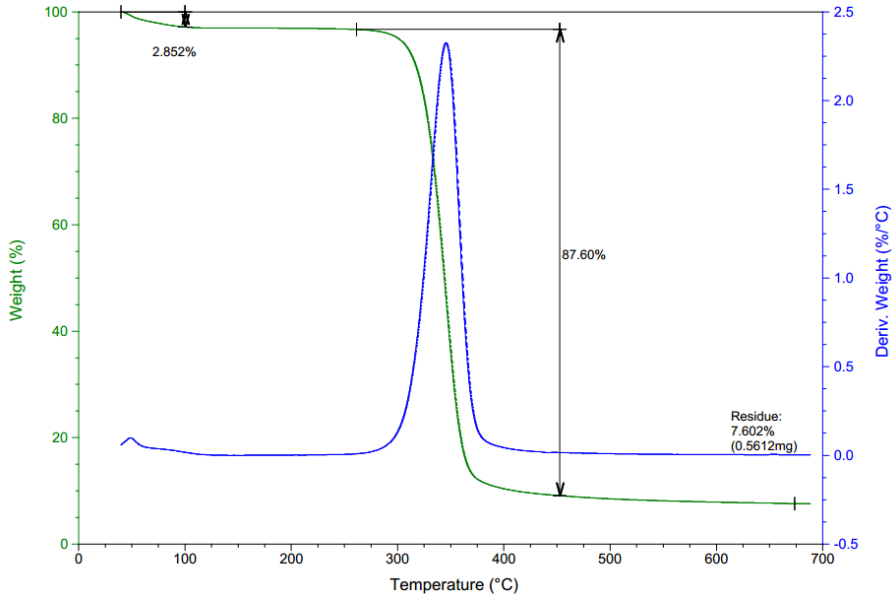

Figure A.17: TGA-DTG curve of Avicel®.

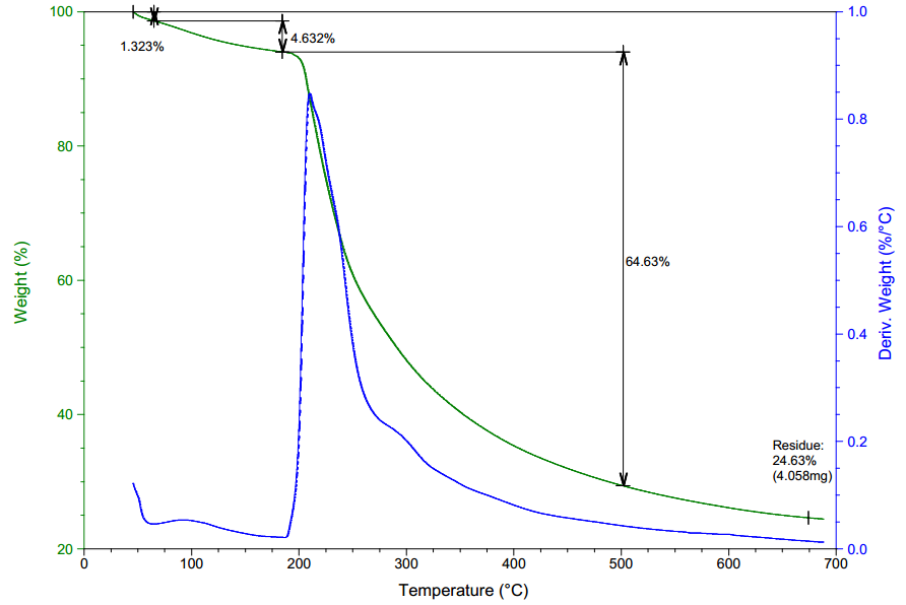

Figure A.18: TGA-DTG curve of CDC.

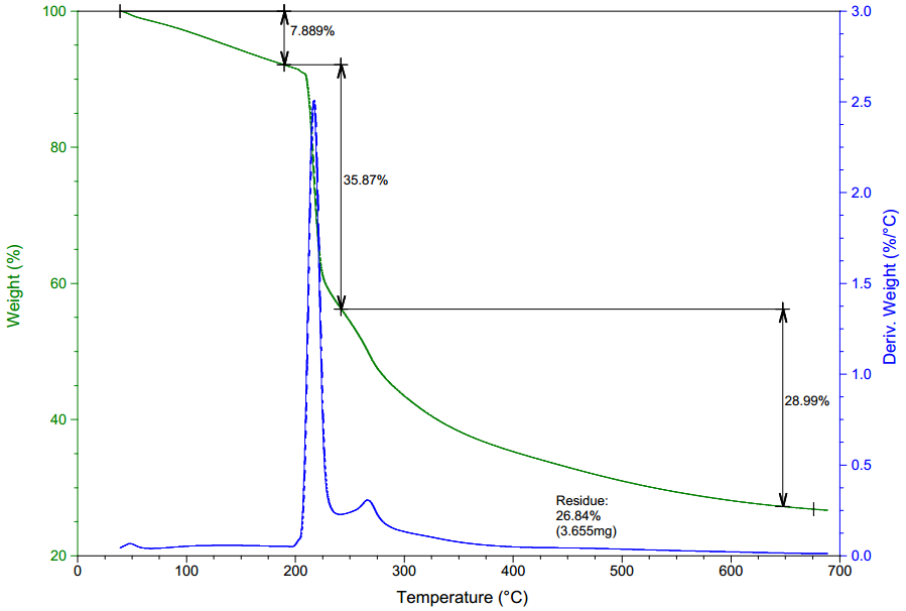

Figure A.19: TGA-DTG curve of CellmimCl.

A.4 Gelation Study - Approach I

A.4.1 BimCl/DMSO - Structural concepts

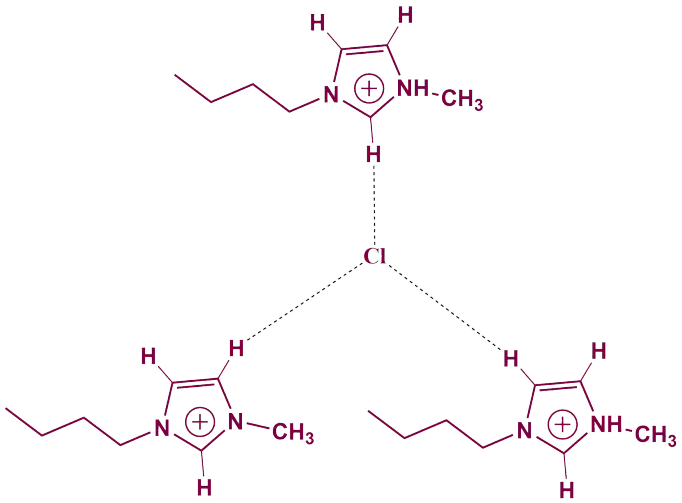

Figure A.20: Three dimensional network of hydrogen-bonding between ring protons. Adapted from reference [81]

A.4.2 CDC experiments

Table A.3: Experimental conditions for CDC samples used in the approach I.

ID	Total (g)	CDC (mg)	CDC (%)	BmimCl (mg)	BmimCl (%)	DMSO (mL)	DMSO (%)	BmimCl/CDC ratio	DMSO/CDC ratio
C1	0.19	4.0	2.12	130.0	69.0	0.05	28.8	33.0	14.0
C2	0.24	4.0	1.65	130.0	53.6	0.10	44.8	33.0	27.0
C3	0.41	4.0	0.99	130.0	32.1	0.25	67.0	33.0	68.0
C4	0.25	4.0	1.57	250.0	98.4			63.0	
E1	1.17	4.0	0.34	250.0	20.9	0.85	78.7	61.0	231.0
E2	1.07	4.0	0.37	250.0	23.4	0.75	76.2	63.0	204.0
H1	1.10	4.0	0.36	50.0	4.5	0.95	95.1	13.0	261.0
H2	1.09	4.0	0.37	100.0	9.1	0.90	90.5	25.0	248.0
H3	1.14	4.0	3.52	50.0	4.4	0.95	92.1	1.0	26.0

A.4.3 CellmimCl experiments

Table A.4: Experimental conditions for CellmimCl samples used in the approach I.

ID	Total (g)	CellmimCl (mg)	CellmimCl (%)	BmimCl (mg)	BmimCl (%)	DMSO (mL)	DMSO (%)	BmimCl/CellmimCl ratio	DMSO/CellmimCl ratio
C5	0.28	14.0	5.05	260.0	95.0			19.0	
F1	1.09	26.0	2.40	250.1	23.0	0.75	74.6	10.0	31.0
F2	1.07	4.7	0.44	470.5	43.9	0.55	55.7	100.0	127.0
F3	0.54	4.0	0.75	125.3	23.4	0.38	75.9	31.0	102.0
F4	0.27	4.0	1.48	62.7	23.2	0.19	75.3	16.0	51.0
PC	1.11	40.0	3.60	256.3	23.1	0.75	73.3	6.0	20.0
H4	1.14	40.0	3.52	50.0	4.4	0.95	92.1	1.0	26.0
H5	2.23	80.0	3.59	500.0	22.4	1.5	74.0	6.0	21.0
R	1.13	50.0	4.43	254.0	22.5	0.75	73.1	5.0	17.0

A.4.4 Approach I - Sample H3

Chemical Shifts

Table A.5: Sample H3 Chemical Shifts.

T (K)	H2	H4,5	OH' CDC	OH CDC	H1' CDC	H6	H10	H_2O	DMSO	H7	H8	H9
296	9.638	7.998	6.204	5.893	4.877	4.374	4.053	3.601	2.677	1.941	1.413	1.065
301	9.637	7.990	6.173	5.861	4.860	4.375	4.053	3.568	2.671	1.941	1.415	1.065
306	9.640	7.985	6.145	5.830	4.860	4.374	4.052	3.543	2.672	1.947	1.423	1.065
311	9.639	7.982	6.109	5.796	4.853	4.374	4.053	3.512	2.666	1.948	1.424	1.065
316	9.637	7.968	6.084	5.765	4.839	4.373	4.053	3.481	2.661	1.947	1.425	1.065
321	9.640	7.957	6.066	5.742	4.832	4.373	4.042	3.457	2.662	1.953	1.432	1.065
326	9.640	7.952	6.043	5.709	4.824	4.374	4.043	3.428	2.659	1.936	1.434	1.065
331	9.637	7.942	5.996	5.668	4.805	4.376	4.052	3.398	2.653	1.937	1.434	1.065
336	9.635	7.947	5.971	5.656	4.806	4.368	4.054	3.381	2.662	1.955	1.447	1.065
341	9.634	7.939	5.941	5.618	4.818	4.367	4.053	3.350	2.657	1.956	1.445	1.065

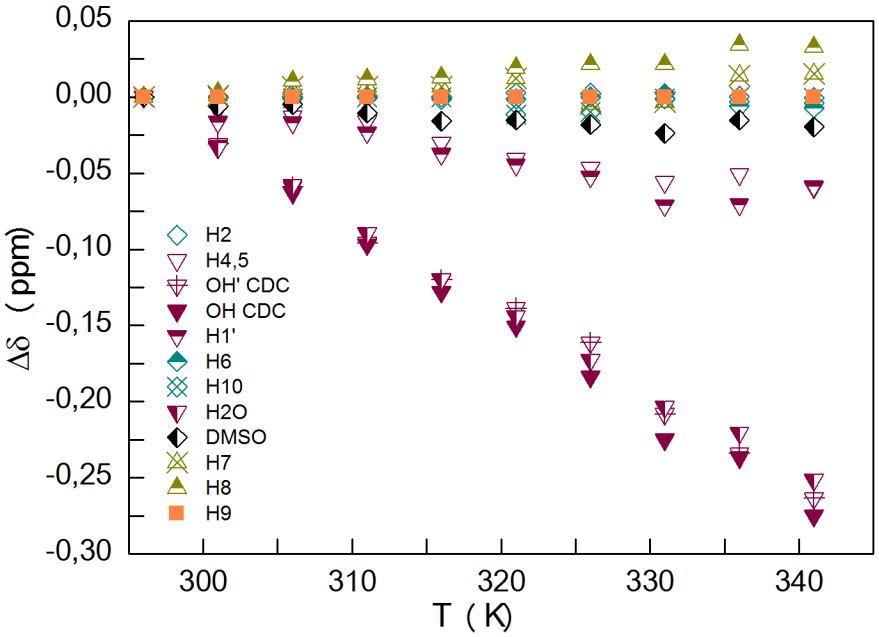

Figure A.21: Chemical shifts deviations with gradient temperature - Sample H3.

^{13}C - T_1 Relaxation

Table A.6: Δ T_1 with increasing temperature.

	ΔT_1 (s)						
T (K)	**C2**	**C4**	**C5**	**C6**	**C10**	**C8**	**C9**
306	-	-	-	-	-	-	-
311	0.15	0.34	-0.01	-0.17	0.42	0.51	0.02
316	0.22	-0.06	0.27	0.46	0.30	0.58	0.76
321	0.27	0.58	0.46	0.03	0.19	0.20	1.03
326	0.40	0.06	0.01	0.42	0.15	0.30	0.57
331	0.58	0.41	0.30	0.25	-0.09	-0.56	-1.76

A.5 Gelation Study - Approach II

A.5.1 CDC experiments

Chemical Shifts

Table A.7: CDC samples - Chemical shift deviations ($\delta_{343\,K} - \delta_{298\,K}$).

	Δ T (K)		
	A	B	C
H2	-0.119	-0.165	0.008
H4	0.017	0.005	0.056
H5	0.008	-0.003	0.039
H6	0.016	0.015	-0.003
H10	0.015	0.010	-0.013
DMSO	0.053	0.053	0.008
H7	-0.008	-0.004	-0.022
H8	-0.027	-0.012	-0.024
H9	0.000	0.000	0.000

Table A.8: Chemical shift deviations of samples B and C comparing with sample A.

	298 K		
	A	B	C
H2	0.000	-0.128	-0.084
H4	0.000	-0.109	-0.105
H5	0.000	-0.099	-0.095
H6	0.000	-0.051	-0.061
H10	0.000	-0.055	-0.064
DMSO	0.000	-0.046	-0.060
H7	0.000	-0.019	-0.027
H8	0.000	-0.004	-0.004
H9	0.000	0.000	0.000

^{13}C - T_1 Relaxation

Table A.9: Deviations of T_1 relaxation times of samples B and C comparing with sample A.

	T_1 (s) 298 K		
	A	**B**	**C**
C2	0.000	0.060	0.060
C4	0.000	0.053	0.045
C5	0.000	0.061	0.059
C6	0.000	0.054	0.027
C10	0.000	0.233	0.269
C7	0.000	0.115	0.050
C8	0.000	0.231	0.142
C9	0.000	0.437	0.331

Diffusion

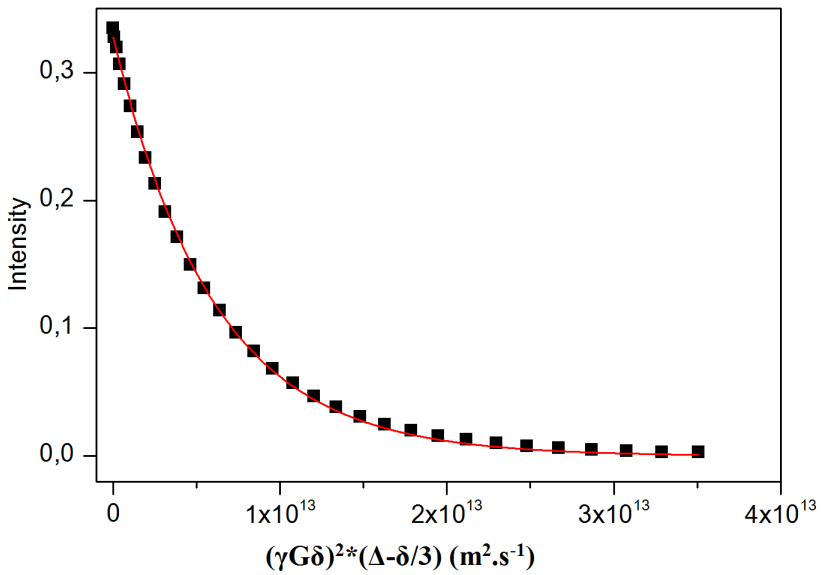

Figure A.22: Representation of effective decay of H2 of CDC - sample B.

Table A.10: Data of the effective decay of H2 for sample B of CDC.

$\gamma^2 g^2 \delta^2 * (\Delta - \delta/3)$ ($m^2.s^{-1}$)	Intensity
5.386E9	0.335
6.870E10	0.328
2.032E11	0.320
4.090E11	0.306
6.860E11	0.291
1.034E12	0.273
1.454E12	0.254
1.944E12	0.233
2.506E12	0.213
3.139E12	0.191
3.843E12	0.171
4.619E12	0.150
5.466E12	0.131
6.384E12	0.114
7.373E12	0.097
8.433E12	0.082
9.565E12	0.068
1.077E13	0.057
1.204E13	0.047
1.339E13	0.038
1.480E13	0.031
1.629E13	0.025
1.785E13	0.020
1.948E13	0.015
2.118E13	0.013
2.295E13	0.010
2.480E13	0.008
2.671E13	0.006
2.870E13	0.005
3.076E13	0.004
3.289E13	0.003
3.509E13	0.003